# Evaluation of physiological traits and identification of QTLs for drought tolerance in hexaploid wheat (*Triticum aestivum L.*)

Ali Izanloo

Thesis submitted for the degree of

Doctor of Philosophy


School of Agriculture, Food and Wine

Discipline of plant and pest science

Australian centre for plant functional genomics (ACPFG)

March 2008

# CHAPTER 5

# IDENTIFICATION OF QTLS FOR AGRONOMIC TRAITS ACROSS DIFFERENT RANGES OF DRY ENVIRONMENTS

# 5 Chapter 5: Identification of QTLs for agronomic traits across different ranges of dry environments

## 5.1 Introduction

Most economically important agronomic traits are genetically complex and quantitatively expressed. Their complexity during the crop cycle is determined by multiple physiological and biochemical pathways as well as environmental influences and their interactions (Shinozaki and Yamaguchi-Shinozaki, 2007). Identifying quantitative trait loci (QTL) associated with these traits is therefore of high interest. However, detecting QTL for these types of traits in environments with varying degrees of stress is potentially difficult as the QTL effects tend to be small and controlled by several genes (Mathews et al., 2008). Identified QTLs can be used as the basis for developing efficient strategies for genomics-based approaches for plant improvement (reviewed by Tuberosa and Salvi, 2006). They can also be used as the basis for positional cloning of genes underlying quantitative traits and for studying the molecular and biochemical mechanisms that condition plant growth and development (reviewed by Remington et al., 2001).

Numerous studies have been conducted to identify QTLs associated with drought tolerance in wheat (Quarrie et al., 1994; Verma et al., 2004; Quarrie et al., 2006; Kirigwi et al., 2007; Mathews et al., 2008; Maccaferri et al., 2008) , barley (Sanguineti et al., 1994; Teulat et al., 1998; Teulat et al., 2001a; Baum et al., 2003; Teulat et al., 2003), rice (Lilley et al., 1996; Ray et al., 1996; Price et al., 2002; Mu et al., 2003; Lanceras et al., 2004; Nguyen et al., 2004; Yue et al., 2005; Yue et al., 2006; Bernier et al., 2007) and maize (Tuberosa et al., 2002; Li et al., 2003; Tuberosa et al., 2003). The aim of this study is to identify QTLs underlying agronomical and physiological traits related to drought tolerance or productivity under drought conditions in the RAC875/Kukri DH population in the field.

### 5.1.1 Materials and methods

### 5.1.2 Field experiments

Five experiments were conducted at five different sites over two years. Three experiments were carried out in the South Australian wheatbelt in 2006, and two experiments were conducted at CIMMYT, Obregon, Mexico in 2007.

Field experiments in 2006 were conducted at Roseworthy (Roseworthy Agricultural College, RAC, University of Adelaide), Minnipa and Booleroo. The geographical locations of the field experiments are illustrated in Fig. 5-1. Roseworthy is an above average site in South Australia with an average annual rainfall of 440 mm. The average growing season (from April to October) rainfall is about 329 mm (http://www.bom.gov.au/climate/averages). The soil type in Roseworthy is a brown soil with clay loam texture with soil pH ranging from 7.6 to 8.3. Minnipa is a dry environment with the long-term average annual rainfall of ~327 mm (1919 - 2001), and the average growing season rainfall is about 242 mm. Main soil type in Minnipa site is moderately calcareous, light sandy loam with occasional patches of limestone and highly alkaline (pH ranging from 7.5 to 8.7). The regular farming practice is no-till cropping; inter-row sowing, controlled traffic and wide-row sowing (http://www.sardi.sa.gov.au). The long-term average rainfall in Booleroo is about 355.6 mm, and the average growing season rainfall is about 250.0 mm with alkaline, sandy-loam and red-brown soils. For each experiment, the design was generated using the DiGGer program (Coombes, 2002). The design was a two-replicate row-column design with plot size of 1.3 × 5 m for Roseworthy and Booleroo, 1.8 × 7 m for Minnipa. There were 6 rows at Roseworthy, eight rows at Minnipa and five rows at Booleroo spacing changed across sites. Plot sizes were then reduced to 3.2 m in length prior to anthesis by herbicide application.Each experiment was laid out in the field as a rectangular array of 69 rows and 12 columns. Parental lines and 10 checks (Drysdale, Excalibur, Frame, Krichauff, RAC1262, Stylet, Tincurren, Westonia, Wyalkatchem, Yitpi and Carinya) with a broad range of biotic and abiotic stress tolerance were included in the experiments and replicated 64 times for Carinya as grid every 12 plot, 4 times for parental lines and 2 times for other checks. The check grid was included to help account for soil spatial variation in the field (Appendix A and B).

Due to soil heterogeneity, plots were evaluated for important soil characteristics. In each of the three sites, 12 soil samples were taken at various depths (0–20, 20–60 and 60+ cm). The climatic data in 2006 were retrieved from nearby weather stations operated by the Australian Bureau of Meteorology (http://www.bom.gov.au) and used to calculate the climatic variables including temperature and rainfall (Table 5-1).

NOTE: This figure is included on page 122 in the print copy of the thesis held in the University of Adelaide Library.

**Figure 5-1. Map showing the locations in South Australia (SA) where field experiments were conducted in 2006. (Source; http://www.ga.gov.au/map/index.jsp)**

**Table 5-1. Average minimum and maximum temperature and total monthly rainfall during wheat growing season at the three trial sites across South Australia, 2006.**
**Source; http://www.bom.gov.au**

NOTE: This table is included on page 122 in the print copy of the thesis held in the University of Adelaide Library.

In 2007, two experiments were conducted in Mexico (CIMMYT, Obregon Experimental Station, Yaqui Valley, Sonora, North-Western Mexico, 27º 25 N, 109º 54 W, 38m above sea level). Obregon is a semi-arid environment with an average annual rainfall of 330 mm, where wheat production is dependent on irrigation. The soil type at Obregon is a coarse sandy clay mixed with montmorillonitic clay, classified as Typic Calciorthid, low in organic matter (0.76%) and slightly alkaline (pH 7.7) (Olivares-Villegas et al., 2007).

Two irrigation regimes were applied: flood irrigation (well-watered treatment) and drip-irrigation simulating a drought stress similar to the South Australian conditions. In the irrigated experiment, four irrigations were applied; at germination, 42, 78 and 130 d after germination with 15 to 18 hours of irrigation time. In the drought experiment, the crop was drip-irrigated and received a total of 152.5 mm of water. Drip-irrigation was applied three times at germination, 28 and 40 days after germination with 14 hours of irrigation time, and no water was applied afterwards. There was a rainfall event followed by lots of cloudy and cool weather after the third irrigation treatment in the drought experiment. The drought experiment was sown on 5$^{th}$ Dec. 2006 in two replicates in the randomized complete block design, and the irrigated experiment was sown on 15$^{th}$ Dec. 2006. Plot size in the irrigation experiment was smaller owing to seed availability. The plot sizes were 0.4 × 2 m for the irrigated experiment and 0.4 × 3.5 m for the drought experiment in 2 rows using bed planting. The experimental layouts for the droughted and drip-irrigated experiments are shown in Appendices C and D, respectively. The climatic data in 2007 at Obregon were collected from a nearby weather station and is presented in Table 5-2.

**Table 5-2. Average minimum and maximum temperature and rainfall, relative humidity and radiation flux at Obregon, Mexico 2007.**

| Month | Temp. (ºC) | | Rainfall | RH (%) | | RAD-FLUX |
|---|---|---|---|---|---|---|
| | Min. | Max. | (mm) | Max. | Min. | MJ/m2 |
| Jan | 6.2 | 21.7 | 19.0 | 88.0 | 33.5 | 14.2 |
| Feb | 7.3 | 25.2 | 0.4 | 92.0 | 31.6 | 19.7 |
| Mar | 8.3 | 28.6 | 0.0 | 91.2 | 26.6 | 23.6 |
| Apr | 10.8 | 29.3 | 0.2 | 91.5 | 25.2 | 25.1 |
| May | 13.6 | 34.2 | 0.4 | 82.6 | 19.1 | 29.9 |
| June | 22.0 | 36.7 | 0.0 | 77.4 | 26.7 | 27.5 |
| July | 25.2 | 36.3 | 46.4 | 77.6 | 35.8 | 23.7 |
| Aug | 25.1 | 37.3 | 12.0 | 85.5 | 37.6 | 22.2 |
| Total | 14.8 | 31.2 | 78.4 | 85.7 | 29.5 | 23.3 |

### 5.1.3 Trait evaluation

The RAC875/Kukri population was evaluated for different phenological, morpho-physiological and agronomical traits under field conditions. As phenological traits, heading time, anthesis and days to maturity were recorded. Morphological traits included early vigour, plant height, peduncle, flag leaf and spike length. Agronomical traits such as grain yield (YLD), number of spikelets per spike (Spn), fertile spikelets (Fspn), non-fertlile spikelets (Nspn), grain number per spike (Gne), thousand grain weight (TGW), biomass and harvest index (only in RAC) were measured. Physiological traits such as leaf waxiness (W), leaf rolling (Lro), leaf chlorophyll content (SPAD) and leaf colour (LC) were also measured in most experiments.

Heading date and maturity were recorded when 50% of the spikes had emerged from the boot and when 50% of the peduncles had turned yellow, respectively. A day of the year was assigned to the planting date and was subtracted from the day of the year of heading to obtain the number of days to heading. Time to anthesis was determined when 50% of the plot showed the first exposed anther in the spike. Maturity differences were also recorded at around grain-filling using the Zadoks scales (Zadoks et al., 1974). Zadoks scale was only recorded in the Minnipa and Bolleroo experiments. Early vigour was scored visually (1 to 5 scale) based on plant vigour at the vegetative stage in each plot. Score 1 was the value for small plants and score 5 was the value for large and vigorous plants.

At maturity, plant height (Ht) was measured from the soil surface to the top of the spikes excluding the awns. Five randomly sampled main stems were used to measure peduncle length (Pdl), flag leaf length (Fl) and ear length (El). The peduncle length was the distance between final node and the spike in centimeters. Leaf length was also measured on five random flag leaves in each plot using a clear ruler placed over the leaves. Lengths were measured from the collar to the tip of the leaf were averaged. Ear length was measured on five selected spikes of each plot and averaged for data analysis.

Crown rot was scored visually in Roseworthy experiment using a 1-9 scale where; 1 = no symptoms of spike whitening, 2 = 5–15%; 3 15-30%, 4 = 30-45%, 5 = 45-60%, 6 = 60-70%, 7 = 70-80%, 8 = 80-90% and 9 = 90-100%.

Leaf waxiness, leaf rolling and leaf colour were assessed visually. For leaf waxiness a score of 1 to 6 scale was used at South Australia (1 was no wax on the back of the flag leaf while 6 was a completely waxy leaf). In the Mexico trails, an improved method of scoring from 1 to 7 was used. Where, 1 = no wax, not even on the stem, 2 = just wax on the stem, 3 = a waxy stem and the bottom part of the back of the flag leaf (no more than a ¼ of the leaf is waxy), 4 = a waxy stem and most of the back of the flag leaf (1/4 to 3/4 of the back of the leaf is waxy), 5 = a waxy stem and all of the back of the flag leaf, 6 = a waxy stem, all of the back of the flag leaf and up to a ¼ of the front of the flag leaf and 7 = a waxy stem, all of the back of the flag leaf and up to a ¾ of the front of the flag leaf. Leaf colour was also scored visually based on 1 to 5 scales (1 = pale green while 5 = dark green).

Leaf rolling was scored (1 to 5 scales) at midday when the difference among the lines became most obvious following the method by O'Toole and Cruz, (1980). A score of 1 indicates no symptom of rolling, and the score 5 indicates complete leaf rolling. The Roseworthy experiment was affected by crown rot disease and to assess crown rot on each plot, a 1-9 scale was used based on the percentage of head whitening where 1= 0-20%, while 9 = 80-90% and other numbers were ranked in between.

Chlorophyll content was measured using a portable chlorophyll meter (SPAD-502, Minolta, Tokyo, Japan). It was measured on two randomly sampled flag leaves in each plot. The SPAD values of four measurements on each flag leaf were averaged. Chlorophyll content was only measured at Roseworthy and Mexico trails. In Mexico, chlorophyll content was assessed on flag leaves at anthesis and during grain-filling. Canopy temperature was only measured in the Mexico experiments using a hand-held infrared thermometer (IRT) (Model AG- 42, Telatemp Crop, Fullerton, CA.) at a field view angle of 2.5º on windless and sunny days as described by (Olivares-Villegas et al., 2007).

For water soluble carbohydrate extractions and measurements, 10 randomly sampled main stems were collected from each plot at the stage of two to five d after anthesis in RAC site. Collected samples were immediately put on dry ice and stored at -80 ºC and freeze-dried. The freeze-dried stems were then oven dried at 60ºC for 24 h. Water soluble carbohydrates (WSC) were extracted from 100 mg of powdered stems with 10 mL of 80% (v/v) ethanol at 80ºC followed by two extractions of the same volume of

water at 60ºC. WSC level in the combined extracts was measured using the anthrone method (Yemm and Willis, 1954) with some modifications (see Chapter 3, Materials and Methods). At RAC, parents along with 20 randomly selected DH lines were prepared for WSC measurements using the anthrone method (these measurements were kindly performed by Dr. Greg Rebetzke, CSIRO Division of Plant Industry, Canberra). However, in the Mexico experiments, stem and spike dry weight were recorded six times from booting stage to pre-harvest. The stem WSC was also analyzed at different stages of development using the anthrone method (data kindly provided by Dr. Matthew Reynolds, CIMMYT, Mexico).

When plants were at full maturity, field plots were machine-harvested, chaff was removed from each grain sample, and the total plot grain weight was recorded. The total plot weight was then converted to the unit ton · $ha^{-1}$. From this, the number of grain per square meter (g · $m^{-2}$) was calculated. A subsample of grain (~100 g) from each plot was passed through a sortimat machine fitted with 3 sieves with a screen hole widths of 2.8, 2.5 and 2.2 mm resulting in 4 fractions that were named fraction F1 (grain remained above 2.8 mm sieve), F2 (2.8–2.5 mm sieves), F3 (2.5–2.2 mm sieves) and F4 (grain that fell below 2.2 mm sieve). All fractions were weighed and used to calculate fraction proportions expressed as percentage of the total sample weight. The weighted average (μ, Equation 5-1) was also calculated. In addition, five hundred grains were counted and weighed to calculate grain weight for harvested samples.

$$\mu = \frac{\sum_{i=1}^{n} F_i w_i}{\sum_{i=1}^{n} F_i} \qquad (5\text{-}1)$$

Where μ is weighted average, $F_i$ is a given fraction and $w_i$ is the weight of seeds in each fraction.

Number of tillers on five randomly sampled plants was counted at three South Australian sites. However, in the Mexico experiments, the numbers of plants and spikes were counted on 0.5 m long rows, and the number of tillers was then estimated by dividing number of spikes per number of plants in the given area. Five spikes corresponding to main stem samples were collected at maturity for each genotype. After all spikes were dried at 40°C for 48 h spikelet number per spike and number of fertile and non-fertile spikelets were counted. Grains of each genotype were threshed, weighed and counted to obtain number of grain per spike, number of grain per spikelet and

thousand grain weights at maturity. Spikelet fertility was measured as the number of grains divided by the total number of spikelets of a plant.

To calculate the harvest index from Roseworthy, plants from a uniform section of 0.5 × 0.5m in each plot were harvested at ground level. Biomass samples were air dried, weighed, and threshed. Total weight of harvested sample was recorded and the grain weight then was recorded after threshing. Harvest index was estimated as the ratio of grain weight to whole plant weight.

### 5.1.4 Statistical analysis and QTL mapping

#### 5.1.4.1 Experimental error and spatial variation

To prepare data for analysis, correlations between the two replicates were calculated to identify outliers. Outliers were carefully inspected and changed or deleted if necessary. Phenotypic correlations between replicates for each trait in each environment as well as traits among environments were calculated based on Pearson's correlation coefficient values using SPSS 13.0 for Windows.

To adjust for spatial variability in the field, especially in the drought-stressed experiments, a series of data analyses were conducted. On the basis of single experiment analysis, spatial methods by Gilmour et al. (1997) were used to remove or minimize spatial effects of field variation by estimating varietal contrasts. A spatial model incorporating row and column effects was fitted to the data along with any other significant spatial terms, such as seeding-side and replications. For each trait in each environment, linear mixed model analysis using the method of residual maximum likelihood (REML) was performed in GenStat release 6.1 (Payne et al., 2002). In the model, all DH lines were considered as one 'DH' and along with checks (parents and other lines) were fitted as fixed effects. Genotypes were considered as random for analyses. The parental and check lines provided the best linear unbiased estimate (BLUE), while the effects of the DH lines were the best linear unbiased predictor (BLUP). First a two-dimensional separable auto-regressive spatial model of first order (AR1 × AR1) was fitted as the basic spatial model. Then, by looking at the pattern of variation (variogram; Fig. 5-2), the best possible model was fitted. The variogram was used by Gilmour et al (1997) as a major diagnostic tool to check for the presence of extraneous variation. When the variogram showed the classical AR1 × AR1 appearance

and there were no outliers or other obvious problems, the model was accepted. Otherwise, terms were added or removed from the model as suggested by the variogram until a reasonable result was obtained. Heading time was also fitted as a covariate for every trait in each environment. When the effect of heading time was not significant, it was excluded from the model. Fitted data based on the best possible model for each genotype were then used for QTL analysis. Broad sense heritabilities were estimated using VFUNCTION procedure of GenStat (Nyquist, 1991).

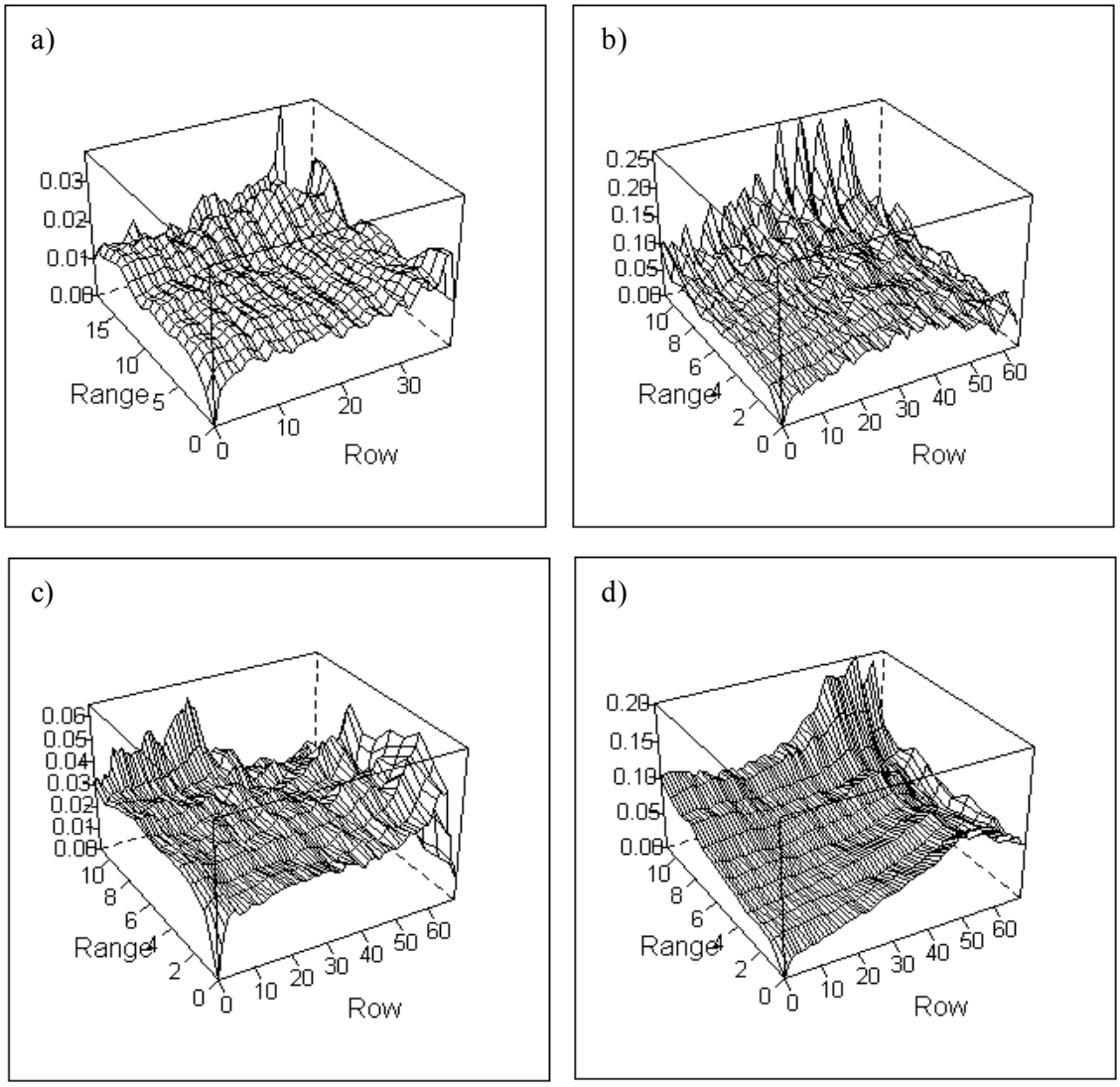


**Figure 5-2. Sample variograms calculated from basic spatial AR1 × AR1 model for grain yield in Mexico irrigated (a), Mexico droughted (b), Minnipa (c) and Booleroo (d) sites.**

### 5.1.4.2 QTL mapping

The QTL analysis was performed by the mixed-model based composite interval mapping (MCIM) using QTLNetwork v2.0 (Yang et al., 2007). To estimate the empirical significance thresholds for detecting putative QTLs of each trait, 1000 permutations with the experimental type I error p = 0.05 significance level were defined (Churchill and Doerge, 1994). The significant threshold was also estimated at p = 0.1 level to detect potential QTLs. The QTLs that were at or above the significance threshold with p = 0.05 value for one or more environment are reported as '*putative* QTLs' and those that were at or above the significance threshold with p = 0.1 for two or more environments are referred as '*suggestive* QTLs'.

In this study, QTL identification was performed using a genetic linkage map containing 440 non-redundant marker loci. The QTL analyses were carried out on different datasets including *non-adjusted data, split-up data* and *adjusted data.* In non-adjusted data, the observed variables did not account for the effects of the heading time. In spilt-up data, QTL analysis was performed on two subpopulations differentiated on the basis of heading time. While for the adjusted data, the phenotypic data of the whole population was adjusted for the heading time effect.

One-way ANOVA was also performed to compare allele classes at each marker locus that was associated with each specific QTL. The trait abbreviations as well as the QTL designations were defined adopting the nomenclature suggested by the wheat catalogue of gene symbols (McIntosh et al., 2003; http://wheat.pw.usda.gov/ggpages/wgc/). However, to easily distinguish the identified QTLs from the different datasets, QTLs were shown with the superscript letter of NA (for non-adjusted data), EF (for early-flowering data), LF (for late-flowering data), and Eet (for adjusted data).

### 5.1.4.3 Adjusting for heading time effect

The ideal populations for QTL mapping of drought tolerance are those with uniformity in plant height and synchrony in flowering time (Reynolds and Tuberosa, 2008). Small differences in phenology between varieties can create very large differences in final yield. Assessing drought is therefore difficult in populations in which flowering times differ (Price and Courtois, 1999). To deal with the difference in phenology, staggered

sowing date has been proposed but it requires knowledge of flowering time of each line in the test environment. However, heading time of a large population still cannot be easily synchronized because of G × E interaction (Price and Courtois 1999). Variation of heading time in segregating populations has often made the phenotyping of drought tolerance inaccurate. The success has been limited because of the difficulty in achieving real synchronization of heading time in a segregating population (Yue et al., 2006).

Three different approaches were adopted to deal with heading time effects on population performance. Firstly, the population was spilt up in two sub-populations with early and late flowering groups (*the spilt-up approach*). Secondly, trait values of each genotype were adjusted for differences in heading time using the regression coefficients (*the adjusted approach*). In the adjusted approach, a linear regression model was fitted between the heading time and the phenotypic values of each genotype for each environment (Flint-Garcia et al., 2003; Zeegers et al., 2004). The linear regression model was tested for significance at p = 0.05. We used the linear model if the linear term was significant. The adjustment for flowering time was done for traits that showed significant regression as follow:

$$\mathrm{Y}adj_i = \mathrm{Y}_i - b_l(\mathrm{FT}_i - \overline{\mathrm{FT}}) \qquad (5\text{-}2)$$

where $b_l$ is the linear regression coefficient between actual yield and flowering time (Flint-Garcia et al., 2003). $\mathrm{Y}adj_i$ and $\mathrm{Y}_i$ are adjusted and actual data values for each individual, respectively. $\mathrm{FT}_i$ and $\overline{\mathrm{FT}}$ are flowering time values for each individual and an averaged flowering time in a given environment, respectively.

Thirdly, the drought response index (DRI) was calculated for each individual in each drought environment (RAC, Minn, Bool and MexD). DRI was developed by Bidinger et al. (1987) to remove the effect of variation in phenology and yield potential in pearl millet. DRI provides an estimate of the genotypic response to drought stress that is independent of both the effects of flowering time and yield potential. In this model drought tolerance is considered as an independent genetic character (Bidinger et al., 1987).

DRI was calculated as described by Bidinger et al. (1987) as follow:

$$DRI = (\mathrm{Y}act_i - \mathrm{Y}est_i)/\mathrm{SE\ of\ Y}est_i \qquad (5\text{-}3)$$

Where $Yact_i$ is the actual grain yield under drought stress for each line, $Yest_i$ is the estimated grain yield for each line, and SE is the standard error of the $Yest$ of all lines. Estimated grain yield ($Yest_i$) was derived from the calculation using multiple linear regression analysis. $Yp_i$ and $FT_i$ are potential yield and flowering time, respectively, under control conditions for $i$th genotype, and a, b and c are the regression coefficients.

$$Yest_i = a + bYp_i + c\mathrm{FT}_i \qquad (5\text{-}4)$$

In this study, the irrigated experiment at CIMMYT, Mexico was considered as non-stressed environment and DRI was calculated for each genotype at the four other environments. In addition, Roseworthy as a good site among South Australian experiments and therefore was considered as a reference for the other two Australian environments (Minnipa and Booleroo); the DRI was calculated for each genotype at these two sites.

The drought susceptible index (DSI) and the stress tolerance index (STI) were also estimated using the adjusted data. Fischer and Maurer (1978) proposed a drought susceptibility index (DSI) based on the relationship of the change in relative yield (yield in drought/yield in the absence of drought) of an individual cultivar to the change in mean relative yield, across a range of stress intensities, of all cultivars in the comparison. They attempted to separate the effects of yield potential from drought susceptibility;

$$\mathrm{DSI} = (1\text{-}Y_{si}/Y_{pi})/\mathrm{DI} \qquad (5\text{-}5)$$

Where, $Y_{si}$ and $Y_{pi}$ are grain yield under drought stressed and non-stressed conditions, respectively. The stress intensity is $\mathrm{DI} = (1\text{-}Y_s/Y_p)$, where Ys and Yp represent average yield of all genotypes under stressed and non-stressed conditions, respectively.

Fernandez (1992) proposed an STI which discriminates genotypes with high yield and stress tolerance potentials. It was used to characterize the relative response of each genotype to stressed field conditions. The index was calculated from genotype/line means using the following formula:

$$\mathrm{STI} = \left(\frac{\mathrm{Yp}_i}{\bar{\mathrm{Y}}\mathrm{p}}\right)\left(\frac{\mathrm{Ys}_i}{\bar{\mathrm{Y}}\mathrm{s}}\right)\left(\frac{\bar{\mathrm{Y}}\mathrm{s}}{\bar{\mathrm{Y}}\mathrm{p}}\right) = \frac{\mathrm{Yp}_i+\mathrm{Ys}_i}{(\bar{\mathrm{Y}}\mathrm{p})^2} \qquad (5\text{-}6)$$

Where $Y_{pi}$ and $Y_{si}$ are the yield of each line in a non-stressed (yield potential) and stressed environments, respectively; $\overline{Y}p$ and $\overline{Y}s$ are the average yield in non-stressed and stressed environments, respectively. Therefore, STI is a function of relative performance of a genotype in non-stressed ($Yp_i/\overline{Y}p$), and stressed ($Ys_i/\overline{Y}s$) environments and the stress intensity ($\overline{Y}s/\overline{Y}p$). Greater values of STI for a genotype indicate greater stress tolerance and yield potential (Fernandez, 1992; Ehdaie et al., 2003). Relationships among different drought indices, heading time, yield under non-stressed (yield potential) and stressed environments were examined by principal component analysis (PCA) using the MINITAB v14.13 statistical software.

## *5.2 Results*

### 5.2.1 Trait performance

The population mean, phenotypic values of the two parental lines (Kukri and RAC875), the range (min.–max.) and heritability of ten traits from five environments are summarized in Table 5-3. Most of the traits showed a normal distribution except heading time and grain yield (Fig. 5-3 and 5-6). Heading time (Eet = ear emergence time) showed a bimodal distribution and grain yield was negatively skewed towards high values in Roseworthy (RAC), Minnipa (Minn), Booleroo (Bool) and Mexico droughted (MexD) datasets. Significant ($P < 0.05$) transgressive segregation occurred in both directions (positive and negative) for all traits except leaf waxiness. For leaf waxiness, transgressive segregation was not significant towards higher values, and it was assumed that this trait was dominantly inherited in this population. Genotype effects were highly significant ($P < 0.001$) for all traits. The maximum range of phenotypic variation was observed for maturity traits, spikelets per spike, spike length, peduncle length, grain yield and thousand grain weight (TGW) while early vigour (EV) and leaf rolling showed the least (Table 5-3).

**Table 5-3. Phenotypic values for the two parental lines (Kukri and RAC875), population mean, range (min.-max.) and heritability of heading time (Eet), days after sowing, (Eet), grain yield (YLD), grain per square meter ($G \cdot m^{-2}$), thousand grain weight (Tgw), plant height (Ht), peduncle length (Pdl), ear length (El), flag leaf length (Fl), spikelet number per ear (Spn), grain number per five stampeded spikes (Gnu), grain number per ears (Gnn), grain weight per five sampled spikes (Gwe), number of grains per spikelet (Gspn), number of fertile spikelets (Fspn), non-fertile spikelets (Nspn), early vigour (Ev) and leaf waxiness in Roseworthy (RAC), Minnipa (Minn), Booleroo (Bool), Mexico irrigated experiment (MexI) and Mexico droughted experiment (MexD).**

| Trial | 2006 | | | | | | | | | | | | | | |
|---|---|---|---|---|---|---|---|---|---|---|---|---|---|---|---|
| | RAC. | | | | | Minn. | | | | | Bool. | | | | |
| | Kukri | RAC875 | Mean | Range | $h^2$ | Kukri | RAC875 | Mean | Range | $h^2$ | Kukri | RAC875 | Mean | Range | $h^2$ |
| Heading (Eet) | 108.6 | 110.8 | 114.1 | 99.2 - 137.5 | 0.83 | 94.7 | 93.9 | 99.8 | 85.7 - 126.7 | 0.82 | 110.4 | 108.7 | 111.2 | 93.9 - 140.9 | 0.87 |
| YLD ($t \cdot ha^{-1}$) | 2.3 | 2.6 | 2.2 | 0.2 - 3.3 | 0.74 | 0.5 | 0.7 | 0.4 | 0.0 - 0.8 | 0.76 | 0.3 | 0.5 | 0.3 | 0.0 - 0.8 | 0.53 |
| $G \cdot m^{-2}$ | 5133.4 | 4578.4 | 5258.9 | 1719.0 - 7233.8 | 0.89 | 1409.9 | 1480.6 | 1355.8 | 404.7-2182.1 | 0.82 | 683.1 | 982.6 | 906.3 | 201.5-1679.4 | 0.75 |
| TGW (g) | 30.6 | 37.4 | 33.1 | 24.5 - 45.2 | 0.49 | 33.8 | 38.1 | 34.8 | 20.1 - 44.1 | 0.68 | 31.6 | 39.4 | 34.0 | 16.2 - 44.6 | 0.47 |
| Ht (cm) | 74.4 | 63.1 | 65.5 | 52.7 - 80.7 | 0.62 | 40.1 | 41.2 | 38.3 | 29.4 - 43.2 | 0.69 | 40.2 | 43.4 | 37.2 | 27.2 - 45.8 | 0.40 |
| Pdl (cm) | 29.5 | 23.2 | 25.4 | 13.9 - 37.8 | 0.65 | 14.4 | 13.6 | 13.6 | 8.2 – 20.0 | 0.76 | 13.8 | 13.6 | 12.7 | 8.1 - 17.5 | 0.62 |
| El (cm) | 9.2 | 8.3 | 9.1 | 7.4 - 12.5 | 0.30 | 6.2 | 5.8 | 6.0 | 4.8 - 7.2 | 0.35 | 5.7 | 5.4 | 5.4 | 4.2 - 6.7 | 0.13 |
| Fl (cm) | 18.6 | 13.8 | 16.5 | 10.7 - 22.6 | 0.78 | 7.3 | 6.3 | 7.5 | 4.1 – 15.0 | 0.80 | 6.6 | 5.7 | 6.5 | 3.9 - 9.9 | 0.72 |
| Spn | 16.8 | 14.9 | 16.4 | 13.1 - 21.7 | 0.67 | 13.8 | 13.0 | 13.3 | 10.1 - 15.6 | 0.35 | 13.1 | 12.4 | 12.2 | 9.2 - 16.3 | 0.25 |
| Gnn | 225.8 | 182.2 | 177.8 | 64 - 240.4 | 0.35 | 86.8 | 93.4 | 82.2 | 23.7 - 141.1 | 0.69 | 66.1 | 86.1 | 62.6 | 6.0 – 112.0 | 0.70 |
| Gwe (g) | 6.3 | 6.5 | 5.9 | 2.0 - 8.9 | 0.48 | 2.9 | 3.5 | 2.9 | 0.6 - 5.2 | 0.68 | 2.1 | 3.4 | 2.2 | 0.0 - 3.7 | 0.72 |
| Gnu | 43.4 | 35.6 | 35.5 | 12 - 48.1 | 0.40 | 17.3 | 18.5 | 16.4 | 1.8 - 30.8 | - | 13.3 | 17.2 | 12.5 | 0.1 - 22.2 | 0.63 |
| Gspn | 2.6 | 2.4 | 2.2 | 0.5 - 3.1 | 0.65 | 1.3 | 1.4 | 1.2 | 0.3 - 2.1 | 0.76 | 1.0 | 1.4 | 1.0 | 0.0 - 1.8 | 0.72 |
| Fspn | 14.5 | 11.9 | 11.8 | 4.0 - 16.0 | 0.40 | 5.8 | 6.1 | 5.7 | 1.6 - 9.4 | 0.33 | 6.5 | 8.4 | 6.3 | 1.5 - 11.3 | 0.67 |
| Nfspn | 2.5 | 3.1 | 4.5 | 0.0 - 13.3 | 0.69 | 8.1 | 6.8 | 7.7 | 2.7 - 12.6 | 0.46 | 6.6 | 3.7 | 6.0 | 0.2 - 13.9 | 0.71 |
| Ev | 4.5 | 3.6 | 3.7 | 1.5 - 5.7 | 0.44 | 4.3 | 5.0 | 4.3 | 1.5 - 7.5 | 0.69 | 2.5 | 3.2 | 2.7 | 0.6 - 5.9 | 0.81 |
| Waxiness (W) | 1.0 | 5.7 | 3.2 | 0.9 - 6.1 | 0.74 | 1.0 | 3.6 | 2.7 | 0.8 - 5.1 | 0.55 | 1.5 | 5.4 | 3.2 | 0.9 - 5.9 | 0.67 |

**Table 5-3. Continued**

| Year | 2007 | | | | | | | | | |
|---|---|---|---|---|---|---|---|---|---|---|
| Trial | MexI | | | | | MexD | | | | |
| | Kukri | RAC875 | Mean | Range | $h^2$ | Kukri | RAC875 | Mean | Range | $h^2$ |
| Heading (Eet) | 75 | 71.5 | 79.3 | 59.4 - 105.3 | 0.81 | 79.0 | 77.5 | 78.2 | 61 - 110 | 0.69 |
| YLD ($t \cdot ha^{-1}$) | 6.2 | 7.1 | 5.6 | 3.5 - 7.6 | 0.22 | 1.3 | 2.1 | 1.8 | 0.0 - 4.1 | 0.71 |
| $G \cdot m^{-2}$ | 2306.0 | 2038.8 | 2198.5 | 1606-3164.4 | 0.68 | - | - | - | - | - |
| TGW (g) | 42.2 | 54.9 | 44.5 | 25.9 - 56.5 | 0.63 | - | - | - | - | - |
| Ht (cm) | 92.5 | 81 | 82.6 | 67.2 - 106.3 | 0.37 | 62.3 | 60.5 | 62.9 | 42.3 - 89.6 | 0.71 |
| Pdl (cm) | - | - | - | - | - | 19.8 | 18.4 | 20.4 | 7.4 - 31.5 | 0.40 |
| El (cm) | - | - | - | - | - | 9.7 | 8.5 | 9.2 | 6.4 - 13.5 | 0.55 |
| Fl (cm) | - | - | - | - | - | 26.0 | 22.6 | 22.8 | 13.7 - 32.7 | 0.39 |
| Spn | - | - | - | - | - | 35.7 | 31.1 | 32.0 | 20.1 - 46.2 | 0.74 |
| Fspn | - | - | - | - | - | 16.5 | 13.5 | 16.0 | 9.0 – 21.0 | 0.37 |
| Nspn | - | - | - | - | - | 4.0 | 1.5 | 2.1 | 0.0 – 11.0 | 0.17 |
| Ev | 9.5 | 9.0 | 8.4 | 3.0 – 10.0 | 0.10 | 6.5 | 6.3 | 6.7 | 4.7 - 9.2 | 0.26 |
| Waxiness (W) | 4.0 | 7.0 | 5.0 | 3.2 - 6.8 | 0.69 | 4.0 | 6.0 | 4.5 | 3.0 – 7.0 | 0.54 |

### 5.2.2 Trait correlations

Phenotypic correlations among traits were estimated at $P < 0.05$ and $P < 0.01$. A summary of correlations between heading time and yield and grain number per square meter ($G \cdot m^{-2}$), thousand grain weight (TGW), hectolitre weight (HL), number of tillers per plant (Tn), number of spikelets per ear (Spn), number of fertile and non-fertile spikelets (Fspn and Nspn, respectively), grain number per five sampled spikes (Gnu), grain number per ear (Gne) and spikelets per ear (Gspn), grain weight per ear (Gwe), plant height (Ht), peduncle length (Pdl), ear length (El), flag leaf length (Fl), chlorophyll content (SPAD unit), leaf waxiness, crown rot (Cre), senescence (Sn), early vigour (Ev) and maturity traits from five environments is given in Table 5-4.

Correlation analysis showed a strong association between heading time, yield and its components, plant height, peduncle length, flag leaf length and spike length, especially under drier environments. Flowering time was found to influence many important agronomic traits such as yield and yield components in this population (Table 5-4). The correlation between yield (YLD) and heading time indicated that early lines yielded better than late lines in this population since lines flowering prior to the drought stress were less affected and lines flowering extremely late were mostly affected by drought as well as high temperatures. Heading time showed negative correlations with grain number per square meter ($G \cdot m^{-2}$) in the three Australian sites RAC, Minn and Bool at -

0.84, -0.88 and -0.80 ($P < 0.001$), respectively, whereas there was a positive correlation (0.53; $P < 0.001$) between these two traits in MexI experiment. Since heading time and YLD showed a negative correlation, the reduction in YLD could, therefore, result from reduced grain size in late flowering genotypes. In the MexI experiment, heading time showed a positive correlation with plant height (r = 0.44, $P < 0.01$), while in drier environments (RAC, Minn, Bool and MexD) it was negative (Table 5-4). For QTL analysis, three different approaches were implemented to remove the potentially confounding effects of heading time on QTLs of smaller effect (see the Materials and Methods; section 5.2.3.3).

**Table 5-4. Phenotypic correlations between heading time and grain yield (Yld) in five environments with grain number per square meter ($G \cdot m^{-2}$), thousand grain weight (TGW), hectolitre weight (HL), number of tillers per plant (Tn), number of spikelets per ear (Spn), number of fertile and non-fertile spikelets (Fspn and Nspn, respectively), grain number per five sampled spikes (Gnu), grain number per ear (Gne) and spikelets per ear (Gspn), grain weight per ear (Gwe), plant height (Ht), peduncle length (Pdl), ear length (El), flag leaf length (Fl), chlorophyll content (SPAD unit), leaf waxiness, crown rot (Cre), senescence (Sn), early vigour (Ev) and maturity in the RAC875/Kukri population.**

| Trait | Heading time | | | | | YLD | | | | |
|---|---|---|---|---|---|---|---|---|---|---|
| | MexI. | MexD. | RAC. | Minn. | Bool. | MexI. | MexD. | RAC. | Minn. | Bool. |
| YLD ($t \cdot ha^{-1}$) | -0.14** | -0.74** | -0.87** | -0.91** | -0.76** | 1 | 1 | 1 | 1 | 1 |
| $G \cdot m^{-2}$ | 0.53** | - | -0.84** | -0.88** | -0.80** | 0.53** | - | 0.94** | 0.94** | 0.91** |
| TGW(g) | -0.75** | - | -0.30** | -0.46** | -0.27** | 0.20** | - | 0.26** | 0.43** | 0.25** |
| HL (g) | - | - | 0.40** | -0.86** | - | - | - | -0.29** | 0.90** | - |
| Tiller (Tn) | - | -0.43** | 0.01 | - | - | - | 0.52** | 0.18** | - | - |
| Nspn | - | 0.33** | 0.80** | 0.67** | 0.77** | - | -0.40** | -0.73** | -0.64** | -0.59** |
| Fspn | - | 0.07 | -0.52** | -0.76** | -0.75** | - | 0.05 | 0.47** | 0.77** | 0.73** |
| Gspn | - | - | -0.76** | -0.78** | -0.80** | - | - | 0.71** | 0.77** | 0.68** |
| Gne | - | - | -0.52** | -0.77** | -0.74** | - | - | 0.47** | 0.79** | 0.71** |
| Gwe | - | - | -0.55** | -0.80** | -0.72** | - | - | 0.50** | 0.80** | 0.72** |
| Gnu | - | - | -0.50** | -0.76** | -0.74** | - | - | 0.48** | 0.77** | 0.71** |
| Spn | - | 0.26** | 0.59** | 0.02 | 0.18** | - | -0.21** | -0.53** | 0.03 | 0.10* |
| Ht (cm) | 0.44** | -0.66** | -0.56** | -0.70** | -0.52** | 0.33** | 0.80** | 0.51** | 0.70** | 0.63** |
| Pdl(cm) | - | -0.52** | -0.91** | -0.77** | -0.65** | - | 0.56** | 0.76** | 0.71** | 0.58** |
| El (cm) | - | 0.37** | 0.41** | -0.28** | -0.13** | - | -0.26** | -0.43** | 0.27** | 0.21** |
| Fl (cm) | - | 0.31** | -0.73** | -0.73** | -0.63** | - | -0.18** | 0.54** | 0.63** | 0.49** |
| SPAD | -0.09* | - | -0.46** | - | - | 0.16** | - | 0.51** | - | - |
| Waxiness | 0.22** | 0.16** | 0.42** | 0.54** | 0.21** | 0.05 | 0.04 | -0.31** | -0.44** | -0.01 |
| Cre | - | - | 0.17** | - | - | - | - | -0.38** | - | - |
| Senescence | - | - | -0.91** | -0.81** | - | - | - | 0.80** | 0.75** | - |
| EV | 0.01 | 0.30** | -0.88** | -0.81** | -0.86** | 0.472** | -0.09* | 0.78** | 0.73** | 0.65** |
| Mat | 0.95** | - | - | 0.95** | 0.96** | -0.142** | - | - | -0.91** | -0.78** |

*, ** Pearson's correlation is significant at the 0.05 and 0.01 levels, respectively (2-tailed)

## 5.2.3 Identifying QTLs using non-adjusted data

### 5.2.3.1 QTLs for grain yield and associated traits

#### *5.2.3.1.1 Heading time and maturity traits QTLs*

Although Kukri and RAC875 did not differ significantly in heading time, days to heading were a range of 30 to 40 d among the DH lines, depending on the environment. Transgressive segregation was well pronounced in the progeny. Heading time distributions showed a bimodal pattern with 3:1 segregation ratio ($\chi^2 = 3.5 < \chi^2_{(0.05,\ 1)}$), suggesting that two major genes of large effect were segregating in the population (Fig. 5-3). The phenotypic variation attributable to those loci are likely to obscure QTLs with smaller effects (Lander and Botstein, 1989). The estimated heritability for heading time in different environments ranged from 69% to 87% (Table 5-3).

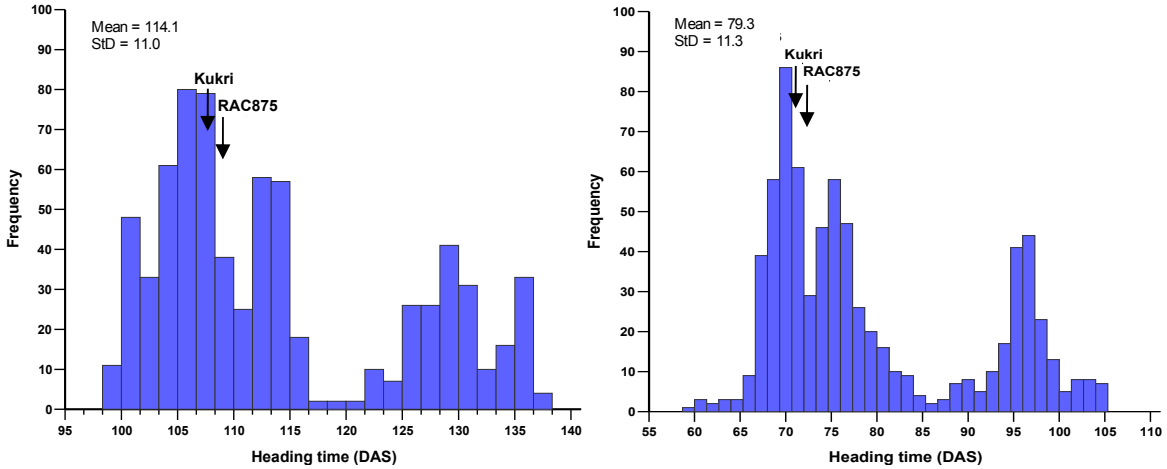


**Figure 5-3. Phenotypic frequency distribution of heading time in DH lines in two different environments (Roseworthy 2006 and Mexico Irrigation 2007). The distribution is bimodal, and approximately twice as many individuals are early-flowering than late-flowering. The population mean (Mean) and the standard error of deviation (StD) are shown in the figure. Arrows indicate the trait value for the two mapping parents.**

Based on the analysis of the original maturity data including heading time, Zadoks scale, anthesis and days to maturity, a total of sixty three QTLs were detected. The estimated positions and effects of QTLs were presented in Table 5-5 and Appendix K. Thirty-six QTLs were detected for heading time in all five environments. Nine QTLs were identified in each of the South Australian environments (RAC, Minn and Bool), eight and six QTLs were detected in Mexico irrigated (MexI) and in Mexico drought

(MexD) experiments, respectively. Sixteen QTLs were identified for 'Zadoks scale' in two environments (Minn and Bool), six and five QTLs were identified for anthesis and day to maturity in MexI, respectively.

Heading time QTLs were located on chromosomes 1A, 2B, 2D, 3D, 5B, and 7B at all five sites and on 7A at four sites. Heading time QTLs on chromosome 1A, 2B, 2D, 3D, 5B, 7A and 7B were identified as putative QTLs with main additive effects. The suggestive QTLs with G × E interactions were also identified on chromosome 5A (three sites). The most significant QTLs were detected on chromosome 2B and 2D, which were designated ***QEet.aww-2BS*** and ***QEet.aww-2DS***. These two QTLs showed the highest LOD score in all five environments ranging from LOD 14.1 to 35.1 and explained an average 21.6% to 16.8% of the phenotypic variation, respectively. These two QTLs were also the largest and the most significant QTL for 'Zadoks scale', anthesis and days to maturity (Table 5-6, Fig. 5-18). ***QEet.aww-2BS*** peaked at *XwPt-7757* (33.0 cM) in the *XwPt-7757–Xbarc0013a* interval, and ***QEet.aww-2DS*** was mapped in a poorly covered region of chromosome 2DS at the marker locus *XwPt-0330* (80.2 cM) in the *XwPt-6003–XwPt-0330* interval. It is very likely that these two maturity related QTLs mapped to the previously described photoperiod insensitivity genes *Ppd-B1* and *Ppd-D1a*, respectively (Worland, 1996; Beales et al., 2007).

***QEet.aww-1AS*** on the distal part of chromosome 1AS was only detected in South Australian experiments with LOD score more than 3.5 and it explained about 1.8 % of the phenotypic variation. ***QEet.aww-3D***, ***QEet.aww-5B*** and ***QEet.aww-7A*** were detected in five environments with LOD > 4. For three QTLs (***QEet.aww-2BS***, ***QEet.aww-7A*** and ***QEet.aww-7B***), the 'RAC875' allele reduced days to heading by 5.1, 2.4 and 1.9 days, respectively, relative to the 'Kukri' allele. For five QTLs (***QEet.aww-1A***, ***QEet.aww-2DS***, ***QEet.aww-3D***, ***QEet.aww-5A*** and ***QEet.aww-5B***), however, the 'Kukri' allele was associated with decreases in days to heading relative to the 'RAC875'allele by 1.4, 10.1, 1.8, 2.3 and 2.2 days, respectively. The QTLs for Zadoks score, anthesis and days to maturity were also mapped to similar positions with heading time QTLs on chromosomes 2B, 2D, 3D, 5B, 7A, and 7B (Table 5-5). The largest QTLs affecting maturity traits were located on the short arm of chromosomes 2B and 2D in the RAC875/Kukri population. The two QTLs, collectively, accounted for 41.5, 43.3, 38.9, and 40.5% of the phenotypic variation on average days to heading, Zadok scale, anthesis and days to maturity, respectively. The results in Table 5-5 show that the

earliness allele for maturity of ***QEet.aww-2BS*** were derived from 'RAC875', while the earliness allele of ***QEet.aww-2DS*** came from 'Kukri' with a stronger additive effect on early flowering. ***QEet.aww-7A.1*** was detected as putative QTLs with a LOD > 4.2 and heritability of 2.6%, 5.5% and 6.6% in RAC, Minn and Bool, respectively. It peaked at *Xcfa2028-7AS* (90.1 cM) near the centromere, where the 'RAC875' allele was associated with earlier flowering. In MexI, however, *QEet.aww-7A.2* was detected as a suggestive QTL, with a negligible contribution to the observed phenotypic variation ($h^2$ = 0.6%). A suggestive QTL (LOD = 2.2; 1.1% of the variation) for anthesis (*QAnth.aww-7A*) was also identified in a similar position with *QEet.aww-7A.2* in MexI. These two QTLs for heading time and anthesis in MexI peaked in the *Xbarc0195–XDuPw0254* interval. In MexD, no QTLs for heading time and anthesis were detected on chromosome 7A (Table 5-5).

Further analysis showed no epistatic interaction between heading time QTLs in four environments. There was, however, only one environment (MexI) where an epistatic effect became significant for a pair of intervals between ***QEet.aww-2BS*** and ***QEet.aww-2DS***, but it was not detectable between other QTLs. Generally, epistatic effects accounted only for a relatively small portion of the observed phenotypic variation for flowering ($h^2$ = 2.8%) compared to the detected additive effect.

**Table 5-5. Detected QTLs with composite interval mapping (CIM) analysis are shown for maturity traits. Heading time (Eet), anthesis (Anth), maturity day (Mat) and Zadoks scale (Zad) QTLs for the RAC875/Kukri population in five environments. The most likely QTL position, range, interval of flanking markers, allelic additive effect, heritability and LOD for each individual QTL is presented. The italic bold loci represent putative QTLs which were detected at a 5% significance threshold. Suggestive QTLs were detected at a 10% significance threshold. QTLs with largest trait effect are highlighted in light gray.**

| Site | Trait | QTL | Position (cM) | Range | Interval | Add | Parent | h2 (%) | LOD |
|---|---|---|---|---|---|---|---|---|---|
| Roseworthy (RAC) | Heading (Eet) | ***QEet.aww-1AS*** | 6.4 | 5.4-7.7 | *XwPt-7541–XwPt-6709* | -1.49 | RAC875 | 1.8 | 4.6 |
| | | ***QEet.aww-2BS*** | 37.0 | 35.0-38.0 | *XwPt-7757–Xbarc0013a* | 5.57 | Kukri | 27.8 | 35.1 |
| | | ***QEet.aww-2DS*** | 45.7 | 41.7-49.7 | *XwPt-6003–XwPt-0330* | -10.82 | RAC875 | 17.4 | 22.8 |
| | | ***QEet.aww-3D*** | 114.7 | 106.1-121.8 | *Xgwm0664-Xgwm0383b* | -1.85 | RAC875 | 2.8 | 4.5 |
| | | ***QEet.aww-5B*** | 79.9 | 73.9-91.6 | *XwPt-4936–XwPt-3457* | -2.38 | RAC875 | 3.0 | 4.3 |
| | | ***QEet.aww-7A.1*** | 54.6 | 39.6-78.6 | *XwPt-5153–Xcfa2028* | 3.72 | Kukri | 2.6 | 4.2 |
| | | *QEet.aww-7B* | 53.8 | 44.0-62.8 | *XwPt-4230–Xwmc0517b* | 1.17 | Kukri | 1.4 | 3.3 |
| Minnipa (Minn) | Heading (Eet) | ***QEet.aww-1AS*** | 6.4 | 5.2-7.7 | *XwPt-7541–XwPt-6709* | -1.84 | RAC875 | 1.6 | 3.6 |
| | | ***QEet.aww-2BS*** | 37.0 | 35.0-39.0 | *XwPt-7757–Xbarc0013a* | 5.18 | Kukri | 26.5 | 28.7 |
| | | ***QEet.aww-2DS*** | 44.7 | 39.7-49.7 | *XwPt-6003–XwPt-0330* | -10.13 | RAC875 | 17.1 | 24.5 |
| | | ***QEet.aww-3D*** | 115.7 | 109.8-120.8 | *Xgwm0664–Xgwm0383b* | -1.52 | RAC875 | 3.0 | 4.1 |
| | | *QEet.aww-5A* | 91.0 | 78.0-101.0 | *Xgwm0186–XwPt-1370* | -1.91 | RAC875 | 1.0 | 2.2 |
| | | *QEet.aww-5B* | 76.9 | 71.4-97.6 | *XwPt-4936–XwPt-3457* | -1.89 | RAC875 | 1.5 | 2.8 |
| | | ***QEet.aww-7A.1*** | 63.6 | 48.6-100.2 | *XwPt_5153–Xcfa2028* | 3.47 | Kukri | 5.5 | 4.3 |
| | | *QEet.aww-7B* | 48.8 | 45.0-61.8 | *XwPt-4230–Xwmc0517b* | 1.26 | Kukri | 0.76 | 3.1 |
| | Zadoks scale | ***QZad.aww-1AS*** | 6.4 | 5.2-7.7 | *XwPt-7541–XwPt-6709* | 1.48 | Kukri | 1.7 | 4.1 |
| | | ***QZad.aww-2BS*** | 37.0 | 35.0-39.0 | *XwPt-7757–Xbarc0013a* | -7.04 | RAC875 | 28.0 | 31.0 |
| | | ***QZad.aww-2DS*** | 44.7 | 40.7-49.7 | *XwPt-6003–XwPt-0330* | 11.57 | Kukri | 14.3 | 18.9 |
| | | ***QZad.aww-3D*** | 115.7 | 111.8-120.8 | *Xgwm0664–Xgwm0383b* | 2.11 | Kukri | 3.0 | 4.0 |
| | | *QZad.aww-5A* | 88.0 | 54.4-103.0 | *Xgwm0186–XwPt-1370* | 2.17 | Kukri | 1.5 | 2.0 |
| | | *QZad.aww-5B* | 57.4 | 47.7-69.4 | *Xbarc0088–XwPt-4936* | 1.22 | Kukri | 0.5 | 1.9 |
| | | *QZad.aww-7A* | 100.2 | 90.1-110.2 | *Xcfa2028–Xbarc0174* | -0.76 | RAC875 | 0.2 | 2.7 |
| Booleroo (Bool) | Heading (Eet) | ***QEet.aww-1AS*** | 6.4 | 4.2-7.7 | *XwPt-7541–XwPt-6709* | 1.51 | Kukri | 2.0 | 3.5 |
| | | ***QEet.aww-2BS*** | 37.0 | 35.0-39.0 | *XwPt-7757–Xbarc0013a* | 4.27 | Kukri | 19.9 | 24.0 |
| | | ***QEet.aww-2DS*** | 45.7 | 41.7-50.7 | *XwPt-6003–XwPt-0330* | -9.62 | RAC875 | 17.1 | 23.3 |
| | | ***QEet.aww-3D*** | 113.7 | 109.8-117.8 | *Xgwm0664–Xgwm0383b* | -1.61 | RAC875 | 2.8 | 3.5 |
| | | *QEet.aww-5A* | 95.0 | 83.0-109.0 | *Xgwm0186–XwPt-1370* | -1.78 | RAC875 | 1.3 | 2.5 |
| | | ***QEet.aww-5B*** | 78.9 | 73.9-89.6 | *XwPt-4936–XwPt-3457* | -2.50 | RAC875 | 3.6 | 6.8 |
| | | ***QEet.aww-7A.1*** | 59.6 | 49.6-81.6 | *XwPt-5153–Xcfa2028* | 4.71 | Kukri | 6.6 | 9.0 |
| | | ***QEet.aww-7B*** | 53.8 | 44.0-62.8 | *XwPt-4230–Xwmc0517b* | 2.06 | Kukri | 3.1 | 6.0 |
| | | *QEet.aww-7D* | 108.9 | 104.2-132.9 | *Xbarc0058–Xgwm0428* | -0.48 | RAC875 | 0.1 | 2.4 |
| | Zadoks scale | *QZad.aww-1AS* | 6.4 | 4.2-7.7 | *XwPt-7541–XwPt-6709* | 1.15 | Kukri | 0.8 | 2.3 |
| | | ***QZad.aww-2BS*** | 37.0 | 35.0-39.0 | *XwPt-7757–Xbarc0013a* | -4.43 | RAC875 | 19.1 | 22.7 |
| | | ***QZad.aww-2DS*** | 43.7 | 39.7-48.7 | *XwPt-6003–XwPt-0330* | 8.68 | Kukri | 15.3 | 20.4 |
| | | *QZad.aww-3D* | 114.7 | 109.8-119.8 | *Xgwm0664–Xgwm0383b* | 1.05 | Kukri | 0.7 | 2.2 |
| | | *QZad.aww-5A* | 97.0 | 83.0-116.0 | *Xgwm0186–XwPt-1370* | 1.93 | Kukri | 2.2 | 2.2 |
| | | ***QZad.aww-5B*** | 79.9 | 72.9-91.6 | *XwPt-4936–XwPt-3457* | 1.99 | Kukri | 2.6 | 4.9 |
| | | ***QZad.aww-7A*** | 95.1 | 90.1-100.1 | *Xcfa2028–Xbarc1004* | -2.46 | RAC875 | 6.5 | 6.7 |
| | | ***QZad.aww-7B*** | 56.8 | 45.0-64.8 | *XwPt-4230–Xwmc0517b* | -2.04 | RAC875 | 4.0 | 4.8 |
| | | *QZad.aww-7D* | 108.9 | 101.2-131.9 | *Xbarc0058–Xgwm0428* | 1.26 | Kukri | 0.95 | 2.3 |

**Table 5-5. Continued**

| Site | Trait | QTL | Position (cM) | Range | Interval | Add | Parent | $h^2$ (%) | LOD |
|---|---|---|---|---|---|---|---|---|---|
| Mexico Irrigation (MexI) | Heading (Eet) | ***QEet.aww-2BS*** | 36.0 | 34.0-38.0 | *XwPt-7757–Xbarc0013a* | 5.48 | Kukri | 24.5 | 34.1 |
| | | ***QEet.aww-2DS*** | 47.7 | 43.7-52.7 | *XwPt-6003–XwPt-0330* | -9.84 | RAC875 | 15.4 | 17.6 |
| | | ***QEet.aww-3D*** | 109.1 | 103.1-109.8 | *XwPt-7894–Xbarc0042* | -1.54 | RAC875 | 3.1 | 4.7 |
| | | *QEet.aww-5A* | 92.0 | 72.0-109.0 | *Xgwm0186–XwPt-1370* | -1.86 | RAC875 | 1.6 | 2.0 |
| | | ***QEet.aww-5B*** | 81.9 | 75.9-91.6 | *XwPt-4936–XwPt-3457* | -2.17 | RAC875 | 2.8 | 4.0 |
| | | *QEet.aww-7A.2* | 126.0 | 125.4-128.0 | *Xbarc0195–XDuPw0254* | 1.12 | Kukri | 0.6 | 2.6 |
| | | ***QEet.aww-7B*** | 55.8 | 46.0-64.8 | *XwPt-4230–Xwmc0517b* | 2.46 | Kukri | 3.1 | 4.7 |
| | Anthesis | ***QAnth.aww-2BS*** | 36.0 | 34.0-38.0 | *XwPt-7757–Xbarc0013a* | 5.67 | Kukri | 25.0 | 31.2 |
| | | ***QAnth.aww-2DS*** | 44.7 | 39.7-49.7 | *XwPt-6003–XwPt-0330* | -8.67 | RAC875 | 13.9 | 17.6 |
| | | ***QAnth.aww-3D*** | 109.1 | 104.1-109.8 | *XwPt-7894–Xbarc0042* | -1.59 | RAC875 | 3.4 | 4.8 |
| | | ***QAnth.aww-5B*** | 82.9 | 50.7-96.6 | *XwPt-4936–XwPt-3457* | -1.75 | RAC875 | 2.3 | 3.0 |
| | | *QAnth.aww-7A* | 126.0 | 125.4-129.0 | *Xbarc0195–XDuPw0254* | 1.42 | Kukri | 1.1 | 2.2 |
| | | ***QAnth.aww-7B*** | 51.8 | 46.0-60.8 | *XwPt-4230–Xwmc0517b* | 2.00 | Kukri | 3.3 | 4.7 |
| | Mat | ***QMat.aww-2BS*** | 37.0 | 35.0-39.0 | *XwPt-7757–Xbarc0013a* | 3.83 | Kukri | 24.9 | 31.9 |
| | | ***QMat.aww-2DS*** | 47.7 | 42.7-52.7 | *XwPt-6003–XwPt-0330* | -7.46 | RAC875 | 15.6 | 20.3 |
| | | ***QMat.aww-3D*** | 113.7 | 109.8-117.7 | *Xgwm0664–Xgwm0383b* | -1.68 | RAC875 | 3.9 | 5.8 |
| | | ***QMat.aww-5B*** | 58.4 | 46.7-69.4 | *Xbarc0088–XwPt-4936* | -1.26 | RAC875 | 2.4 | 3.4 |
| | | ***QMat.aww-7B*** | 28.4 | 21.0-37.2 | *Xgwm0297–Xbarc0065* | 1.26 | Kukri | 2.9 | 4.3 |
| Mexico Drought (MexD) | Heading (Eet) | ***QEet.aww-2BS*** | 37.0 | 33.0-42.1 | *XwPt-7757–Xbarc0013a* | 3.41 | Kukri | 9.2 | 10.0 |
| | | ***QEet.aww-2DS*** | 49.7 | 43.7-56.7 | *XwPt-6003–XwPt-0330* | -7.52 | RAC875 | 17.2 | 14.1 |
| | | ***QEet.aww-3D*** | 78.6 | 65.9-90.1 | *Xwmc0533–XwPt-6262* | -1.74 | RAC875 | 4.4 | 4.5 |
| | | *QEet.aww-5B* | 92.6 | 71.9-106.3 | *XwPt-3457–Xgwm0271b* | -1.50 | RAC875 | 0.9 | 2.3 |
| | | ***QEet.aww-7B*** | 35.6 | 26.4-41.2 | *Xgwm0297–Xbarc0065* | 2.32 | Kukri | 5.2 | 4.6 |
| | Anth | ***QAnth.aww-2BS*** | 23.6 | 18.6-26.8 | *XwPt-1489–XwPt-9644* | 5.03 | Kukri | 9.7 | 10.5 |
| | | ***QAnth.aww-2DS*** | 47.7 | 42.7-52.7 | *XwPt-6003–XwPt-0330* | -2.97 | RAC875 | 3.4 | 4.2 |

#### *5.2.3.1.2 Phenotypic data for plant height and peduncle length*

Plant height values in five environments were normally distributed suggesting multiple genes controlling height in this population (Fig. 5-4). Peduncle length distribution was also normally distributed in Minn, Bool, MexD, but in RAC it was negatively skewed towards large numbers (Fig. 5-5). Drought, on average, reduced plant height by 20.6%, 23.8%, 53.6% and 55.0% in RAC, MexD, Minn and Bool, respectively. Drought significantly ($P < 0.01$) reduced peduncle length and, thus, reduced the length of the main stem. The peduncle length made up 32.5%, 34.2%, 35.6% and 39.2% of final plant height in MexD, Minn, Bool and RAC, respectively. Ehdaie et al. (2006a) reported 37 to 47% of peduncle length contributed to final stem length in modern dwarf and semi-dwarf wheats. Correlations between plant height and peduncle length in different environments ranged from 0.59 to 0.65 ($P < 0.001$). Average plant height and peduncle length of the DH lines are given in Table 5-3. Plant height ranged from 37.2 to 82.6 cm. Despite the fact that both parental lines (Kukri and RAC875) are semi-dwarfing genotypes and possess the *Rht-D1b* genes, RAC875 and Kukri differed in plant height under favorable environments. Under favorable conditions in MexI and RAC, Kukri was significantly taller (10 cm) than RAC875, whereas under drought stress environments in MexD and Minn no significant difference ($P > 0.05$) between the two parents in plant height was observed. In the Bool environment (severely drought affected site), however, RAC875 was significantly taller (3.4 cm; $P < 0.001$) than Kukri (Table 5-3). The average height for plants grown under well irrigated conditions (MexI) was higher (82.6 cm) than for plants grown under drought including RAC, MexD, Minn and Bool (65.5 cm, 62.9 cm, 38.3 cm and 37.2 cm, respectively; Table 5-3). The heritabilities of this trait in different environments ranged from 0.37to 0.71, (Table 5-3).

Phenotypic correlation analysis showed a significant ($p = 0.001$) association between heading time and plant height in all five environments. In the drought-affected environments, RAC, Minn, Bool and MexD, negative correlations (-0.56, -0.70, -0.52 and -0.66, respectively; Table 5-4) between heading time and plant height occurred, while in the irrigated experiment (MexI) there was a positive correlation ($r = 0.44$). The associations between plant height and grain yield in different environments were positively significant at $p = 0.001$ level (0.51, 0.70, 0.63, 0.33 and 0.80 for RAC, Minn, Bool, MexI and MexD, respectively).

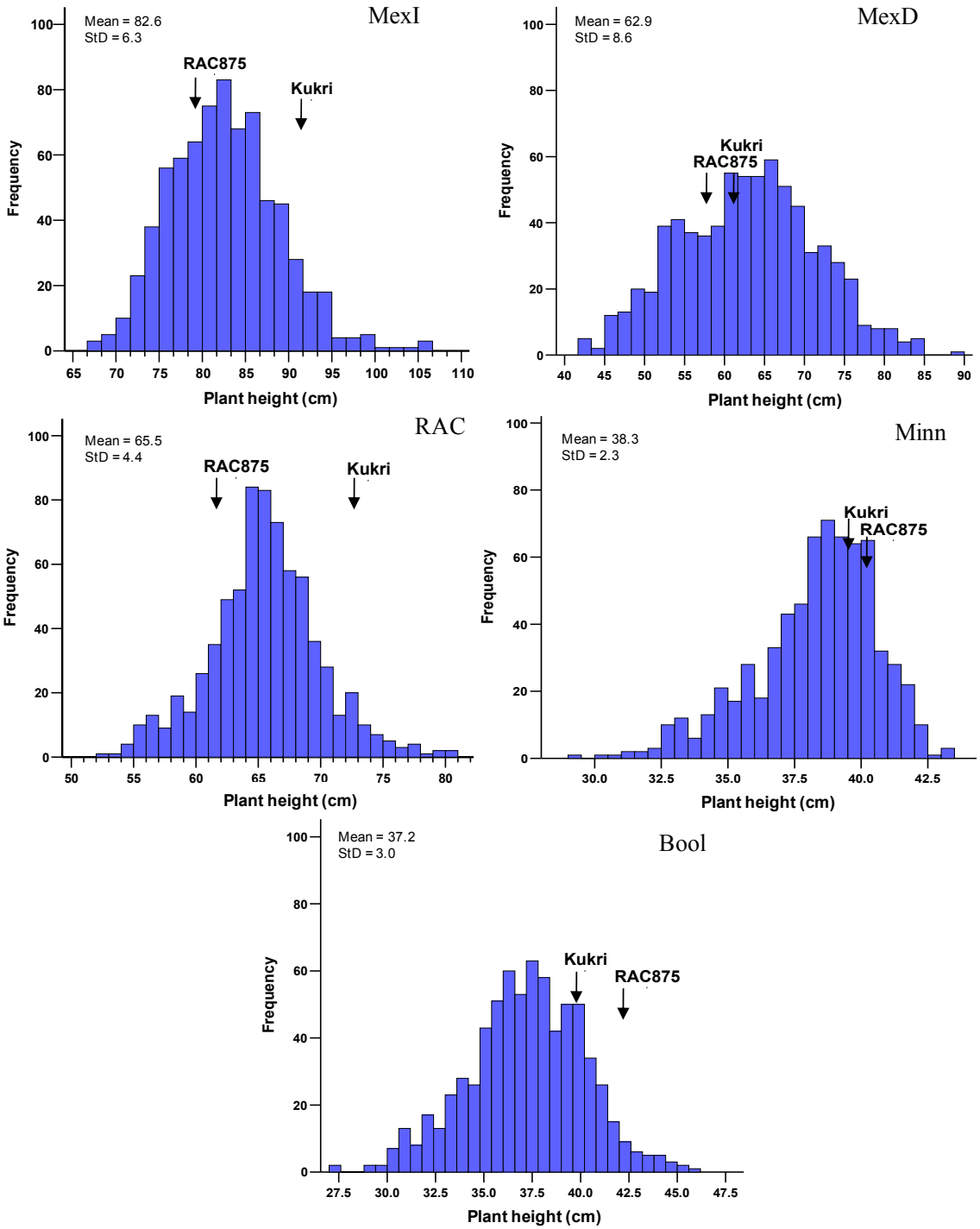


**Figure 5-4. Phenotypic frequency distribution of plant height at five sites; Mexico irrigation (MexI), Mexico drought (MexD), Roseworthy (RAC), Minnipa (Minn) and Booleroo (Bool). The population mean (Mean) and the standard error of deviation (StD) are shown in the figure. Arrows indicate the trait value for the two mapping parents.**

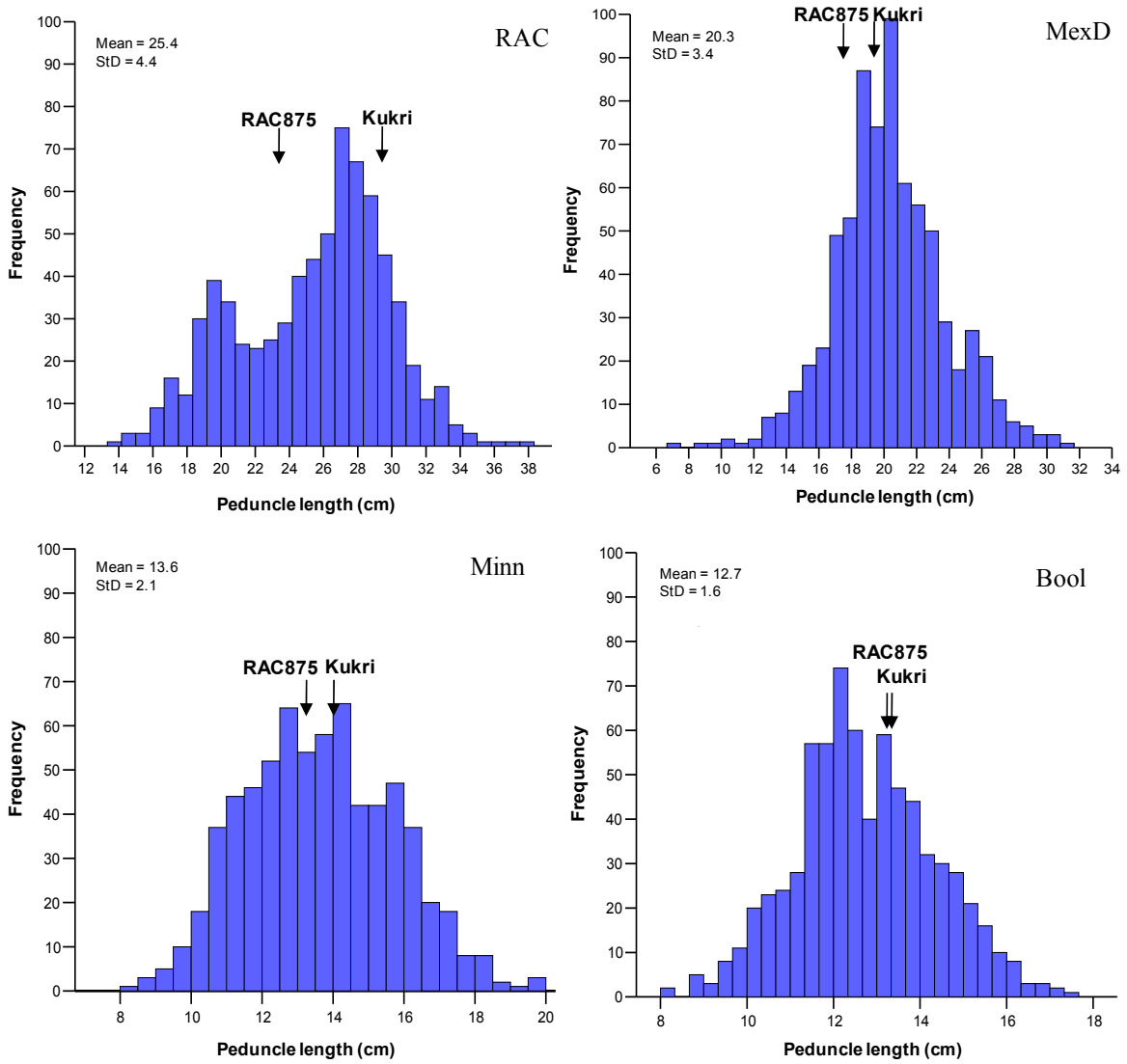


**Figure 5-5. Phenotypic frequency distribution of peduncle length in four sites; Roseworthy (RAC), Obregon, Mexico drought (MexD), Minnipa (Minn) and Booleroo (Bool). The population mean (Mean) and the standard error of deviation (StD) are shown in the figure. Arrows indicate the trait value for the two mapping parents.**

### *5.2.3.1.3 QTLs for plant height (non-adjusted data)*

Thirty three QTLs controlling plant height were identified in five environments (Table 5-6; Appendix K). Twenty three QTLs showed strong additive effects on plant height and the rest were potential QTLs with smaller effects. Plant height QTLs were, overall, located on 9 chromosomes including 1A, 2B, 2D, 3A, 3D, 4A, 5A, 5B and 7A. Plant height QTL on chromosome 1AS (***QHt.aww-1AS***$^{NA}$) was detected in four environments as a suggestive QTL at similar position with maturity traits. The strongest height QTL in all environments was ***QHt.aww-2DS.1***$^{NA}$ on chromosome 2D with LOD score of

more than 3.2 and heritability of 18.1%. In the MexI experiment, ***QHt.aww-2DS.2$^{NA}$*** QTL was located at the distal part of 2DS at the position of 0.0 cM in the *Xbarc0095–Xwmc0111* interval. However, in the other four environments, ***QHt.aww-2DS.1$^{NA}$*** peaked at *XwPt-0330* at about 50 cM. The 'RAC875' allele reduced plant height by 3.05, 1.53, 0.63, 1.43 and 6.7 cm relative to the 'Kukri' allele in RAC, Minn, Bool, MexI and MexD, respectively. The second major QTL for plant height was detected on chromosome 2B (***QHt.aww-2BS$^{NA}$***) at *XwPt-7757* with the peak LOD score of > 5.7 and explained 7.6% of the phenotypic variation for plant height (Table 5-6). The additive effect of this QTL for reduced plant height at RAC, Minn, Bool and MexD was 0.99, 0.68, 0.68 and 3.1 cm, respectively, where the 'Kukri' allele was associated with reduced plant height relative to the 'RAC875' allele. However, under irrigated conditions (MexI), , the 'RAC875' allele was associated with reduced plant height. The two plant height QTLs on chromosome 2B and 2D overlapped with heading time QTLs at every drought site. Other significant QTLs for plant height were identified on chromosome 3A, 5A, 5B and 7A (at three sites), 3D (at two sites) and 4A (at one site). These QTLs collectively accounted for 20.6% of the phenotypic variation, whereas their individual contributions to plant height varied depending on the environment being sampled. A plant height QTL on chromosome 7A (*QHt.aww-7A.1$^{NA}$*) was identified as a suggestive QTL in RAC. It peaked at *Xcfa2028* (90.1 cM) with LOD = 4.4. In MexD, ***QHt.aww-7A.1$^{NA}$*** was significantly identified with a LOD of 4.2 in the *XwPt-5153-Xcfa2028* interval, in which the 'Kukri' allele contributed to reduce plant height at this QTL. Under irrigation, however, two other QTLs for plant height on chromosome 7A (***QHt.aww-7A.2$^{NA}$*** and ***QHt.aww-7A.3$^{NA}$***) were found. ***QHt.aww-7A.2$^{NA}$*** was located at 113.3 cM in *Xbarc0259-Xbarc0281* interval with a LOD of 5.2 and $h^2$ of 6.8%. For this QTL, the 'RAC875' allele reduced plant height by 1.7 cm relative to the 'Kukri' allele. ***QHt.aww-7A.3$^{NA}$*** peaked at 224.5 cM in the *XwPt-7763–XwPt-6495* interval, with a LOD of 4.3 and heritability of 3.7%. The 'Kukri' allele contributed to reduce plant height by 1.2 cm. Most of the QTLs for plant height were coincident with heading time QTLs except the QTL on chromosome 3A (***QHt.aww-3A$^{NA}$***), which was detected in three datasets (RAC, Minn and MexI). This QTL was located at *Xgwm0002* (56.9 cM) with LOD of 8.0, 2.1 and 8.0, and it explained 9.1%, 1.1% and 7.7% of phenotypic variations in the RAC, Minn and MexI datasets, respectively (Table 5-6; Appendix K). None of the detected plant height QTLs mapped on chromosome 4B and 4D, the expected locations for *Rht-B1b* and *Rht-D1b* semi-dwarfing genes, respectively (Börner

et al., 1997; Ellis et al., 2002). This suggests that this population did not segregate for the major plant height genes *Rht-B1b* and *Rht-D1b.*

#### *5.2.3.1.4 QTLs for peduncle length (non-adjusted data)*

In total, twenty three QTLs for peduncle length were identified in four drought environments (RAC, Minn, Bool and MexD; Table 5-7). The heritability of individual QTLs ranged from 0.7 to 19.8%. These QTLs were detected on nine chromosomes (1A, 2B, 2D, 3A, 3D, 5A, 5B, 6D, 7A and 7B), of which ***QPdl.aww-2BS$^{NA}$***, ***QPdl.aww-2DS$^{NA}$*** and ***QPdl.aww-7A$^{NA}$***were detected in four environments as putative QTLs with main additive effect. ***QPdl.aww-5A$^{NA}$*** and ***QPdl.aww-5B$^{NA}$*** were detected in three environments. ***QPdl.aww-1AS$^{NA}$*** was identified as only a suggestive QTL with a LOD of 2.7 and 2.3 in RAC and Minn, respectively. ***QPdl.aww-3A$^{NA}$***, ***QPdl.aww-3D$^{NA}$*** and ***QPdl.aww-7B$^{NA}$*** were detected in only one environment (RAC, Minn and MexD, respectively). Two QTLs on chromosome 2B and 2D (***QPdl.aww-2BS$^{NA}$*** and ***QPdl.aww-2DS$^{NA}$***), in particular, were significant across four environments, with LOD of more than 3.9 and 6.6, respectively. These two QTLs overlapped with heading time and plant height QTLs, indicating that flowering time largely affected peduncle length. ***QPdl.aww-2BS$^{NA}$*** explained on average 8.1% of the phenotypic variation, while ***QPdl.aww-2DS$^{NA}$*** explained on average 14.1% of the phenotypic variation in peduncle length (Table 5-8; Fig. 5-18). The 'Kukri' allele was associated with reduced peduncle length at ***QPdl.aww-2BS$^{NA}$*** QTL, whereas at ***QPdl.aww-2DS$^{NA}$*** QTL the 'RAC875' allele was associated with reduced peduncle length. Other peduncle length QTLs on chromosome 1A, 3D, 5A, 5B, 7A and 7B were also associated with variation in peduncle length, but their contributions to the phenotypic variation were small (1.4 to 4.3%). These QTLs also coincided with heading time QTLs. ***QPdl.aww-3A$^{NA}$*** was detected just in RAC on chromosome 3A at *Xgwm0002* (56.9 cM) with a LOD of 7.4 and $h^2$ of 2.4%, coinciding with the plant height QTL.

**Table 5-6. Detected QTLs with composite interval mapping (CIM) analysis are shown for plant height (Ht) in the RAC875/Kukri population from five different environments. QTL analysis was performed without taking heading time effects into account (non-adjusted data = NA). The most likely QTL position, range, interval of flanking markers, allelic additive effect, heritability and LOD for each individual QTL is presented. The italic bold loci represent putative QTLs which were detected at a 5% significance threshold. Suggestive QTLs were detected at a 10% significance threshold. QTLs with largest trait effect are highlighted in light gray.**

| Site | QTL | Position (cM) | Range | Interval | Add | Parent | $h^2$ (%) | LOD |
|---|---|---|---|---|---|---|---|---|
| RAC | *QHt.aww-1AS$^{NA}$* | 6.7 | 2.0-7.7 | *XwPt-6709–Xgdm0033a* | 0.59 | Kukri | 1.5 | 2.2 |
| | ***QHt.aww-2BS$^{NA}$*** | 33.3 | 30.5-37.0 | *XwPt-5556–XwPt-7757* | -0.99 | RAC875 | 6.1 | 5.5 |
| | ***QHt.aww-2DS.1$^{NA}$*** | 53.7 | 46.7-60.7 | *XwPt-6003–XwPt-0330* | 3.05 | Kukri | 10.3 | 13.1 |
| | ***QHt.aww-3A$^{NA}$*** | 52.1 | 42.1-58.9 | *XwPt-0714–Xgwm0002* | -1.22 | RAC875 | 9.1 | 8.0 |
| | ***QHt.aww-4A$^{NA}$*** | 19.2 | 3.0-24.2 | *Xbarc0106–XDuPw0328* | 0.97 | Kukri | 3.8 | 4.2 |
| | ***QHt.aww-5A$^{NA}$*** | 172.7 | 160.7-180.7 | *Xcfa2141–XwPt-5231* | 1.15 | Kukri | 3.9 | 3.9 |
| | *QHt.aww-7A.1$^{NA}$* | 76.6 | 54.6-98.1 | *XwPt-5153–Xcfa2028* | -0.64 | RAC875 | 1.8 | 2.2 |
| Minn | *QHt.aww-1AS$^{NA}$* | 6.4 | 5.7-7.7 | *XwPt-7541–XwPt-6709* | 0.28 | Kukri | 1.0 | 3.2 |
| | ***QHt.aww-2BS$^{NA}$*** | 25.8 | 21.6-27.8 | *XwPt-9644–XwPt-5672* | -0.68 | RAC875 | 9.7 | 8.0 |
| | ***QHt.aww-2DS.1$^{NA}$*** | 47.7 | 40.7-54.7 | *XwPt-6003–XwPt-0330* | 1.53 | Kukri | 7.0 | 6.0 |
| | *QHt.aww-3A$^{NA}$* | 35.1 | 20.3-45.1 | *XwPt-0714–Xgwm0002* | -0.29 | RAC875 | 1.1 | 2.1 |
| | ***QHt.aww-3D$^{NA}$*** | 109.8 | 106.1-113.7 | *Xbarc0042–Xgwm0664* | 0.58 | Kukri | 4.5 | 4.1 |
| | *QHt.aww-5A$^{NA}$* | 172.7 | 160.7-190.5 | *Xcfa2141–XwPt-5231* | 0.35 | Kukri | 1.5 | 2.4 |
| | *QHt.aww-5B$^{NA}$* | 49.7 | 43.7-54.3 | *XwPt-5914–Xbarc0216* | 0.54 | Kukri | 2.6 | 2.8 |
| Bool | ***QHt.aww-2BS$^{NA}$*** | 37.0 | 33.0-44.1 | *XwPt-7757–Xbarc0013a* | -0.68 | RAC875 | 4.6 | 5.7 |
| | ***QHt.aww-2DS.1$^{NA}$*** | 94.2 | 84.2-107.1 | *XwPt-0330–Xbarc0328b* | 0.63 | Kukri | 3.9 | 3.2 |
| | ***QHt.aww-5A$^{NA}$*** | 186.5 | 167.7-200.1 | *XwPt-5231–Xgwm0126* | 0.67 | Kukri | 4.5 | 2.9 |
| MexI | *QHt.aww-1AS$^{NA}$* | 4.2 | 1.0-5.7 | *XwPt-2527–XwPt-6564* | 0.80 | Kukri | 1.6 | 2.6 |
| | ***QHt.aww-2BS$^{NA}$*** | 39.1 | 36.0-44.1 | *Xbarc0013a–Xgwm0271a* | 1.52 | Kukri | 5.7 | 6.3 |
| | ***QHt.aww-2DS.2$^{NA}$*** | 0.0 | 0.0-1.5 | *Xbarc0095–Xwmc0111* | 1.43 | Kukri | 6.2 | 7.3 |
| | ***QHt.aww-3A$^{NA}$*** | 56.9 | 50.1-58.9 | *Xgwm0002–Xbarc0328a* | -1.50 | RAC875 | 7.7 | 8.0 |
| | ***QHt.aww-5B$^{NA}$*** | 63.4 | 55.8-70.4 | *Xbarc0088–XwPt-4936* | -1.30 | RAC875 | 4.3 | 5.4 |
| | ***QHt.aww-7A.2$^{NA}$*** | 113.3 | 103.2-115.3 | *Xbarc0174–Xbarc0259* | 1.67 | Kukri | 6.8 | 5.2 |
| | ***QHt.aww-7A.3$^{NA}$*** | 224.5 | 217.1-225.2 | *XwPt-7763–XwPt-6495* | -1.23 | RAC875 | 3.7 | 4.3 |
| | ***QHt.aww-7B$^{NA}$*** | 44.0 | 37.2-65.8 | *Xwmc0396–XwPt-4230* | 0.93 | Kukri | 2.4 | 3.0 |
| MexD | *QHt.aww-1AS$^{NA}$* | 6.7 | 4.2-7.7 | *XwPt-6709–Xgdm0033a* | 0.94 | Kukri | 0.8 | 2.7 |
| | ***QHt.aww-2BS$^{NA}$*** | 37.0 | 34.0-43.1 | *XwPt-7757–Xbarc0013a* | -3.06 | RAC875 | 11.8 | 11.1 |
| | ***QHt.aww-2DS.1$^{NA}$*** | 51.7 | 46.7-57.7 | *XwPt-6003–XwPt-0330* | 6.66 | Kukri | 18.3 | 22.6 |
| | *QHt.aww-3D$^{NA}$* | 75.6 | 62.9-85.6 | *Xwmc0533–XwPt-6262* | 1.11 | Kukri | 1.1 | 2.0 |
| | ***QHt.aww-5B.1$^{NA}$*** | 9.0 | 0.0-22.0 | *Xgwm0234b–XwPt-8604* | 1.22 | Kukri | 3.1 | 3.4 |
| | ***QHt.aww-5B.2$^{NA}$*** | 92.6 | 80.9-101.3 | *XwPt-3457–Xgwm0271b* | 1.50 | Kukri | 2.1 | 3.1 |
| | ***QHt.aww-7A.1$^{NA}$*** | 68.6 | 55.6-96.1 | *XwPt-5153–Xcfa2028* | -2.27 | RAC875 | 5.3 | 4.2 |
| | *QHt.aww-7B$^{NA}$* | 35.6 | 26.0-39.2 | *Xgwm0297–Xbarc0065* | -0.89 | RAC875 | 0.7 | 2.5 |

**Table 5-7. Detected QTLs with composite interval mapping (CIM) analysis are shown for peduncle length (Pdl) in the RAC875/Kukri population from four environments. QTL analysis was performed without taking heading time effects into account (non-adjusted data = NA). The most likely QTL position, range, interval of flanking markers, allelic additive effect, heritability and LOD for each individual QTL is presented. The italic bold loci represent putative QTLs which were detected at a 5% significance threshold. Suggestive QTLs were detected at a 10% significance threshold. QTLs with largest trait effect are highlighted in light gray.**

| Site | QTL | Position (cM) | Range | Interval | Add | Parent | $h^2$ (%) | LOD |
|---|---|---|---|---|---|---|---|---|
| RAC | *QPdl.aww-1AS$^{NA}$* | 6.4 | 5.4-7.7 | *XwPt-7541–XwPt-6709* | 0.65 | Kukri | 2.0 | 2.7 |
| | ***QPdl.aww-2BS$^{NA}$*** | 37.0 | 35.0-39.0 | *XwPt-7757–Xbarc0013a* | -2.02 | RAC875 | 19. 8 | 30.8 |
| | ***QPdl.aww-2DS$^{NA}$*** | 90.2 | 87.2-94.2 | *XwPt-0330–Xbarc0328b* | 1.82 | Kukri | 16.1 | 22.9 |
| | ***QPdl.aww-3A$^{NA}$*** | 58.9 | 50.1-61.9 | *Xgwm0002–Xbarc0328a* | 0.70 | Kukri | 2.4 | 3.4 |
| | ***QPdl.aww-5A$^{NA}$*** | 168.7 | 157.7-179.7 | *Xcfa2141–XwPt-5231* | 0.89 | Kukri | 3.8 | 2.9 |
| | ***QPdl.aww-5B$^{NA}$*** | 89.6 | 71.4-97.6 | *XwPt-3457–Xgwm0271b* | 0.97 | Kukri | 4.6 | 5.1 |
| | *QPdl.aww-7A$^{NA}$* | 62.6 | 47.6-93.1 | *XwPt-5153–Xcfa2028* | -0.86 | RAC875 | 3.6 | 2.2 |
| Minn | *QPdl.aww-1AS$^{NA}$* | 12.0 | 9.1-17.0 | *XwPt-3870–XwPt-6122* | 0.22 | Kukri | 0.7 | 2.3 |
| | ***QPdl.aww-2BS$^{NA}$*** | 37.0 | 34.0-39.0 | *XwPt-7757–Xbarc0013a* | -0.81 | RAC875 | 17.1 | 17.9 |
| | ***QPdl.aww-2DS$^{NA}$*** | 49.7 | 44.7-55.7 | *XwPt-6003–XwPt-0330* | 1.77 | Kukri | 16.3 | 18.3 |
| | ***QPdl.aww-3D$^{NA}$*** | 114.7 | 109.1-120.8 | *Xgwm0664–Xgwm0383b* | 0.32 | Kukri | 2.6 | 3.0 |
| | ***QPdl.aww-5A$^{NA}$*** | 163.7 | 148.7-174.7 | *Xcfa2141–XwPt-5231* | 0.45 | Kukri | 3.1 | 3.5 |
| | ***QPdl.aww-5B$^{NA}$*** | 92.6 | 83.6-101.3 | *XwPt-3457–Xgwm0271b* | 0.53 | Kukri | 2.9 | 3.4 |
| | ***QPdl.aww-7A$^{NA}$*** | 90.1 | 61.6-94.1 | *Xcfa2028–Xbarc1004* | -0.31 | RAC875 | 2.9 | 2.8 |
| Bool | *QPdl.aww-2BS$^{NA}$* | 37.0 | 32.3-46.1 | *XwPt-7757–Xbarc0013a* | -0.23 | RAC875 | 1.2 | 2.8 |
| | ***QPdl.aww-2DS$^{NA}$*** | 45.7 | 40.7-51.7 | *XwPt-6003–XwPt-0330* | 1.33 | Kukri | 15.4 | 14.1 |
| | ***QPdl.aww-5A$^{NA}$*** | 168.7 | 155.7-183.7 | *Xcfa2141–XwPt-5231* | 0.39 | Kukri | 4.2 | 2.8 |
| | ***QPdl.aww-7A$^{NA}$*** | 65.6 | 51.6-93.1 | *XwPt-5153–Xcfa2028* | -0.54 | RAC875 | 4.4 | 3.5 |
| MexD | ***QPdl.aww-2BS$^{NA}$*** | 37.0 | 31.5-45.1 | *XwPt-7757–Xbarc0013a* | -0.60 | RAC875 | 4.3 | 3.9 |
| | ***QPdl.aww-2DS$^{NA}$*** | 48.7 | 40.7-56.7 | *XwPt-6003–XwPt-0330* | 2.02 | Kukri | 8.2 | 6.6 |
| | *QPdl.aww-5B$^{NA}$* | 101.3 | 91.6-110.3 | *Xgwm0271b–Xwmc0215b* | 0.48 | Kukri | 1.5 | 2.0 |
| | ***QPdl.aww-7A$^{NA}$*** | 93.1 | 66.6-99.1 | *Xcfa2028–Xbarc1004* | -0.68 | RAC875 | 4.3 | 3.9 |
| | ***QPdl.aww-7B$^{NA}$*** | 14.0 | 6.6-21.0 | *Xbarc0338–Xstm0671acag* | -0.79 | RAC875 | 4.9 | 5.5 |

#### *5.2.3.1.5 Grain yield data*

Grain yield can be dissected into a number of component traits. Important yield components in cereals are the number of spikes per unit area, the number of spikelets per spike and spikelet weights (Fageria et al., 2006). These component traits are also under genetic control (Kato et al., 2000). Therefore, in addition to identifying QTLs for grain yield, QTLs for yield components were also determined in order to dissect grain yield genetically.

Drought strongly affected grain yield in the four droughted environments. The population mean for grain yield under flood-irrigation (MexI) was 5.6 $t \cdot ha^{-1}$, and only 0.3 $t \cdot ha^{-1}$ in the most severely affected drought experiment (Bool). The drought stress intensities were 58.6%, 92.2%, 93.8% and 66.4% for RAC, Minn, Bool and MexD, respectively relative to the grain yield in MexI. Figure 5-6 shows the phenotypic frequency distribution for grain yield in the five different environments. Transgression segregation for grain yield in the population was very high in both directions, indicating that multiple genes or QTLs controlling this trait. In the drought-affected environments, grain yield distributions were negatively skewed as a result of the heading time effect. Late flowering genotypes produced fewer or no grains in Minn, Bool and MexD environments (Table 5-3; Fig. 5-6). The heritability of grain yield, depending on the environment, ranged from 0.22 to 0.76 (Table 5-3). Overall, RAC875 was the better parent under droughted environments (Fig. 5-6) and yielded significantly ($P < 0.05$) higher than Kukri in all environments. The highest correlations were found between yield and $G \cdot m^{-2}$, fertile spikelets, grain number per spike, and between yield and grain weight per sample of spike, indicating that an increase in the number of grain per spike and grain weight are important components of yield. There were also significant correlations between yield and TGW, peduncle length, spike length and flag leaf length (Table 5-4). The number of grains per square meter ($G \cdot m^{-2}$), grain weight per sampled spikes (Gwe), number of grains from sampled spikes (Gnu) and spike fertility were the most prominent yield components in this population.

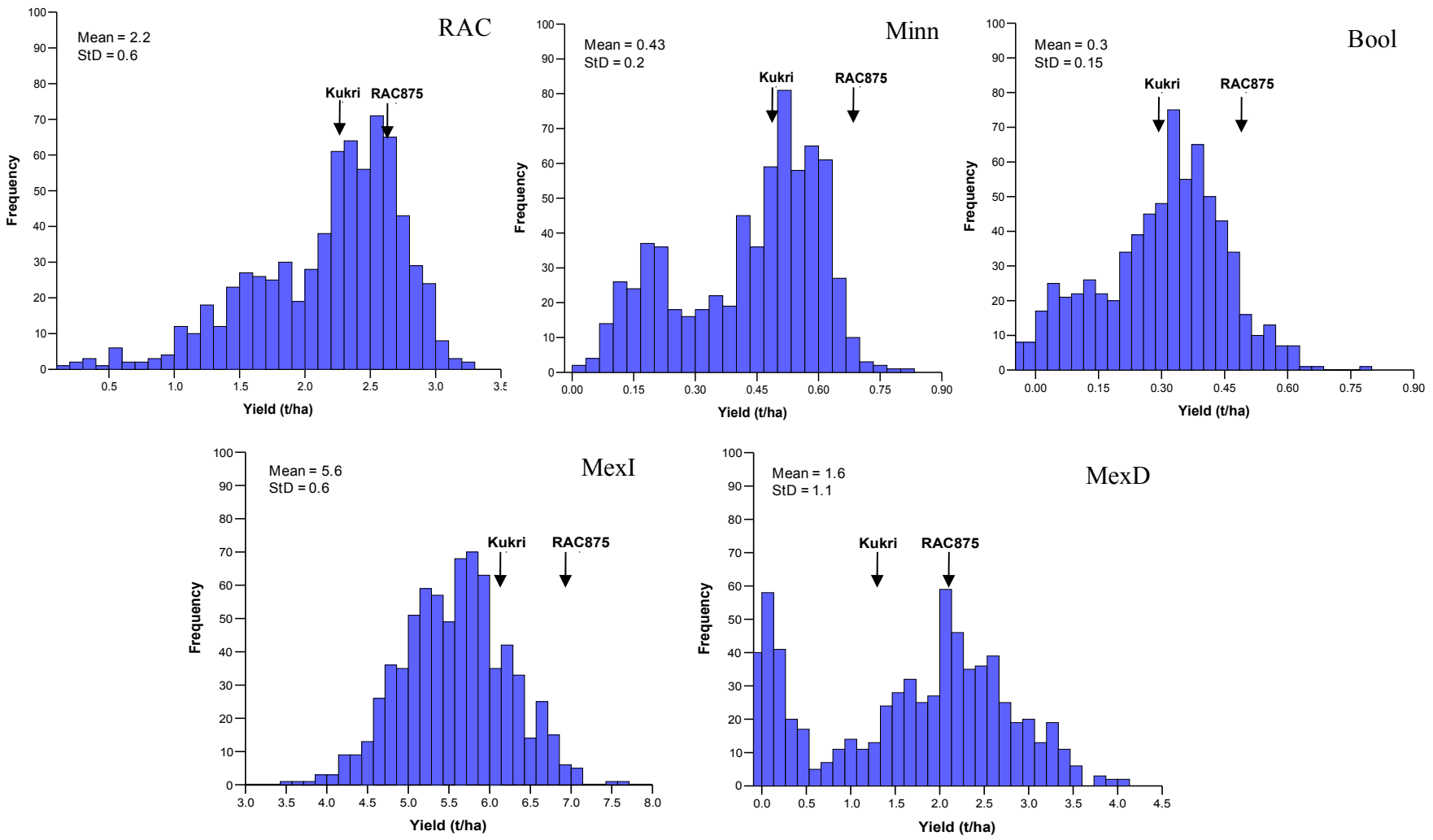


**Figure 5-6. Phenotypic frequency distribution of grain yield in the RAC875/Kukri DH population across five environments (RAC, Minn and Bool, MexI and MexD). The population mean (Mean) and the standard error of deviation (StD) are shown in the figure. Arrows indicate the trait value for the two mapping parents.**

#### *5.2.3.1.6 QTLs for grain yield (non-adjusted data)*

In total, thirty QTLs with main additive effects were associated with grain yield (YLD) on nine chromosomes and in five environments (Table 5-8; Appendix K). Twenty one QTLs were detected in more than one environment. Yield QTLs on chromosomes 1A, 2B, 2D, 3B, 3D, 5B and 7A were detected as putative QTLs. Two suggestive QTLs were also detected on chromosomes 5A (one environment, Bool) and 7B in four environments (RAC, Minn, Bool and MexD). The phenotypic variation explained by individual QTLs ranged from 0.7 to 24.0%. 'Kukri' alleles were associated with yield increases at five loci on chromosome 1A, 2D, 3D, 5A and 5B, while 'RAC875' alleles contributed to yield increases at three loci on chromosome 2B, 7A and 7B. Almost all grain yield QTLs identified under drought stress, were associated with QTLs for early heading and increased grain yield.

The yield QTL (***QYld.aww-1A***$^{NA}$) was only detected in RAC with a LOD of 6.4 peaking at the *XwPt-7541–XwPt-6709* interval in a similar position with heading time, plant height and peduncle length QTLs. The most significant yield QTL was ***QYld.aww-2BS.1***$^{NA}$ which was detected in all five environments with a LOD of >14.9 in the drought environments and 4.9 under irrigation (MexI). ***QYld.aww-2BS.1***$^{NA}$ explained on average 19.0% and 4.3% of phenotypic variations in drought-affected environments and in MexI, respectively (Table 5-8; Fig 5-7). This QTL was also coincident with heading time QTLs (***QEet.aww-2BS***) in stress environments but not in MexI. In MexI, ***QYld.aww-2BS.2***$^{NA}$ was located at *XwPt-0335* (54.2 cM) in the *XwPt-0335–XwPt-0950* interval, whereas ***QEet.aww-2BS*** was located at *XwPt-7757* (33.0 cM) the more distal *XwPt-7757–Xbarc0013a* interval. Therefore, ***QYld.aww-2B.2***$^{NA}$ in MexI may be a yield QTL unaffected by heading time. ***QYld.aww-2D***$^{NA}$ was detected in four drought environments in a very similar position as ***QEet.aww-2DS***, with LOD more than 8.1. On average, it explained 12.4% of the phenotypic variation.

Other prominent QTLs on chromosome 3D (***QYld.aww-3D***$^{NA}$), 5B (***QYld.aww-5B***$^{NA}$) and 7A (***QYld.aww-7A.1***$^{NA}$ and ***QYld.aww-7A.2***$^{NA}$) with a LOD > 3 accounted collectively for about 9.4% of the observed variation in grain yield in the drought-affected environments. ***QYld.aww-3D***$^{NA}$ and ***QYld.aww-5B***$^{NA}$ individually accounted for 2.0% of the observed phenotypic variation and overlapped with heading time QTLs,

whereas ***QYld.aww-7A.2***$^{NA}$ explained, on average, 5.5% of the observed variation for grain yield. It peaked at *Xgwm0275* (130.9 cM) between *Xbarc0195* and *Xbarc0292* in RAC, Minn and MexD datasets (Fig. 5-21). However, in Bool, ***QYld.aww-7A.1***$^{NA}$ peaked at *Xbarc0259* (110.0 cM) between *Xbarc0174* and *Xbarc0259*. ***QYld.aww-7A.2***$^{NA}$ did not overlap with the heading time QTL on chromosome 7A, since ***QEet.aww-7A*** and other maturity QTLs were located around the more distal marker locus *Xcfa2028-7A* (90.1 cM). It seems that these two QTLs for heading time and grain yield were located near the centromere on chromosome 7A in adjacent intervals. The ***QEet.aww-7A*** peaked toward the short arm, while ***QYld.aww-7A.2***$^{NA}$ from the three drought-affected environments peaked toward the long arm. However, ***QYld.aww-7A.1***$^{NA}$ in Bool peaked between ***QEet.aww-7A*** and ***QYld.aww-7A.2***$^{NA}$. For both yield QTLs (***QYld.aww-7A.1***$^{NA}$ and ***Yld.aww-7A.2***$^{NA}$) the 'RAC875' allele was associated with increases in grain yield under drought conditions. It is very likely that these loci to be specifically associated with higher grain yield under drought stress since it was not detectable under irrigation in MexI.

In MexI, two yield QTLs (***QYld.aww-3B.1***$^{NA}$ and ***QYld.aww-3B.2***$^{NA}$; Table 5-8 and Fig. 5-7) were detected on chromosome 3B, in which both parental alleles contributed to yield increase. In ***QYldaww.3B.1***$^{NA}$, the 'Kukri' allele was associated with yield increase by 0.17 t·ha$^{-1}$, while the 'RAC875' allele was associated with yield increase in ***QYld.aww-3B.2***$^{NA}$ locus by 0.2 t.ha$^{-1}$. These two QTLs were only detected under well-irrigated conditions (MexI), and did not overlap with heading time and plant height QTLs. Therefore, they could be considered as yield potential *per se* QTLs in this population.

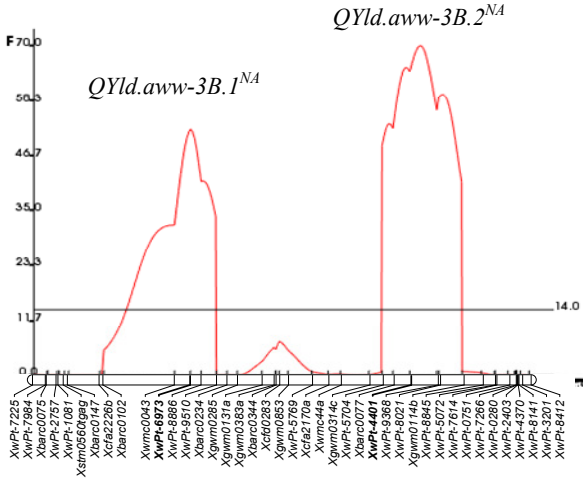


**Figure 5-7. Detected QTLs with CIM analysis are shown for grain yield, QYld.aww-3B.1NA and QYld.aww-3B.2NA, on chromosome 3B in the flood-irrigated experiment, Mexico 2007.**

**Table 5-8. Detected QTLs with composite interval mapping (CIM) analysis are shown for grain yield (YLD) in the RAC875/Kukri population in five environments. QTL analysis was performed without taking heading time effects into account (non-adjusted data = NA). The most likely QTL position, range, interval of flanking markers, allelic additive effect, heritability and LOD for each individual QTL is presented. The italic bold loci represent putative QTLs which were detected at a 5% significance threshold. Suggestive QTLs were detected at a 10% significance threshold. QTLs with largest trait effect are highlighted in light gray.**

| Site | QTL | Position (cM) | Range | Interval | Add | Parent | h2 (%) | LOD |
|---|---|---|---|---|---|---|---|---|
| RAC | ***QYld.aww-1AS$^{NA}$*** | 6.4 | 5.4-7.7 | *XwPt-7541–XwPt-6709* | 0.08 | Kukri | 2.2 | 3.9 |
| | ***QYld.aww-2BS.1$^{NA}$*** | 37.0 | 34.0-44.1 | *Xbarc0013a–Xgwm0271a* | -0.26 | RAC875 | 23.1 | 22.8 |
| | ***QYld.aww-2DS$^{NA}$*** | 42.7 | 37.7-47.7 | *XwPt-6003–XwPt-0330* | 0.43 | Kukri | 10.4 | 14.7 |
| | ***QYld.aww-3D$^{NA}$*** | 114.7 | 110.8-117.9 | *Xgwm0664–Xgwm0383b* | 0.12 | Kukri | 4.2 | 5.3 |
| | ***QYld.aww-5B$^{NA}$*** | 57.4 | 53.3-66.4 | *Xbarc0088–XwPt-4936* | 0.11 | Kukri | 2.9 | 5.0 |
| | ***QYld.aww-7A.2$^{NA}$*** | 132.8 | 126.3-135.8 | *Xgwm0276–Xbarc0292* | -0.22 | RAC875 | 5.3 | 6.8 |
| | *QYld.aww-7B$^{NA}$* | 48.8 | 44.0-64.8 | *XwPt-4230–Xwmc0517b* | -0.06 | RAC875 | 0.7 | 3.0 |
| Minn | ***QYld.aww-2BS.1$^{NA}$*** | 37.0 | 35.0-39.0 | *XwPt-7757–Xbarc0013a* | -0.09 | RAC875 | 24.0 | 25.9 |
| | ***QYld.aww-2DS$^{NA}$*** | 44.7 | 38.7-49.7 | *XwPt-6003–XwPt-0330* | 0.14 | Kukri | 11.1 | 14.8 |
| | ***QYld.aww-3D$^{NA}$*** | 113.7 | 109.8-119.8 | *Xgwm0664–Xgwm0383b* | 0.03 | Kukri | 2.6 | 3.3 |
| | *QYld.aww-5B$^{NA}$* | 60.4 | 47.7-69.4 | *Xbarc0088–XwPt-4936* | 0.02 | Kukri | 0.8 | 2.4 |
| | ***QYld.aww-7A.2$^{NA}$*** | 131.4 | 125.3-135.8 | *XDuPw0254–Xgwm0276* | -0.04 | RAC875 | 4.7 | 6.1 |
| | *QYld.aww-7B$^{NA}$* | 27.4 | 21.0-37.2 | *Xstm0671acag–Xgwm0297* | -0.02 | RAC875 | 0.6 | 3.0 |
| Bool | ***QYld.aww-2BS.1$^{NA}$*** | 38.0 | 35.0-43.1 | *XwPt-7757–Xbarc0013a* | -0.05 | RAC875 | 6.7 | 14.9 |
| | ***QYld.aww-2DS$^{NA}$*** | 37.7 | 27.7-45.7 | *XwPt-6003–XwPt-0330* | 0.08 | Kukri | 15.0 | 8.1 |
| | *QYld.aww-3D$^{NA}$* | 113.7 | 104.1-116.7 | *Xgwm0664–Xgwm0383b* | 0.03 | Kukri | 2.7 | 2.4 |
| | *QYld.aww-5A$^{NA}$* | 78.0 | 54.4-92.0 | *Xgwm0186–XwPt-1370* | 0.03 | Kukri | 2.1 | 2.5 |
| | ***QYld.aww-5B$^{NA}$*** | 81.9 | 72.9-93.6 | *XwPt-4936–XwPt-3457* | 0.02 | Kukri | 2.2 | 3.8 |
| | ***QYld.aww-7A.1$^{NA}$*** | 111.0 | 105.2-122.8 | *Xbarc0174–Xbarc0259* | -0.04 | RAC875 | 7.0 | 6.2 |
| | *QYld.aww-7B$^{NA}$* | 55.8 | 43.0-68.8 | *XwPt-4230–Xwmc0517b* | -0.03 | RAC875 | 2.8 | 2.7 |
| MexI | ***QYld.aww-2BS.2$^{NA}$*** | 54.2 | 48.1-61.2 | *XwPt-0335–XwPt-0950* | -0.11 | RAC875 | 4.3 | 4.9 |
| | ***QYld.aww-3B.1$^{NA}$*** | 75.8 | 72.1-79.8 | *XwPt-6973–XwPt-8886* | 0.17 | Kukri | 6.9 | 11.2 |
| | ***QYld.aww-3B.2$^{NA}$*** | 187.0 | 182.0-192.0 | *XwPt-4401–XwPt-9368* | -0.20 | RAC875 | 10.7 | 15.5 |
| MexD | ***QYld.aww-2BS.1$^{NA}$*** | 37.0 | 34.0-39.0 | *XwPt-7757–Xbarc0013a* | -0.45 | RAC875 | 22.1 | 25.4 |
| | ***QYld.aww-2DS$^{NA}$*** | 44.7 | 38.7-50.7 | *XwPt-6003–XwPt-0330* | 0.86 | Kukri | 12.9 | 17.4 |
| | ***QYld.aww-3D$^{NA}$*** | 111.8 | 103.1-119.8 | *Xbarc0042–Xgwm0664* | 0.13 | Kukri | 3.0 | 3.8 |
| | ***QYld.aww-5B$^{NA}$*** | 56.4 | 55.8-63.4 | *Xbarc0088–XwPt-4936* | 0.19 | Kukri | 2.4 | 3.5 |
| | ***QYld.aww-7A.2$^{NA}$*** | 126.3 | 125.3-135.8 | *Xbarc0195–XDuPw0254* | -0.22 | RAC875 | 3.8 | 4.0 |
| | *QYld.aww-7B$^{NA}$* | 17.0 | 3.6-30.4 | *Xbarc0338–Xstm0671acag* | -0.12 | RAC875 | 0.9 | 3.0 |

#### *5.2.3.1.7 QTLs for number of grains per square meter (non-adjusted data)*

Grain number per square meter (Kpsm) was the most important yield component and it was highly correlated with YLD under both drought and well-irrigated environments (r = 0.94, 0.94, 0.91 and 0.53, $P < 0.001$; in RAC, Minn, Bool and MexI, respectively). The Kukri parent showed higher value of $G \cdot m^{-2}$ compared to RAC875 at MexI and RAC sites, while in Minn and Bool, the RAC875 parent exceeded Kukri for this trait (Table 5-3). QTL analysis showed twenty-three QTLs on eight chromosomes (1A, 2B, 2D, 3B, 3D, 5B, 7A and 7B) in four environments (Table 5-10; Appendix L). ***QKpsm.aww-1AL***$^{NA}$ was putatively detected in Minn and Bool sites with LOD > 3.6 that was located on the long arm of the chromosome 1A at *XwPt-8644* (181.2 cM) in the *XwPt-8644–XwPt-0864* interval, and it was also declared as a suggestive QTL (LOD = 2.9) for the RAC site. The 'Kukri' allele in this QTL was associated with higher number of grain per unit area relative to the 'RAC875' allele.

Other QTLs for $G \cdot m^{-2}$ on chromosome 2BS, 2DS, 3D, 5B and 7B (LOD > 3.3) were coincident with heading time QTLs. Alleles that were associated with decreases in time to heading contributed to increases in $G \cdot m^{-2}$, consequently increased grain yield. In MexI, two QTLs for $G \cdot m^{-2}$ were identified on chromosome 3B (***QKpsm.aww-3B.1***$^{NA}$ and ***QKpsm.aww-3B.2***$^{NA}$) with LOD > 5.1 overlapping with yield QTLs. Other prominent QTL for $G \cdot m^{-2}$ were detected on chromosome 7A in the three drought-affected environments in South Australia (RAC, Minn and Bool). ***QKpsm.aww-7A***$^{NA}$ peaked at *XDuPw0259* (127.5 cM) and explained about 4.0% of the observed phenotypic variation. This QTL also collocated with yield QTL which were evidently different from heading time QTLs (***QEet.aww-7A***). The 'RAC875' allele was associated with increases in $G \cdot m^{-2}$ in this locus relative to the 'Kukri' allele.

**Table 5-9. Detected QTLs with CIM analysis for grain number per square meter (Kpsm) in the RAC875/Kukri population from four environments (RAC, Minn, Bool and MexI). QTL analysis was performed without taking heading time effects into account (non-adjusted data = NA). The most likely QTL position, range, interval of flanking markers, allelic additive effect, heritability and LOD for each individual QTL is presented. The italic bold loci represent putative QTLs which were detected at a 5% significance threshold. Suggestive QTLs were detected at a 10% significance threshold. QTLs with largest trait effect are highlighted in light gray.**

| Site | QTL | Position (cM) | Range | Interval | Add | Parent | $h^2$ (%) | LOD |
|---|---|---|---|---|---|---|---|---|
| RAC | *QKpsm.aww-1AL$^{NA}$* | 181.2 | 168.0-190.6 | *XwPt-8644–XwPt-0864* | 100.8 | Kukri | 2.3 | 2.9 |
| | ***QKpsm.aww-2BS$^{NA}$*** | 37.0 | 34.0-44.1 | *XwPt-7757–Xbarc0013a* | -440.5 | RAC875 | 16.3 | 17.8 |
| | ***QKpsm.aww-2DS$^{NA}$*** | 39.7 | 28.7-48.7 | *XwPt-6003–XwPt-0330* | 720.7 | Kukri | 10.3 | 9.9 |
| | ***QKpsm.aww-3D$^{NA}$*** | 114.7 | 110.8-118.8 | *Xgwm0664–Xgwm0383b* | 233.9 | Kukri | 4.9 | 6.3 |
| | ***QKpsm.aww-5B$^{NA}$*** | 79.9 | 71.4-89.6 | *XwPt-4936–XwPt-3457* | 238.2 | Kukri | 4.1 | 5.0 |
| | ***QKpsm.aww-7A$^{NA}$*** | 132.8 | 125.3-137.3 | *XDuPw0254–Xgwm0276* | -181.3 | RAC875 | 3.1 | 3.8 |
| | ***QKpsm.aww-7B$^{NA}$*** | 48.8 | 44.0-59.8 | *XwPt-4230–Xwmc0517b* | -208.3 | RAC875 | 3.6 | 5.2 |
| Minn | ***QKpsm.aww-1AL$^{NA}$*** | 181.2 | 168.0-190.6 | *XwPt-8644–XwPt-0864* | 73.5 | Kukri | 5.6 | 3.6 |
| | ***QKpsm.aww-2BS$^{NA}$*** | 36.0 | 33.0-39.0 | *XwPt-7757–Xbarc0013a* | -196.2 | RAC875 | 19.8 | 20.9 |
| | ***QKpsm.aww-2DS$^{NA}$*** | 46.7 | 39.7-54.7 | *XwPt-6003–XwPt-0330* | 331.3 | Kukri | 12.4 | 18.1 |
| | ***QKpsm.aww-3D$^{NA}$*** | 114.7 | 110.8-118.8 | *Xgwm0664–Xgwm0383b* | 233.9 | Kukri | 2.0 | 3.4 |
| | ***QKpsm.aww-7A$^{NA}$*** | 131.4 | 125.3-136.8 | *XDuPw0254–Xgwm0276* | -89.6 | RAC875 | 4.2 | 5.3 |
| | ***QKpsm.aww-7B$^{NA}$*** | 50.8 | 44.0-65.8 | *XwPt-4230–Xwmc0517b* | -75.8 | RAC875 | 2.7 | 4.4 |
| Bool | ***QKpsm.aww-1AL$^{NA}$*** | 182.3 | 172.0-189.1 | *XwPt-0864–XwPt-6754* | 47.0 | Kukri | 5.8 | 4.0 |
| | ***QKpsm.aww-2BS$^{NA}$*** | 36.0 | 32.3-42.1 | *XwPt-7757–Xbarc0013a* | -101.1 | RAC875 | 12.7 | 12.2 |
| | ***QKpsm.aww-2DS$^{NA}$*** | 38.7 | 26.7-48.7 | *XwPt-6003–XwPt-0330* | 175.9 | Kukri | 7.6 | 9.2 |
| | ***QKpsm.aww-3D$^{NA}$*** | 113.7 | 96.1-125.8 | *Xgwm0664–Xgwm0383b* | 50.4 | Kukri | 3.5 | 4.0 |
| | ***QKpsm.aww-7A$^{NA}$*** | 127.3 | 125.3-139.3 | *Xbarc0195–XDuPw0254* | -60.8 | RAC875 | 4.6 | 5.3 |
| | ***QKpsm.aww-7B$^{NA}$*** | 46.0 | 12.0-63.8 | *Xwmc0396–XwPt-4230* | -47.4 | RAC875 | 2.6 | 3.3 |
| MexI | ***QKpsm.aww-2BS$^{NA}$*** | 36.0 | 30.5-40.1 | *XwPt-7757–Xbarc0013a* | -88.3 | RAC875 | 9.6 | 10.7 |
| | ***QKpsm.aww-2DS$^{NA}$*** | 87.2 | 46.7-97.2 | *XwPt-0330–Xbarc0328b* | 62.6 | Kukri | 5.6 | 5.3 |
| | ***QKpsm.aww-3B.1$^{NA}$*** | 73.1 | 50.9-79.8 | *Xwmc0043–XwPt-6973* | 55.0 | Kukri | 4.1 | 5.1 |
| | ***QKpsm.aww-3B.2$^{NA}$*** | 201.1 | 195.1-207.1 | *XwPt-8021–Xgwm0114b* | -80.9 | RAC875 | 8.6 | 9.2 |

#### *5.2.3.1.8 QTLs for grain weight and number of grains from the sampled spikes (non-adjusted data)*

Grain weight from the sampled spikes (Gwe) was the function of grain number and grain size. Adverse environmental conditions such as drought, heat, frost and N deficiency during the reproductive stage (about one week before flowering) reduce seed set and consequently grain number (Fageria et al., 2006). The distribution of the population showed that RAC875 exceeded Kukri for grain number from sampled spikes

in Minn and Bool (Table 5-3). This trait was significantly correlated ($P < 0.001$) with grain yield (Table 5-4).

Twelve significant QTL for Gwe were identified on five chromosomes (2B, 2D, 5B, 6A and 7A) in the three South Australian sites (Table 5-10; Appendix L). ***QGwe.aww-2BS$^{NA}$***, ***QGwe.aww-2DS$^{NA}$*** and ***QGwe.aww-5B$^{NA}$*** were identified in more than one environment and they were coincident with heading time QTLs. One QTL on chromosome 6A (***QGwe.aww-6A$^{NA}$***) was only detected in RAC with a LOD of 4.0 and heritability of 3.7%, in which the 'RAC875' allele was associated with increases in grain weight per spike. Other QTL for grain weight were found on chromosome 7A (***QGwe.aww-7A$^{NA}$***) in all three Australian sites, with LOD > 3.7, and it explained on average 5.7% of the observed phenotypic variation. ***QGwe.aww-7A$^{NA}$*** peaked at *Xbarc0259* (113.3 cM) in a similar position with ***QYld.aww-7A.1$^{NA}$*** between ***QEet.aww-7A*** for heading time and ***QYld.aww-7A.2$^{NA}$*** for grain yield. It could reflect the pleiotropic effect of heading time effect, grain number or grain size (Table 5-10).

In total, eighteen QTLs for number of grains from the sampled spike were identified on eight chromosomes (1A, 1B, 2B, 2D, 3A, 5B, 7A and 7D) in three South Australian environments (Table 5-10; Appendix K). ***QGne.aww-1AL$^{NA}$*** was detected (LOD = 4.5) in Minn and it was also identified as a suggestive QTL (LOD = 2.7) in Bool. This QTL peaked at *XwPt-0864* (182.3 cM) in the *XwPt-8644–XwPt-0864* interval that explained 6.4 and 1.2% of the phenotypic variation in Minn and Bool, respectively. The 'Kukri' allele at this QTL was associated with increases in grain number from the sampled spike. ***QGne.aww-1BL$^{NA}$*** was detected (LOD = 3.9) in RAC at *XwPt-9809* (151.0 cM). *QGne.aww-1BL$^{NA}$* was also identified as a suggestive QTL (LOD = 1.8) in Bool and explained 4.4 and 0.2% of the phenotypic variation in RAC and Bool, respectively. For this QTL, the 'RAC875' allele was associated with increases in grain number per sampled spike relative to the 'Kukri' allele. The most significant QTLs were located on chromosome 2BS and 2DS coinciding with heading time QTLs (Table 5-10). ***QGne.aww2BS$^{NA}$*** and ***QGne.aww2DS$^{NA}$*** together explained 12.0%, 24.9% and 18.9% of the phenotypic variation in RAC, Minn and Bool, respectively.

Another QTL for this trait was detected on chromosome 5B (***QGne.aww-5B$^{NA}$***) in a similar position with heading time QTL (***QEet.aww-5B***). This QTL was detected (LOD > 3.0) in RAC and Bool, while in Minn, it was identified as a suggestive QTL (LOD =

2.5). ***QGne.aww-7A$^{NA}$*** was identified in Minn and Bool. In the Minn environment, this QTL was located at *Xgwm0276* (130.9 cM) with a LOD of 3.7 and heritability of 3.4%. However, in Bool, it was located at *Xbarc0259* (113.3 cM) with a LOD of 5.1 and heritability of 5.9%. For ***QGne.aww-7A$^{NA}$***, the 'RAC875' allele contributed to increase a grain number compared to the 'Kukri' allele. A significant QTL on chromosome 7D (***QGne.aww-7D$^{NA}$***) was only detected in Minn, with LOD of 3.2 and heritability of 2.6%. This QTL peaked at *Xbarc058* (108.9 cM) in the same position with heading time QTL in this region.

**Table 5-10. Detected QTLs with CIM analysis for grain weight and grain number from sample spikes in three South Australian environments (RAC, Minn and Bool; 2006). QTL analysis was performed without taking heading time effects into account (non-adjusted data = NA). The most likely QTL position, range, interval of flanking markers, allelic additive effect, heritability and LOD for each individual QTL is presented. The italic bold loci represent putative QTLs which were detected at a 5% significance threshold. Suggestive QTLs were detected at a 10% significance threshold. QTLs with largest trait effect are highlighted in light gray.**

| Trait | Site | QTL | Position (cM) | Range | Interval | Add | Parent | $h^2$ (%) | LOD |
|---|---|---|---|---|---|---|---|---|---|
| Grain weight | RAC | ***QGwe.aww-2BS$^{NA}$*** | 56.2 | 50.6-61.2 | *XwPt-0335–XwPt-0950* | -0.335 | RAC875 | 14.9 | 17.7 |
| | | ***QGwe.aww-2DS$^{NA}$*** | 45.7 | 33.7-58.7 | *XwPt-6003–XwPt-0330* | 0.489 | Kukri | 8.2 | 6.4 |
| | | ***QGwe.aww-5B$^{NA}$*** | 80.9 | 71.9-93.6 | *XwPt-4936–XwPt-3457* | 0.218 | Kukri | 5.2 | 4.9 |
| | | ***QGwe.aww-6A$^{NA}$*** | 94.5 | 85.0-105.5 | *Xwmc0256a–XwPt-7599* | -0.163 | RAC875 | 3.7 | 4.0 |
| | | ***QGwe.aww-7A$^{NA}$*** | 94.1 | 65.6-113.3 | *Xcfa2028–Xbarc0174* | -0.189 | RAC875 | 5.5 | 6.8 |
| | Minn | ***QGwe.aww-2BS$^{NA}$*** | 41.1 | 35.0-45.1 | *Xbarc0013a–Xgwm0271a* | -0.391 | RAC875 | 21.9 | 21.0 |
| | | ***QGwe.aww-2DS$^{NA}$*** | 39.7 | 28.7-48.7 | *XwPt-6003–XwPt-0330* | 0.563 | Kukri | 9.1 | 10.1 |
| | | ***QGwe.aww-7A$^{NA}$*** | 113.0 | 104.2-122.8 | *Xbarc0174–Xbarc0259* | -0.166 | RAC875 | 3.6 | 3.7 |
| | Bool | ***QGwe.aww-2BS$^{NA}$*** | 42.1 | 32.3-48.1 | *Xbarc0013a–Xgwm0271a* | -0.198 | RAC875 | 9.1 | 7.8 |
| | | ***QGwe.aww-2DS$^{NA}$*** | 44.7 | 35.7-53.7 | *XwPt-6003–XwPt-0330* | 0.420 | Kukri | 8.6 | 11.2 |
| | | ***QGwe.aww-5B$^{NA}$*** | 87.6 | 57.4-99.6 | *XwPt-3457–Xgwm0271b* | 0.125 | Kukri | 2.3 | 3.0 |
| | | ***QGwe.aww-7A$^{NA}$*** | 112.0 | 105.2-115.3 | *Xbarc0174–Xbarc0259* | -0.186 | RAC875 | 7.7 | 6.4 |
| Gran number | RAC | ***QGne.aww-1B$^{NA}$*** | 161.0 | 151.0-182.1 | *XwPt-9809–XwPt-0944* | -4.25 | RAC875 | 4.4 | 3.9 |
| | | ***QGne.aww-2BS$^{NA}$*** | 46.1 | 40.1-58.2 | *Xbarc0013a–Xgwm0271a* | -5.31 | RAC875 | 5.8 | 6.5 |
| | | ***QGne.aww-2DS$^{NA}$*** | 41.7 | 23.7-55.7 | *XwPt-6003–XwPt-0330* | 8.81 | Kukri | 6.1 | 4.3 |
| | | *QGne.aww-3A$^{NA}$* | 58.9 | 48.1-61.9 | *Xbarc0328a–Xgwm0666a* | 2.46 | Kukri | 1.1 | 2.6 |
| | | ***QGne.aww-5B$^{NA}$*** | 82.9 | 76.9-88.6 | *XwPt-4936–XwPt-3457* | 6.55 | Kukri | 9.6 | 9.1 |
| | Minn | ***QGne.aww-1AL$^{NA}$*** | 182.2 | 172.0-188.1 | *XwPt-8644–XwPt-0864* | 4.25 | Kukri | 6.4 | 4.5 |
| | | ***QGne.aww-2BS$^{NA}$*** | 37.0 | 33.0-43.1 | *XwPt-7757–Xbarc0013a* | -8.39 | RAC875 | 15.1 | 15.6 |
| | | ***QGne.aww-2DS$^{NA}$*** | 42.7 | 32.7-50.7 | *XwPt-6003–XwPt-0330* | 15.49 | Kukri | 9.8 | 10.5 |
| | | *QGne.aww-3A$^{NA}$* | 57.9 | 52.1-66.1 | *Xgwm0002–Xbarc0328a* | 3.03 | Kukri | 1.4 | 1.8 |
| | | *QGne.aww-5B$^{NA}$* | 73.9 | 71.4-83.6 | *XwPt-4936–XwPt-3457* | 3.23 | Kukri | 1.5 | 2.5 |
| | | ***QGne.aww-7A.2$^{NA}$*** | 131.4 | 126.3-135.8 | *XDuPw0254–Xgwm0276* | -3.95 | RAC875 | 3.4 | 3.7 |
| | | ***QGne.aww-7D$^{NA}$*** | 114.9 | 102.2-140.9 | *Xbarc0058–Xgwm0428* | 3.99 | Kukri | 2.6 | 3.2 |
| | Bool | *QGne.aww-1A$^{NA}$* | 182.3 | 172.0-189.1 | *XwPt-8644–XwPt-0864* | 2.53 | Kukri | 1.2 | 2.7 |
| | | *QGne.aww-1B$^{NA}$* | 151.0 | 143.5-159.0 | *XwPt-9809–XwPt-0944* | -1.12 | RAC875 | 0.2 | 1.8 |
| | | ***QGne.aww-2BS$^{NA}$*** | 35.0 | 25.8-39.1 | *XwPt-7757–Xbarc0013a* | -4.63 | RAC875 | 7.2 | 6.2 |
| | | ***QGne.aww-2DS$^{NA}$*** | 43.7 | 34.7-52.7 | *XwPt-6003–XwPt-0330* | 13.74 | Kukri | 11.7 | 11.1 |
| | | ***QGne.aww-5B$^{NA}$*** | 80.9 | 58.4-97.6 | *XwPt-4936–XwPt-3457* | 3.96 | Kukri | 3.1 | 3.0 |
| | | ***QGne.aww-7A.1$^{NA}$*** | 113.0 | 103.2-116.3 | *Xbarc0174–Xbarc0259* | -4.64 | RAC875 | 5.9 | 5.1 |

#### *5.2.3.1.9 QTLs for spikelet number per spike (non-adjusted data)*

Among components for grain yield of cereal crops, number of spikelets appears to be important in developing high-yielding cultivars (Feil, 1992). Producing more grains per unit area in modern cultivars is probably the result of more grains per spikelet (Feil, 1992). Total numbers of spikelet per spike (including fertile and non-fertile spikelets) in Kukri were higher than RAC875 in the four environments (Table 5-3). Number of spikelets per spike was negatively correlated with grain yield in RAC and MexD sites. It showed no or small correlations with grain yield in Minn and Bool (r = 0.03 and 0.10, respectively; Table 5-4).

Fourteen QTLs for spikelets per spike (Spn) were detected on seven chromosomes (2B, 2D, 3A, 4A, 6A, 7A and 7B) in four environments (Table 5-11; Appendix L). Spikelet QTLs on chromosome 2B, 2D, 3A and 4A were only detected in RAC with LOD > 3.5 and collectively explained 37.0% of the observed phenotypic variation in this environment. 2B and 2D QTLs (***QSpn.aww-2BS***$^{NA}$ and ***QSpn.aww-2DS***$^{NA}$) overlapped with heading time QTL, while ***QSpn.aww-3A***$^{NA}$ co-located with plant height and peduncle length QTLs (***QHt.aww-3A***$^{NA}$ and ***QPdl.aww-3A***$^{NA}$, respectively). ***QSpn.aww-4A***$^{NA}$ peaked at the *Xcfe0254* (27.9 cM) in the *Xcfe0254–Xbarc0170* interval. This QTL explained 3.0% of the phenotypic variation, in which the 'RAC875' allele was associated with increases in spikelet number per spike. Spikelet QTLs on chromosome 6A, 7A and 7B were detected in more than two environments. ***QSpn.aww-6A***$^{NA}$ was identified (LOD > 4.7) in RAC, Minn and Bool at *Xwmc0256a* (91.5 cM) which explained on average 4.5% of the observed phenotypic variation.

The most significant QTL was ***QSpn.aww-7A***$^{NA}$ (LOD > 4.2) that was located on the long arm of chromosome 7A in the *Xbarc0292–Xgwm0746* interval. The contribution of ***QSpn.aww-7A***$^{NA}$ QTL to the phenotypic variation, depending on the environment, ranged from 8.1% to 22.6%. The 'Kukri' allele was associated with increases in spikelet number per spike. Although ***QSpn.aww-7A***$^{NA}$ overlapped with grain yield QTL (***QYld.aww-7A.2***$^{NA}$) in RAC, Minn, and MexD, it did not associate with grain yield QTLs since there was a weak correlation between Spn and grain yield in these environments. Although a higher number of spikelets per spike are important as a

potential sink to produce more grains, the higher proportion of fertile spikelets with a reasonable grain size is more important under drought stress conditions.

***QSpn.aww-7B$^{NA}$*** was identified in the Bool and MexD environments, while it was detected as a suggestive QTL in RAC. However, this QTL was coincident with heading time QTLs. An increased number of spikelet per spike was associated with the later flowering allele from 'Kukri'.

**Table 5-11. Detected QTLs with CIM analysis for the number of spikelets per spike (Spn) in the four droughted environments (RAC, Minn, Bool and MexD). QTL analysis was performed without taking heading time effects into account (non-adjusted data = NA). The most likely QTL position, range, interval of flanking markers, allelic additive effect, heritability and LOD for each individual QTL is presented. The italic bold loci represent putative QTLs which were detected at a 5% significance threshold. Suggestive QTLs were detected at a 10% significance threshold. QTLs with largest trait effect are highlighted in light gray.**

| Site | QTL | Position (cM) | Range | Interval | Add | Parent | $h^2$ (%) | LOD |
|---|---|---|---|---|---|---|---|---|
| RAC | ***QSpn.aww-2BS$^{NA}$*** | 35.0 | 33.0-38.0 | *XwPt-7757–Xbarc0013a* | 0.59 | Kukri | 13.7 | 14.4 |
| | ***QSpn.aww-2DS$^{NA}$*** | 41.7 | 27.7-54.7 | *XwPt-6003–XwPt-0330* | -0.65 | RAC875 | 4.1 | 5.5 |
| | ***QSpn.aww-3A$^{NA}$*** | 37.1 | 20.3-50.1 | *XwPt-0714–Xgwm0002* | 0.33 | Kukri | 3.7 | 3.5 |
| | ***QSpn.aww-4A$^{NA}$*** | 36.9 | 27.9-45.9 | *Xcfe0254–Xbarc0170* | -0.24 | RAC875 | 3.0 | 4.0 |
| | ***QSpn.aww-6A$^{NA}$*** | 98.5 | 87.0-107.5 | *Xwmc0256a–XwPt-7599* | -0.38 | RAC875 | 4.9 | 5.9 |
| | ***QSpn.aww-7AL$^{NA}$*** | 133.8 | 130.4-144.3 | *Xgwm0276–Xbarc0292* | 0.42 | Kukri | 8.1 | 7.7 |
| | *QSpn.aww-7B$^{NA}$* | 80.8 | 67.8-88.6 | *XwPt-4230–Xwmc0517b* | 0.31 | Kukri | 3.8 | 2.4 |
| Minn | ***QSpn.aww-6A$^{NA}$*** | 90.1 | 86.0-105.5 | *Xbarc0118–Xwmc0256a* | -0.19 | RAC875 | 3.9 | 4.7 |
| | ***QSpn.aww-7AL$^{NA}$*** | 148.3 | 143.3-154.3 | *Xbarc0292–Xgwm0746* | 0.41 | Kukri | 15.9 | 15.1 |
| Bool | ***QSpn.aww-6A$^{NA}$*** | 93.5 | 87.0-103.5 | *Xwmc0256a–XwPt-7599* | -0.24 | RAC875 | 4.8 | 4.9 |
| | ***QSpn.aww-7AL$^{NA}$*** | 146.3 | 141.3-151.3 | *Xbarc0292–Xgwm0746* | 0.44 | Kukri | 16.3 | 15.5 |
| | ***QSpn.aww-7B$^{NA}$*** | 71.8 | 61.8-85.6 | *XwPt-4230–Xwmc0517b* | 0.33 | Kukri | 6.3 | 5.9 |
| MexD | ***QSpn.aww-7AL$^{NA}$*** | 159.9 | 149.3-166.4 | *Xgwm0746–XwPt-5558* | 0.92 | Kukri | 22.6 | 4.2 |
| | ***QSpn.aww-7B$^{NA}$*** | 33.6 | 28.4-39.2 | *Xgwm0297–Xbarc0065* | 0.52 | Kukri | 7.7 | 8.6 |

### *5.2.3.1.10 QTLs for fertile and non-fertile spikelets (non-adjusted data)*

Grain yield showed a positive correlation ($P < 0.001$) with fertile spikelets (Fspn) and it showed a significantly negative correlation with non-fertile spikelets (Table 5-4). QTL analysis revealed twenty QTLs for fertile spikelets on eight chromosomes (1A, 1B, 2B, 2D, 5B, 6A, 7A and 7B) in the four drought environments (Table 5-12; Appendix L).

Overall, eight putative QTL were identified and one potential QTL was detected for fertile spikelets. The phenotypic variation explained by individual QTL ranged from 1.3 to 24.9%. Fertile spikelet QTL on 1A (***QFspn.aww-1AL$^{NA}$***) was identified as putative QTL (LOD = 4.7) in Minn and as a suggestive QTL (LOD = 2.7) in Bool. ***QFspn.aww-1AL$^{NA}$*** was located on the long arm of chromosome 1A in a similar position with grain number per square meter as well as grain number per sample spike, and it explained 6.5% and 1.7% of the phenotypic variation in Minn and Bool, respectively. ***QFspn.aww-1B$^{NA}$*** was detected in RAC (LOD = 4.1), but in Bool it was identified as a suggestive QTL (LOD = 1.8). ***QFspn.aww-1B$^{NA}$*** co-located with a QTL for grain number from sampled spikes, in which the 'RAC875' allele was associated with higher spikelet fertility.

In the South Australian environments, two major heading time QTL on 2B and 2D (***QEet.aww-2BS*** and ***QEet.aww-2DS***) affected spikelet fertility. ***QFspn.aww-2BS$^{NA}$*** and ***QFspn.aww-2DS$^{NA}$*** were only detected in three South Australian experiments in 2006 (Table 5-12; Fig. 5-21). These two QTLs collectively accounted for about 13.2%, 24.3% and 19.9% of the phenotypic variations in RAC, Minn and Bool environments, respectively. Another QTL for spikelet fertility was identified on chromosome 5B (***QFspn.aww-5B$^{NA}$***) in RAC as a significant QTL (LOD = 9.9; 10.23% of the variation) and as a suggestive QTL (LOD = 2.8; 2.9% of the variation) in the Bool environment. ***QFspn.aww-5B$^{NA}$*** also overlapped with heading time QTL on chromosome 5B at *XwPt-3457* (83.6 cM). A small QTL on chromosome 6A (***QFspn.aww-6A$^{NA}$***) was only identified in MexD with a LOD of 3.3 and heritability of 2.9%, in which the 'RAC875' allele was associated with increases in fertile spikelets.

One prominent QTL for spikelet fertility was identified on chromosome 7A in three out of four environments with LOD > 3.4. In Minn ***QFspn.aww-7A.2$^{NA}$*** was located at *Xgwm0276* (130.9 cM) in a similar position with QTLs for grain yield (***QYld.aww-7A.2$^{NA}$***), grain number per unit area (***QKpsm.aww-7A$^{NA}$***), grain number (***QGne.aww-7A$^{NA}$***) and grain weight from the sampled spike (***QGwe.aww-7A$^{NA}$***) (Fig. 5-21). In Bool, ***QFspn.aww-7A.1$^{NA}$*** was also coincident with grain number from sample spike which peaked at *Xbarc0259* (113.3 cM) about 8.0 cM away from ***QFspn.aww-7A.2$^{NA}$*** detected in Minn. An increased number of fertile spikelets at ***QFspn.aww-7A.2$^{NA}$*** were associated with the 'RAC875' allele. However, in the MexD environment, two significant QTLs were found on chromosome 7A, where the 'Kukri' allele was

associated with increases in spikelet fertility indicating genotype x environment interaction at ***QFspn.aww-7A.1***$^{NA}$ and ***QFspn.aww-7A.2***$^{NA}$ between Mexican and Australian sites (Table 5-12). ***QFspn.aww-7A.1***$^{NA}$ was detected in a similar position to ***QFspn.aww-7A.1***$^{NA}$ in Bool, with a LOD of 3.5 and heritability of 24.9%, whereas ***QFspn.aww-7A.2***$^{NA}$ LOD = 4.2; 8.8% of the phenotypic variation) was detected at *Xgwm0746* (154.0 cM), about 37.3 cM apart from ***QFspn.aww-7A.1***$^{NA}$. A QTL on 7B (***QFspn.aww-7B***$^{NA}$) was detected in MexD at *XwPt-4230* (48.8 cM) with a LOD of 4.0 and explained 3.7% of the phenotypic variation. This QTL was also identified as a suggestive QTL in RAC and Bool environments with LOD of 2.2.

For the non-fertile spikelets per spike (Nspn) trait, twenty two QTLs were found on eight chromosomes (1A, 1B, 2B, 2D, 5B, 6A, 7A and 7B) in four environments (Table 5-12; Appendix L). The phenotypic variation explained by individual QTL ranged from 1.1 to 18.7% depending on the environment. Most of the QTLs for Nspn co-located with fertile spikelets QTLs and both were coincident with heading time QTLs, except QTLs on chromosome 6A and 7A. Alleles associated with later-flowering were also associated with increases in number of spikelets per spike, decreases in fertile spikelets as well as increases in non-fertile spikelts. ***QNspn.aww-6A***$^{NA}$ (LOD = 3.1; 4.44% of variation) was only detected at MexD. ***QNspn.aww-7A.2***$^{NA}$ however, was detected in the three tested environments (RAC, Minn and MexD) with a clear main additive effect. ***QNspn.aww-7A.2***$^{NA}$ peaked at *Xgwm0276* (130.9 cM) in a similar position with ***QYld.aww-7A.2***$^{NA}$ in the *Xbarc0195-Xgwm0276* interval (Fig. 5-21). The contribution of this QTL to phenotypic variation, depending on the environment, ranged from 4.06% to 10.9%. In Bool, ***QNspn.aww-7A.1***$^{NA}$ was located in the *Xbarc1004–Xbarc0259* interval, with a LOD of 13.8 and heritability of 13.05%. The 'Kukri' allele in this QTL was associated with a higher number of non-fertile spikelets compared to the 'RAC875' allele.

**Table 5-12. Detected QTLs with CIM analysis for fertile spikelets (Fspn) and non-fertile spikelets (Nspn) for four drought environments (RAC, Minn, Bool and MexD). QTL analysis was performed without taking heading time effects into account (non-adjusted data = NA). The most likely QTL position, range, interval of flanking markers, allelic additive effect, heritability and LOD for each individual QTL is presented. The italic bold loci represent putative QTLs which were detected at a 5% significance threshold. Suggestive QTLs were detected at a 10% significance threshold. QTLs with largest trait effect are highlighted in light gray.**

| Trait | Site | QTL | Position (cM) | Range | Interval | Add | Parent | $h^2$ (%) | LOD |
|---|---|---|---|---|---|---|---|---|---|
| Fspn | RAC | ***QFspn.aww-1BL$^{NA}$*** | 161.0 | 151.0-182.1 | *XwPt-9809–XwPt-0944* | -0.29 | RAC875 | 4.5 | 4.1 |
| | | ***QFspn.aww-2BS$^{NA}$*** | 45.1 | 39.1-57.2 | *Xbarc0013a–Xgwm0271a* | -0.38 | RAC875 | 6.3 | 7.1 |
| | | ***QFspn.aww-2DS$^{NA}$*** | 41.7 | 26.7-54.7 | *XwPt-6003–XwPt-0330* | 0.64 | Kukri | 6.9 | 5.0 |
| | | ***QFspn.aww-5B$^{NA}$*** | 83.6 | 76.9-89.6 | *XwPt-3457–Xgwm0271b* | 0.46 | Kukri | 10.2 | 9.9 |
| | | *QFspn.aww-7B$^{NA}$* | 37.2 | 32.6-56.8 | *Xbarc0065–Xbarc0137b* | -0.18 | RAC875 | 1.3 | 2.2 |
| | Minn | ***QFspn.aww-1AL$^{NA}$*** | 181.2 | 170.0-189.1 | *XwPt-8644–XwPt-0864* | 0.55 | Kukri | 6.5 | 4.7 |
| | | ***QFspn.aww-2BS$^{NA}$*** | 37.0 | 33.0-43.1 | *XwPt-7757–Xbarc0013a* | -1.05 | RAC875 | 15.4 | 15.9 |
| | | ***QFspn.aww-2DS$^{NA}$*** | 42.7 | 32.7-51.7 | *XwPt-6003–XwPt-0330* | 1.79 | Kukri | 8.9 | 9.5 |
| | | ***QFspn.aww-7A.2$^{NA}$*** | 131.4 | 124.3-135.8 | *XDuPw0254–Xgwm0276* | -0.49 | RAC875 | 3.1 | 3.4 |
| | Bool | *QFspn.aww-1AL$^{NA}$* | 201.6 | 196.1-201.6 | *Xcfe0242b–Xwmc0215a* | 0.30 | Kukri | 1.7 | 2.7 |
| | | *QFspn.aww-1BL$^{NA}$* | 151.0 | 142.5-161.0 | *XwPt-9809–XwPt-0944* | -0.15 | RAC875 | 0.4 | 1.8 |
| | | ***QFspn.aww-2BS$^{NA}$*** | 35.0 | 24.8-39.1 | *XwPt-7757–Xbarc0013a* | -0.48 | RAC875 | 7.6 | 6.6 |
| | | ***QFspn.aww-2DS$^{NA}$*** | 43.7 | 34.7-52.7 | *XwPt-6003–XwPt-0330* | 1.37 | Kukri | 11.3 | 10.7 |
| | | *QFspn.aww-5B$^{NA}$* | 79.9 | 58.4-96.6 | *XwPt-4936–XwPt-3457* | 0.39 | Kukri | 2.9 | 2.8 |
| | | ***QFspn.aww-7A.1$^{NA}$*** | 112.0 | 103.2-116.3 | *Xbarc0174–Xbarc0259* | -0.48 | RAC875 | 6.0 | 5.2 |
| | | *QFspn.aww-7B$^{NA}$* | 48.8 | 46.0-61.8 | *XwPt-4230–Xwmc0517b* | -0.26 | RAC875 | 1.3 | 2.2 |
| | MexD | ***QFspn.aww-6A$^{NA}$*** | 65.7 | 51.1-79.7 | *Xbarc0353b–Xstm0519actc* | -0.30 | RAC875 | 2.9 | 3.3 |
| | | ***QFspn.aww-7A.1$^{NA}$*** | 103.2 | 96.1-112.0 | *Xbarc1004–Xbarc0174* | 0.58 | Kukri | 24.9 | 3.5 |
| | | ***QFspn.aww-7A.2$^{NA}$*** | 158.9 | 149.3-166.4 | *Xgwm0746–XwPt-5558* | 0.55 | Kukri | 8.8 | 4.2 |
| | | ***QFspn.aww-7B$^{NA}$*** | 57.8 | 26.4-70.8 | *XwPt-4230–Xwmc0517b* | 0.37 | Kukri | 3.7 | 4.0 |
| Nspn | RAC | *QNspn.aww-1AL$^{NA}$* | 178.2 | 169.0-191.6 | *XwPt-8644–XwPt-0864* | -0.29 | RAC875 | 1.1 | 2.4 |
| | | ***QNspn.aww-1BL$^{NA}$*** | 159.0 | 146.5-169.1 | *XwPt-9809–XwPt-0944* | 0.37 | Kukri | 3.6 | 3.9 |
| | | ***QNspn.aww-2BS$^{NA}$*** | 44.1 | 40.1-47.1 | *Xbarc0013a–Xgwm0271a* | 1.07 | Kukri | 18.7 | 26.2 |
| | | ***QNspn.aww-2DS$^{NA}$*** | 38.7 | 25.7-47.7 | *XwPt-6003–XwPt-0330* | -1.36 | RAC875 | 10.2 | 9.1 |
| | | ***QNspn.aww-5B.2$^{NA}$*** | 83.6 | 74.9-91.6 | *XwPt-3457–Xgwm0271b* | -0.54 | RAC876 | 5.2 | 5.5 |
| | | ***QNspn.aww-7A.2$^{NA}$*** | 133.8 | 125.3-141.3 | *Xgwm0276–Xbarc0292* | 0.46 | Kukri | 4.1 | 5.9 |
| | | ***QNspn.aww-7B$^{NA}$*** | 27.4 | 19.0-37.2 | *Xstm0671acag–Xgwm0297* | 0.50 | Kukri | 4.6 | 4.9 |
| | Minn | ***QNspn.aww-2BS$^{NA}$*** | 36.0 | 33.0-39.0 | *XwPt-7757–Xbarc0013a* | 1.11 | Kukri | 16.9 | 20.5 |
| | | ***QNspn.aww-2DS$^{NA}$*** | 44.7 | 37.7-52.7 | *XwPt-6003–XwPt-0330* | -1.88 | RAC875 | 10.6 | 15.4 |
| | | ***QNspn.aww-5B.2$^{NA}$*** | 79.9 | 53.3-97.6 | *XwPt-4936–XwPt-3457* | -0.50 | RAC875 | 3.0 | 4.0 |
| | | ***QNspn.aww-7A.2$^{NA}$*** | 132.4 | 129.4-136.8 | *XDuPw0254–Xgwm0276* | 0.88 | Kukri | 10.9 | 12.7 |
| | | ***QNspn.aww-7B$^{NA}$*** | 55.8 | 42.6-66.8 | *XwPt-4230–Xwmc0517b* | 0.68 | Kukri | 4.6 | 5.8 |
| | Bool | ***QNspn.aww-1AL$^{NA}$*** | 179.2 | 170.0-190.6 | *XwPt-8644–XwPt-0864* | -0.38 | RAC875 | 3.8 | 3.6 |
| | | ***QNspn.aww-1BL$^{NA}$*** | 153.0 | 141.5-162.0 | *XwPt-9809–XwPt-0944* | 0.48 | Kukri | 4. 6 | 4.2 |
| | | ***QNspn.aww-2BS$^{NA}$*** | 34.0 | 29.5-39.0 | *XwPt-7757–Xbarc0013a* | 0.63 | Kukri | 7.6 | 8.7 |
| | | ***QNspn.aww-2DS$^{NA}$*** | 45.7 | 38.7-52.7 | *XwPt-6003–XwPt-0330* | -1.90 | RAC875 | 11.6 | 17.3 |
| | | ***QNspn.aww-5B.1$^{NA}$*** | 19.0 | 7.0-31.3 | *Xgwm0234b–XwPt-8604* | -0.46 | RAC875 | 2.2 | 3.8 |
| | | ***QNspn.aww-7A.1$^{NA}$*** | 107.2 | 103.2-116.3 | *Xbarc1004–Xbarc0259* | 0.92 | Kukri | 13.1 | 13.8 |
| | | ***QNspn.aww-7B$^{NA}$*** | 60.8 | 48.8-68.8 | *XwPt-4230–Xwmc0517b* | 0.77 | Kukri | 5.9 | 9.1 |
| | MexD | ***QNspn.aww-2B$^{NA}$*** | 75.4 | 70.6-83.4 | *XwPt-7200–XwPt-5128* | 0.29 | Kukri | 9.0 | 6.0 |
| | | ***QNspn.aww-6A$^{NA}$*** | 91.5 | 64.7-102.5 | *Xwmc0256a–XwPt-7599* | 0.20 | Kukri | 4.4 | 3.1 |
| | | ***QNspn.aww-7A.2$^{NA}$*** | 129.4 | 123.3-132.8 | *XDuPw0254–Xgwm0276* | 0.25 | Kukri | 6.7 | 5.0 |

#### *5.2.3.1.11 QTLs for TGW (non-adjusted data)*

The mean thousand grain weight (TGW) of the two parental lines in different environments differed significantly, and ranged from 30.6 g to 42.2 g for Kukri and from 35.5 g to 55.9 g for RAC875 (Table 5-3). The TGW of the RAC875 parent were 5 to 13 g heavier than the TGW of the Kukri parent in the four tested environments (RAC, Minn, Bool and MexI). TGW was not measured in the MexD experiment. The mean TGW of individual DH lines in different environments ranged from 16.2 g to 56.5 g with a grand mean ranging from 33.1 g to 44.5 g in different environments. The TGW values for DH lines in each environment were normally distributed, and transgressed the low TGW parent (Kukri) and the high TGW parent (RAC875) in all environments, suggesting that several genes control TGW. Alleles from RAC875 resulted in higher TGW in most of detected QTLs (Table 5-13).

Twenty-five QTL were detected for TGW on ten chromosomes (1A, 2A, 2B, 2D, 3A, 4A, 4B, 6A, 6B and 7A) in four environments (Table 5-13; Appendix L). The most significant QTL for TGW was detected on chromosomes 2BS (***QTgw.aww-2B.1***$^{NA}$) with LOD > 6.9 in four environments, and overlapped with the heading time QTL. The phenotypic variation explained by ***QTgw.aww-2B.1***$^{NA}$, depended on the environment and ranged from 7.6% to 28.7%. In the MexI environment, ***QTgw.aww-2B.1***$^{NA}$ was the strongest QTL with LOD = 32.1 and heritability of 28.7%. For this QTL the 'RAC875' allele was associated with increases in TGW. A potential QTL for TGW on the long arm of chromosome 2B (***QTgw.aww-2B.2***$^{NA}$) was also identified with a smaller additive effect in RAC, Minn and Bool, with LOD of 2.7, 3.7 and 2.6, respectively. ***QTgw.aww-2D***$^{NA}$ was detected in two environments in the same position with heading time QTL, and explained 1.7% and 8.2% of the observed phenotypic variation in the RAC and MexI environments, respectively. The effect of heading time QTL in this region was not as strong as the 2B QTL on TGW. TGW QTLs on 3A (***QTgw.aww-3A***$^{NA}$), 4B (***QTgw.aww-4B***$^{NA}$) and 6B (***QTgw.aww-6B***$^{NA}$) were only detected in the Minn, with a LOD > 4.6 and almost similar magnitudes of additive effect, which collectively accounted for 15.9% of the phenotypic variation. For 3A and 4B QTLs, the 'RAC875' allele was associated with larger grain size relative to the 'Kukri' allele, while in ***QTgw.aww-6B***$^{NA}$, the 'Kukri' allele contributed to large grain size. A QTL for TGW on chromosome 2A (***QTgw.aww-2A***$^{NA}$) was only identified in MexI with a LOD of 3.2 and

heritability of 2.53%. Two other prominent QTLs were detected on chromosome 6A and 7A in four environments, for both loci the 'RAC875' allele was associated with larger grain size. ***QTgw.aww-6A$^{NA}$*** was located at *Xwmc0256a* (91.5 cM) with LOD > 3.2 and its heritability ranged from 1.97% to 16.8%. This QTL was coincident with QTLs for the number of spikelets per spike, grain weight from sampled spikes, screening fractions and leaf waxiness. However, ***QTgw.aww-7A$^{NA}$*** was located in a range from 90.0 cM to 123.3 cM on chromosome 7A. In the RAC, Minn and Bool, it was detected at *Xcfa2028* (90.1 cM) between *Xcfa2028* and *Xbarc1004*. In the MexI environment, it peaked at *Xbarc0259* (110.0 cM) in the *Xbarc0259–Xbarc0281* interval with a LOD of 4.7 and heritability of 4.5%. Overall, QTLs for TGW on chromosome 2B, 6A and 7A were most detected in four tested environments.

#### *5.2.3.1.12 QTLs for screening and hectolitre weight (non-adjusted data)*

Screening fractions were only determined for the RAC site. QTL analyses were performed on four screening fractions as well as weighted average of screening. Nine QTLs for weighted screening were detected on eight chromosomes (1A, 2B, 2D, 3A, 4D, 6A, 7A and 7D) in RAC (Table 5-14; Appendix L). Of those, eight QTLs were highly significant with LOD of > 3.2 and their contribution to the phenotypic variation ranged from 1.13% to 10.42%, and one suggestive QTL was detected on chromosome 7D with a LOD of 2.7 and heritability of 4.02%. All markers that were associated with TGW also exhibited significant associations with average screening as well as screening fractions. For six out of nine QTLs, the 'RAC875' allele was associated with greater additive effect on screening relative to the 'Kukri' allele (Table 5-14; Appendix L). The most significant QTL was ***QScr.aww-2BS$^{NA}$*** with LOD of 10.7 and heritability of 10.42% (Table 5-14; Fig. 5-21). This QTL peaked at *Xbarc0013a* (39.1 cM) in the *Xbarc0013a-Xgwm0271a* interval. The second most significant QTL was ***QScr.aww-7A$^{NA}$*** on chromosome 7A (LOD = 6.3), which alone explained 7.83% of the phenotypic variation for average screening. Two QTLs for screening were detected on chromosome 2D (***QScr.aww- 2D.1$^{NA}$*** and ***QScr.aww- 2D.2$^{NA}$***) with a small additive effect on average screening and both explained 3.97% of the observed phenotypic variation. ***QScr.aww-2D.1$^{NA}$*** coincided with the heading time QTL, while ***QScr.aww- 2D.2$^{NA}$*** was located on the long arm of chromosome 2D at *Xwpt-0021* (123.4 cM) about 20.0 cM apart from the heading time QTL. A suggestive QTL for average screening was also identified on

chromosome 7D (*QScr.aww-7D*$^{NA}$), with a LOD of 2.7 and heritability of 4.02% (Table 5-14 and Fig. 5-21).

For screening fraction of more than 2.8 mm (N>2.8), eight significant QTLs on chromosomes 1A, 2B, 2D, 3A, 4D, 6A, 7A and 7D were identified with LOD > 3.2 and their contribution to the phenotypic variation ranged from 2.32% to 11.51%. Of them ***QN>2.8.aww-2B***$^{NA}$ and ***QN>2.8.aww-7A***$^{NA}$ showed the greatest contribution (20.5%) to the phenotypic variation. A further six QTLs collectively accounted for about 22.3% (Table 5-15). For almost all identified loci the 'RAC875' allele was associated with larger grain sizes relative to the 'Kukri', except ***QN>2.8.aww-2D***$^{NA}$ QTL, in where the 'Kukri' allele contributed to larger grain size.

For fraction of 2.5 mm (N2.5), only one significant QTL was detected (LOD of 3.3; 4.09% of the phenotypic variation) on chromosome 7B (***QN2.5.aww-7B***$^{NA}$). Two suggestive QTLs were also detected on chromosome 1A and 4B with LOD of 2.2 and 2.7, respectively.

For fraction of 2.2 mm (N2.2), however, eight QTLs on chromosomes 1A, 2B, 2D, 3A, 3B, 6A, 7A, and 7D were detected. Again, QTLs for this screening fraction on chromosome 2B and 7A (***QN2.2.aww-2B***$^{NA}$ and ***QN2.2.aww-7A***$^{NA}$) were the most significant QTLs which explained 11.01% and 6.28% of the phenotypic variation, respectively. The other six QTLs collectively explained 22.87%. Most QTLs for the N2.2 fraction overlapped those detected QTLs for N>2.8 fraction, except ***QN2.2.aww-3B***$^{NA}$ QTL. ***QN2.2.aww-3B***$^{NA}$ peaked between *Xgwm0131a–Xgwm0383a* at 111.4 cM distance with a LOD of 3.7 and the heritability of 2.93%. This QTL did not co-locate with the yield potential QTL ***QYld.aww-3B.1***$^{NA}$ on chromosome 3B (Appendix L).

For fraction less than 2.2 mm (N<2.2), six QTLs (LOD > 3.2) were detected on chromosomes 1AL, 1B, 2BL, 2D, 3A and 7A. A suggestive QTL for this trait was also identified on chromosome 5A with a LOD of 2.8 and heritability of 4.21%. For almost all of identified QTLs for small fractions, the 'Kukri' allele was associated with bigger values, except the 2D QTL, where the allele from 'RAC875' parent was associated with greater values. Overall, the allele from 'RAC875' was associated with large grain in the large size fractions, while the 'Kukri' allele was associated with grain size in the small size fractions. In total, six QTLs on chromosomes 1A, 2B, 2D, 3A, 6A and 7A were

associated with grain size traits. QTLs on 2B, 2D and 7A overlapped heading time QTL, while 1AL, 3A and 6A QTLs were not associated with heading time QTLs.

Four QTLs for hectolitre weight (Hlw) were detected on chromosomes 2A, 2B, 3B and 7A (LOD > 3.2) in the RAC environment that accounted for 2.8%, 5.8%, 5.6% and 6.2% of the observed phenotypic variation (Table 5-14; Appendix L).

**Table 5-13. Detected QTLs with CIM analysis for thousand grain weight (TGW) for four environments (RAC, Minn, Bool and MexI). QTL analysis was performed without taking heading time effects into account (non-adjusted data = NA). The most likely QTL position, range, interval of flanking markers, allelic additive effect, heritability and LOD for each individual QTL is presented. The italic bold loci represent putative QTLs which were detected at a 5% significance threshold. Suggestive QTLs were detected at a 10% significance threshold. QTLs with largest trait effect are highlighted in light gray.**

| Site | QTL | Position | Range | Interval | Add | Parent | $h^2$ (%) | LOD |
|---|---|---|---|---|---|---|---|---|
| RAC | ***QTgw.aww-1AL$^{NA}$*** | 189.1 | 171.0-201.6 | *XwPt-6005–XwPt-9802* | -0.46 | RAC875 | 3.80 | 3.6 |
| | ***QTgw.aww-2B.1$^{NA}$*** | 50.6 | 41.1-61.2 | *Xbarc0091–XwPt-0335* | -0.74 | RAC875 | 8.77 | 7.9 |
| | *QTgw.aww-2B.2$^{NA}$* | 133.9 | 129.0-140.3 | *XwPt-3378–XwPt-7360* | -0.45 | RAC875 | 3.63 | 2.7 |
| | ***QTgw.aww-2D$^{NA}$*** | 82.2 | 53.7-94.2 | *XwPt-0330–Xbarc0328b* | 0.49 | Kukri | 1.71 | 3.3 |
| | ***QTgw.aww-4A$^{NA}$*** | 108.7 | 74.3-121.7 | *XwPt-5694–XwPt-7939* | 0.45 | Kukri | 3.24 | 3.5 |
| | ***QTgw.aww-6A$^{NA}$*** | 90.1 | 84.0-98.5 | *Xbarc0118–Xwmc0256a* | -0.53 | RAC875 | 5.17 | 3.9 |
| | ***QTgw.aww-7A$^{NA}$*** | 92.1 | 60.6-99.1 | *Xcfa2028–Xbarc1004* | -0.71 | RAC875 | 8.39 | 6.7 |
| Minn | *QTgw.aww-1AL$^{NA}$* | 181.2 | 175.0-186.9 | *XwPt-8644–XwPt-0864* | -0.52 | RAC875 | 2.59 | 2.8 |
| | ***QTgw.aww-2B.1$^{NA}$*** | 40.1 | 36.0-46.1 | *Xbarc0013a–Xgwm0271a* | -1.28 | RAC875 | 13.09 | 9.1 |
| | ***QTgw.aww-2B.2$^{NA}$*** | 132.0 | 118.6-137.3 | *Xcfd0050a–XwPt-3378* | -0.94 | RAC875 | 8.57 | 3.7 |
| | ***QTgw.aww-3A$^{NA}$*** | 60.9 | 53.1-68.1 | *Xbarc0328a–Xgwm0666a* | -0.82 | RAC875 | 5.58 | 7.4 |
| | ***QTgw.aww-4A$^{NA}$*** | 108.7 | 101.8-111.7 | *XwPt-5694–XwPt-7939* | 0.67 | Kukri | 3.39 | 5.0 |
| | ***QTgw.aww-4B$^{NA}$*** | 51.8 | 35.6-59.1 | *Xbarc0114–XwPt-0391* | -0.67 | RAC875 | 4.57 | 4.6 |
| | ***QTgw.aww-6A$^{NA}$*** | 90.1 | 88.0-93.5 | *Xbarc0118–Xwmc0256a* | -1.35 | RAC875 | 16.81 | 19.8 |
| | ***QTgw.aww-6B$^{NA}$*** | 100.2 | 93.1-115.6 | *Xbarc0223–Xbarc0247* | 0.76 | Kukri | 5.74 | 5.1 |
| | ***QTgw.aww-7A$^{NA}$*** | 92.1 | 51.6-103.2 | *Xcfa2028– Xbarc1004* | -0.7 | RAC875 | 2.20 | 3.5 |
| Bool | ***QTgw.aww-2B.1$^{NA}$*** | 42.1 | 37.0-48.1 | *Xbarc0013a–Xgwm0271a* | -1.22 | RAC875 | 7.56 | 6.9 |
| | *QTgw.aww-2B.2$^{NA}$* | 129.0 | 120.0-140.3 | *Xcfd0050a–XwPt-3378* | -0.45 | RAC875 | 3.63 | 2.6 |
| | ***QTgw.aww-6A$^{NA}$*** | 91.5 | 87.0-98.5 | *Xwmc0256a–XwPt-7599* | -1.11 | RAC875 | 7.13 | 6.4 |
| | *QTgw.aww-7A$^{NA}$* | 92.1 | 60.6-99.1 | *Xcfa2028–Xbarc1004* | -0.70 | RAC875 | 2.66 | 2.5 |
| MexI | ***QTgw.aww-1B$^{NA}$*** | 59.2 | 49.6-67.3 | *Xbarc0008–Xgwm0413* | 1.00 | Kukri | 0.90 | 3.3 |
| | ***QTgw.aww-2A$^{NA}$*** | 149.4 | 147.4-152.4 | *Xgdm0093–XwPt-9793* | -0.91 | RAC875 | 2.53 | 3.2 |
| | ***QTgw.aww-2B.1$^{NA}$*** | 42.1 | 39.1-45.1 | *Xbarc0013a–Xgwm0271a* | -2.98 | RAC875 | 28.72 | 32.1 |
| | ***QTgw.aww-2D$^{NA}$*** | 92.2 | 85.2-108.1 | *XwPt-0330–Xbarc0328b* | 1.86 | Kukri | 8.22 | 9.2 |
| | ***QTgw.aww-6A$^{NA}$*** | 90.1 | 85.0-92.5 | *Xbarc0118–Xwmc0256a* | -0.80 | RAC875 | 1.97 | 3.2 |
| | ***QTgw.aww-7A$^{NA}$*** | 117.3 | 102.2-123.3 | *Xbarc0259–Xbarc0281* | -1.17 | RAC875 | 4.55 | 4.7 |

**Table 5-14. Detected QTLs with CIM analysis for screening fractions, weighted average of screening (Scr) and hectolitre weight (Hlw) in RAC environment. QTL analysis was performed without taking heading time effects into account (non-adjusted data = NA). The most likely QTL position, range, interval of flanking markers, allelic additive effect, heritability and LOD for each individual QTL is presented. The italic bold loci represent putative QTLs which were detected at a 5% significance threshold. Suggestive QTLs were detected at a 10% significance threshold. QTLs with largest trait effect are highlighted in light gray.**

| QTL | Position | Range | Interval | Add | Parent | $h^2$ (%) | LOD |
|---|---|---|---|---|---|---|---|
| ***QN>2.8.aww-1AL$^{NA}$*** | 179.2 | 169.0-201.6 | *XwPt-8644–XwPt-0864* | -2.54 | RAC875 | 4.77 | 4.0 |
| ***QN>2.8.aww-2BS$^{NA}$*** | 47.1 | 42.1-52.6 | *Xbarc0013a–Xgwm0271a* | -4.76 | RAC875 | 11.51 | 11.9 |
| ***QN>2.8.aww-2DS$^{NA}$*** | 65.7 | 49.7-97.2 | *XwPt-6003–XwPt-0330* | 4.82 | Kukri | 3.07 | 7.3 |
| ***QN>2.8.aww-3A$^{NA}$*** | 56.9 | 47.1-65.3 | *Xgwm0002–Xbarc0328a* | -2.83 | RAC875 | 4.46 | 3.4 |
| ***QN>2.8.aww-4D$^{NA}$*** | 5.0 | 0.0-8.0 | *Xgwm0297b–Xwmc0457* | -2.28 | RAC875 | 3.05 | 3.2 |
| ***QN>2.8.aww-6A$^{NA}$*** | 68.7 | 55.1-78.7 | *Xbarc0353b–Xstm0519actc* | -3.59 | RAC875 | 4.64 | 4.8 |
| ***QN>2.8.aww-7A$^{NA}$*** | 93.1 | 58.6-100.1 | *Xcfa2028–Xbarc1004* | -4.00 | RAC875 | 7.97 | 6.7 |
| ***QN>2.8.aww-7D$^{NA}$*** | 48.8 | 24.4-57.8 | *Xbarc0092–Xgwm295* | -2.19 | RAC875 | 2.32 | 3.5 |
| *QN2.5.aww-1AL$^{NA}$* | 192.1 | 178.0-196.1 | *XwPt-6568–Xcfe0242b* | -1.05 | RAC875 | 2.90 | 2.2 |
| *QN2.5.aww-4B$^{NA}$* | 28.7 | 23.9-32.6 | *Xwmc0349–Xwmc0047* | -0.93 | RAC875 | 2.26 | 2.7 |
| ***QN2.5.aww-7B$^{NA}$*** | 26.4 | 20.0-31.4 | *Xstm0671acag–Xgwm0297* | 1.22 | Kukri | 4.09 | 3.3 |
| ***QN2.2.aww-1AL$^{NA}$*** | 178.2 | 170.0-190.6 | *XwPt-8644–XwPt-0864* | 1.70 | Kukri | 5.07 | 3.2 |
| ***QN2.2.aww-2BS$^{NA}$*** | 46.1 | 41.1-52.6 | *Xbarc0013a–Xgwm0271a* | 3.47 | Kukri | 11.01 | 11.6 |
| ***QN2.2.aww-2DS$^{NA}$*** | 84.2 | 52.7-94.2 | *XwPt-0330–Xbarc0328b* | -2.28 | RAC875 | 2.15 | 5.2 |
| ***QN2.2.aww-3A$^{NA}$*** | 96.7 | 86.9-110.8 | *Xwmc0264–Xcfa2193b* | 2.37 | Kukri | 5.85 | 4.0 |
| ***QN2.2.aww-3B$^{NA}$*** | 111.4 | 102.5-130.1 | *Xgwm0131a–Xgwm0383a* | 1.89 | Kukri | 2.93 | 3.7 |
| ***QN2.2.aww-6A$^{NA}$*** | 85.0 | 80.7-97.5 | *Xstm0519actc–Xbarc0118* | 2.31 | Kukri | 4.43 | 3.8 |
| ***QN2.2.aww-7A$^{NA}$*** | 93.1 | 55.6-100.1 | *Xcfa2028–Xbarc1004* | 2.59 | Kukri | 6.28 | 5.2 |
| *QN2.2.aww-7D$^{NA}$* | 49.8 | 28.4-59.8 | *Xgwm295–XwPt-4115* | 1.61 | Kukri | 2.44 | 2.7 |
| ***QN<2.2.aww-1AL$^{NA}$*** | 179.2 | 173.0-190.6 | *XwPt-8644–XwPt-0864* | 1.17 | Kukri | 8.27 | 5.4 |
| ***QN<2.2.aww-1B$^{NA}$*** | 79.0 | 77.8-80.8 | *XwPt-3679–Xbarc1138b* | 1.24 | Kukri | 3.43 | 4.2 |
| ***QN<2.2.aww-2BL$^{NA}$*** | 134.3 | 129.0-138.3 | *XwPt-7360–XwPt-2135* | 1.20 | Kukri | 5.48 | 4.2 |
| ***QN<2.2.aww-2D$^{NA}$*** | 85.2 | 56.7-96.2 | *XwPt-0330–Xbarc0328b* | -1.17 | RAC875 | 2.32 | 3.5 |
| ***QN<2.2.aww-3A$^{NA}$*** | 96.7 | 85.9-119.8 | *Xwmc0264–Xcfa2193b* | 1.36 | Kukri | 4.29 | 3.2 |
| *QN<2.2.aww-5A$^{NA}$* | 61.4 | 50.4-86.0 | *Xgwm0304b–Xbarc0360* | 1.18 | Kukri | 4.21 | 2.8 |
| ***QN<2.2.aww-7A$^{NA}$*** | 90.1 | 57.6-96.1 | *Xcfa2028–Xbarc1004* | 1.25 | Kukri | 4.77 | 4.5 |
| ***QScr.aww-1AL$^{NA}$*** | 179.2 | 169.0-190.6 | *XwPt-8644–XwPt-0864* | -0.23 | RAC875 | 5.93 | 5.3 |
| ***QScr.aww-2BS$^{NA}$*** | 47.1 | 42.1-53.6 | *Xbarc0013a–Xgwm0271a* | -0.38 | RAC875 | 10.42 | 10.7 |
| ***QScr.aww-2D.1$^{NA}$*** | 85.2 | 48.7-95.2 | *XwPt-0330–Xbarc0328b* | 0.32 | Kukri | 2.84 | 5.5 |
| ***QScr.aww-2D.2$^{NA}$*** | 130.4 | 117.7-142.4 | *XwPt-0021–XwPt-4559* | 0.14 | Kukri | 1.13 | 3.8 |
| ***QScr.aww-3A$^{NA}$*** | 60.9 | 48.1-65.3 | *Xbarc0328a–Xgwm0666a* | -0.26 | RAC875 | 5.19 | 3.7 |
| ***QScr.aww-4D$^{NA}$*** | 6.3 | 0.0-8.0 | *Xbarc0288–XwPt-2379* | -0.19 | RAC875 | 3.20 | 3.2 |
| ***QScr.aww-6A$^{NA}$*** | 88.0 | 50.1-100.5 | *Xstm0519actc–Xbarc0118* | -0.23 | RAC875 | 3.77 | 3.9 |
| ***QScr.aww-7A$^{NA}$*** | 92.1 | 57.6-99.1 | *Xcfa2028–Xbarc1004* | -0.33 | RAC875 | 7.83 | 6.3 |
| *QScr.aww-7D$^{NA}$* | 49.8 | 46.8-56.8 | *Xgwm295–XwPt-4115* | -0.26 | RAC875 | 4.02 | 2.7 |
| *QHlw.aww-2A$^{NA}$* | 166.0 | 145.4-166.0 | *XwPt-6687–XwPt-7901* | 2.6 | Kukri | 2.8 | 3.2 |
| *QHlw.aww-2BS$^{NA}$* | 29.5 | 28.0-37.0 | *XwPt-4125–XwPt-5556* | 3.5 | Kukri | 5.8 | 5.4 |
| *QHlw.aww-3B$^{NA}$* | 222.5 | 214.4-230.4 | *XwPt-5072–XwPt-7614* | -3.3 | RAC875 | 5.6 | 4.4 |
| *QHlw.aww-7A$^{NA}$* | 155.9 | 148.3-162.9 | *Xgwm0746–XwPt-5558* | -3.5 | RAC875 | 6.2 | 4.8 |

#### *5.2.3.1.13 QTLs for spike length (non-adjusted data)*

Spike or ear length (El) was affected greatly by environmental conditions. The average spike length in RAC and MexD (relatively mild drought stress) was 91.5 mm, while it was about 60.0 mm in Minn and Bool (severely stressed) environments. This trait correlated positively with heading time (0.41 and 0.37; $P < 0.001$) and negatively with grain yield (-43 and -0.26; $P < 0.001$) in the RAC and MexD environments. In contrast, in the Minn and Bool environments, spike length was negatively correlated with heading time and positively correlated with grain yield (Table 5-4). The 'Kukri' parent showed 3 to 12 mm longer spikes compared to 'RAC875' in all tested environments (Table 5-3).

Fifteen QTLs for El were detected on seven chromosomes (1A, 2B, 3A, 3D, 6D, 4B and 7A) in four environments (Table 5-15). For ten QTLs, the 'Kukri' allele was associated with longer spikes relative to the 'RAC875' allele. Three putative QTLs on 3A, 3D and 7A were detected in more than three environments with LOD > 2.6. The phenotypic variation explained by these QTLs, depending on environments, ranged from 2.0% to 16.9%. ***QEl.aww-3A$^{NA}$*** was located on the short arm of chromosome 3A at *Xgwm0002* (56.9 cM), overlapping plant height, peduncle length, number of spikelets per spike and TGW. ***QEl.aww-3D$^{NA}$*** peaked at *Xwmc0533* (69.7 cM) in RAC, Minn and MexD, but it was located at *Xgwm0664* (113.7 cM) at the same position with heading time QTL. The 'RAC875' allele was associated with longer spikes relative to the 'Kukri' allele. Spike length QTL on the long arm of 7A (***QEl.aww-7A$^{NA}$***) was identified in three environments. ***QEl.aww-7A$^{NA}$*** was the most significant QTL in Minn and MexD (LOD of 6.6 and 11.4, respectively), and was identified as a suggestive QTL in Bool (LOD = 2.9; 3.4% of the phenotypic variation). ***QEl.aww-7A$^{NA}$*** peaked at *Xgwm0276* (130.9 cM) overlapped with QTLs for number of spikelets per spike and in repulsion with hectolitre weight and grain yield QTLs.

A spike length QTL on the short arm of chromosome 1A (***QEl.aww-1AS$^{NA}$***; LOD = 4.0 and 3.7% of the phenotypic variation) was only detected in Minn, overlapping heading time QTL. ***QEl.aww-2BS$^{NA}$*** was identified in RAC with LOD of 8.4 and heritability of 9.2%, also colocated with heading time QTL. A suggestive QTL on chromosome 4B (*QEl.aww-4B;* LOD = 2.9; 3.7% of the phenotypic variation) was detected at

*Xwmc0047* (31.6 cM) in Minn in a similar position with TGW and the screening fraction of N>2.8 QTLs. For this QTL, the 'RAC875' allele was associated with longer spikes relative to the 'Kukri' allele. Only one QTL on chromosome 6D (***QEl.aww-6D$^{NA}$***) was significantly identified in RAC at *Xcfd0287* (73.1 cM) with a LOD of 3.8 and the phenotypic variation explained by this QTL was 3.7%. No QTLs for other measured traits were found on this chromosome.

#### *5.2.3.1.14 Flag leaf length (non-adjusted data)*

Flag leaf length (Fl), provided an indication of flag leaf area. This trait was highly correlated with heading time and grain yield (Table 5-4). In the South Australian sites (RAC, Minn and Bool), this trait was negatively correlated with heading time (r = -0.73, -0.73 and -0.63, respectively; $P < 0.001$), since the late-flowering lines suffered more severe drought and heat stress compared to the early flowering lines. However, in the MexD experiment, it showed relatively small and positive correlation with heading time (r = 0.31, $P < 0.001$). This different response might be related to the type of stress in these environments. In South Australia, drought progressed as the plants developed, while in MexD (drip-irrigation) plants had no experience of drought until 50-60 d after sowing, while heading time in this experiment ranged from 61 to 110 d after sowing, indicating that the flag leaf had already developed under non-stressed conditions before heading time (McMaster et al., 2005). The population means for flag leaf length in RAC, Minn, Bool and MexD were 16.5, 13.3, 12.2 and 22.8 cm, respectively (Table 5-4). 'Kukri' had a longer flag leaf compared to 'RAC875'. Flag leaf length of 'Kukri' was about 3.5 cm longer than RAC875 in RAC and MexD, while this difference in flag leaf length reduced to 1.0 cm in Minn and Bool.

Nineteen QTLs for flag leaf length were detected on ten chromosomes (1A, 2B, 2D, 3D, 4B, 5B, 6A, 7A, and 7B) in four drought environments (Table 5-15; Appendix L). The most significant QTLs in RAC, Minn and Bool were located on chromosomes 2BS, 2DS, and 5B (***QFl.aww-2BS$^{NA}$***, ***QFl.aww-2DS$^{NA}$*** and ***QFl.aww-5B$^{NA}$***; LOD > 5.6), and they were coincident with heading time QTLs. Those early flowering alleles were associated with longer flag leaf in these QTLs. ***QFl.aww-4B$^{NA}$*** was detected in RAC with a LOD = 3.5 and it explained 1.5% of the observed phenotypic variation. A QTL for Fl with a small additive effect was detected on chromosome 3D (***QFl.aww-3D$^{NA}$)*** in Minn (LOD = 3.3), which overlapped with heading time QTL. ***QFl.aww-6A$^{NA}$*** was

detected in Minn as a putative QTL with a LOD of 4.0, and it was also identified as a suggestive QTL in Bool with a LOD of 2.5. This QTL was located at *XwPt-7599* (108.5 cM) in a similar position, in repulsion, with number of spikelets, TGW and screening fractions QTLs.

***QFl.aww-7A$^{NA}$*** was detected as a putative QTL (LOD = 5.1; 7.7% of the phenotypic variation) in MexD, and it was also identified as a suggestive QTL (LOD = 2.5) in RAC. This QTL overlapped with grain yield, number of spikelets, spike length and hectolitre weight QTLs. A QTL for flag leaf length with small additive effect (LOD = 3.0; 4.1% of the phenotypic variation) was identified on chromosome 7B in MexD, which co-located with heading time QTL (***QEet.aww-7B$^{NA}$***). Chromosome 7D also contained a QTL for flag leaf length (***QFl.aww-7D$^{NA}$***), which was detected in RAC and Minn as putative and suggestive QTL with LOD of 5.8 and 2.9, respectively. ***QFl.aww-7D$^{NA}$*** explained 4.0% and 1.9% of the phenotypic variation in RAC and Minn, respectively. Overall, the 'Kukri' alleles were associated with longer flag leaves relative to the 'RAC875' alleles in most of the identified QTLs, except in ***QFl.aww-2B$^{NA}$*** and ***QFl.aww-4B$^{NA}$***.

**Table 5-15. Detected QTLs with CIM analysis for spike length (El) and flag leaf length (Fl) in four environments. QTL analysis was performed without taking heading time effects into account (non-adjusted data = NA). The most likely QTL position, range, interval of flanking markers, allelic additive effect, heritability and LOD for each individual QTL is presented. The italic bold loci represent putative QTLs which were detected at a 5% significance threshold. Suggestive QTLs were detected at a 10% significance threshold. QTLs with largest trait effect are highlighted in light gray.**

| Trait | Site | QTL | Position | Range | Interval | Add | Parent | $h^2$ (%) | LOD |
|---|---|---|---|---|---|---|---|---|---|
| El | RAC | ***QEl.aww-2BS$^{NA}$*** | 34.0 | 29.5-38.0 | *XwPt-7757–Xbarc0013a* | 0.24 | Kukri | 9.2 | 8.4 |
| | | ***QEl.aww-3A$^{NA}$*** | 38.1 | 22.3-48.1 | *XwPt-0714–Xgwm0002* | 0.19 | Kukri | 5.8 | 4.9 |
| | | ***QEl.aww-3D$^{NA}$*** | 83.6 | 74.6-94.1 | *Xwmc0533–XwPt-6262* | -0.16 | RAC875 | 5.0 | 5.1 |
| | | ***QEl.aww-6D$^{NA}$*** | 73.1 | 67.9-79.1 | *Xcfd0287–Xwmc0278* | 0.13 | Kukri | 3.7 | 3.8 |
| | Minn | ***QEl.aww-1AS$^{NA}$*** | 29.4 | 25.5-39.4 | *Xcfd0021–XwPt-1657* | 0.07 | Kukri | 3.7 | 4.0 |
| | | *QEl.aww-3A$^{NA}$* | 49.1 | 38.1-61.9 | *XwPt-0714–Xgwm0002* | 0.06 | Kukri | 2.0 | 2.6 |
| | | *QEl.aww-3D$^{NA}$* | 62.9 | 52.7-74.6 | *Xcfd0034–Xwmc0533* | -0.08 | RAC875 | 3.8 | 2.9 |
| | | *QEl.aww-4B$^{NA}$* | 35.6 | 19.9-44.6 | *Xwmc0047–Xbarc0114* | -0.07 | RAC875 | 3.7 | 2.9 |
| | | ***QEl.aww-7A$^{NA}$*** | 159.9 | 150.3-166.4 | *Xgwm0746–XwPt-5558* | 0.10 | Kukri | 8.0 | 6.6 |
| | Bool | ***QEl.aww-3A$^{NA}$*** | 49.1 | 38.1-61.9 | *XwPt-0714–Xgwm0002* | 0.07 | Kukri | 3.3 | 4.3 |
| | | ***QEl.aww-3D$^{NA}$*** | 113.7 | 98.1-116.7 | *Xgwm0664–Xgwm0383b* | -0.08 | RAC875 | 4.5 | 3.7 |
| | | *QEl.aww-7A$^{NA}$* | 157.9 | 146.3-174.2 | *Xgwm0746–XwPt-5558* | 0.07 | Kukri | 3.4 | 2.9 |
| | MexD | *QEl.aww-3A$^{NA}$* | 2.0 | 0.0-14.0 | *Xbarc0057–Xwmc0532* | 0.21 | Kukri | 2.3 | 3.1 |
| | | ***QEl.aww-3D$^{NA}$*** | 82.6 | 69.6-94.1 | *Xwmc0533–XwPt-6262* | -0.24 | RAC875 | 5.9 | 4.1 |
| | | ***QEl.aww-7A$^{NA}$*** | 133.8 | 130.4-146.3 | *Xgwm0276–Xbarc0292* | 0.40 | Kukri | 16.9 | 11.4 |
| Fl | RAC | ***QFl.aww-2BS$^{NA}$*** | 38.0 | 35.0-43.1 | *XwPt-7757–Xbarc0013a* | -0.99 | RAC875 | 17.6 | 24.5 |
| | | ***QFl.aww-2DS$^{NA}$*** | 51.7 | 45.7-59.7 | *XwPt-6003–XwPt-0330* | 2.06 | Kukri | 20.6 | 25.3 |
| | | ***QFl.aww-4B$^{NA}$*** | 37.6 | 4.9-62.6 | *Xwmc0047–Xbarc0114* | -0.43 | RAC875 | 1.5 | 3.5 |
| | | ***QFl.aww-5B$^{NA}$*** | 90.6 | 84.6-96.6 | *XwPt-3457–Xgwm0271b* | 0.87 | Kukri | 10.1 | 13.6 |
| | | *QFl.aww-7A$^{NA}$* | 146.1 | 137.1-155.1 | *Xbarc0292–Xgwm0746* | 0.36 | Kukri | 1.4 | 2.5 |
| | | ***QFl.aww-7D$^{NA}$*** | 103.2 | 88.2-127.9 | *Xstm0535–Xstm0001tcac* | 0.50 | Kukri | 4.0 | 5.8 |
| | Minn | *QFl.aww-1AS$^{NA}$* | 12.0 | 9.1-15.0 | *XwPt-3870–XwPt-6122* | 0.20 | Kukri | 0.5 | 2.2 |
| | | ***QFl.aww-2BS$^{NA}$*** | 37.0 | 34.0-41.1 | *XwPt-7757–Xbarc0013a* | -0.93 | RAC875 | 19.6 | 23.7 |
| | | ***QFl.aww-2DS$^{NA}$*** | 48.7 | 42.7-56.7 | *XwPt-6003–XwPt-0330* | 1.80 | Kukri | 19.3 | 21.0 |
| | | ***QFl.aww-3D$^{NA}$*** | 117.8 | 111.8-124.8 | *Xgwm0383b–Xgwm0314b* | 0.19 | Kukri | 0.5 | 3.3 |
| | | ***QFl.aww-5B$^{NA}$*** | 89.6 | 72.9-99.6 | *XwPt-3457–Xgwm0271b* | 0.51 | Kukri | 4.4 | 5.6 |
| | | ***QFl.aww-6A$^{NA}$*** | 108.5 | 98.5-114.5 | *XwPt-7599–Xksm0098* | 0.36 | Kukri | 3.1 | 4.0 |
| | | *QFl.aww-7D$^{NA}$* | 108.9 | 101.2-133.9 | *Xbarc0058–Xgwm0428* | 0.30 | Kukri | 1.9 | 2.9 |
| | Bool | ***QFl.aww-2BS$^{NA}$*** | 39.1 | 35.0-43.1 | *Xbarc0013a–Xgwm0271a* | -0.26 | RAC875 | 7.3 | 8.0 |
| | | ***QFl.aww-2DS$^{NA}$*** | 50.7 | 43.7-58.7 | *XwPt-6003–XwPt-0330* | 0.88 | Kukri | 22.2 | 21.1 |
| | | ***QFl.aww-5B$^{NA}$*** | 90.6 | 79.9-97.6 | *XwPt-3457–Xgwm0271b* | 0.30 | Kukri | 7.0 | 8.4 |
| | | *QFl.aww-6A$^{NA}$* | 93.0 | 82.7-108.5 | *Xbarc0118–XwPt-7599* | 0.15 | Kukri | 1.4 | 2.5 |
| | MexD | ***QFl.aww-7A$^{NA}$*** | 94.1 | 67.6-99.1 | *Xcfa2028–Xbarc1004* | 0.70 | Kukri | 7.7 | 5.1 |
| | | ***QFl.aww-7B$^{NA}$*** | 7.0 | 2.6-20.0 | *Xbarc0338–Xstm0671acag* | 0.54 | Kukri | 4.1 | 3.0 |

#### *5.2.3.1.15 QTLs for number of spikes per square meter (non-adjusted data)*

Number of spikes per square meter (Spsm) was only measured in MexD environments. It was significantly correlated with grain yield (r = 0.52; $P < 0.001$) and also negatively correlated with heading time (r = -0.43; $P < 0.001$). Four QTLs for number of spikes per unit area were detected on chromosomes 1A, 2B, 2D and 3D with LODs of more than 3.1, and together they explained 41.2% of phenotypic variation (Table 5-16; Appendix L). ***QSpsm.aww-1AS$^{NA}$*** on the short arm of chromosome 1A with a LOD = 3.1 and heritability of 1.6% was located at the estimated position of 6.4 cM in the *XwPt-7541–XwPt-6709* interval. ***QSpsm.aww-2BS$^{NA}$*** was detected at the estimated position of 37.0 cM in the *XwPt-7757–Xbarc0013a* interval with a LOD = 25.0 that alone explained 23.9% of the observed phenotypic variation. The QTL for this trait on the short arm of 2D (***QSpsm.aww-2DS$^{NA}$***) peaked at the position of 45.7 cM in the *XwPt-6003–XwPt-0330* interval with a LOD of 15.0 that explained 11.6% of the phenotypic variation. Other QTL for this trait on 3D (***QSpsm.aww-3D$^{NA}$***) peaked at the estimated position of 116.7 cM in the *Xgwm0664–Xgwm0383b* interval with a LOD = 5.1 and the heritability of 4.1%. All four QTLs for number of spikes per unit area were coincident with heading time QTLs. Early flowering lines had more spikes per unit area compared to late flowering lines. This could result from tiller abortion in the late flowering lines under drought stress.

#### *5.2.3.1.16 QTLs for harvest index (HI) (non-adjusted data)*

HI was only estimated for the RAC experiment in 2006. Phenotypic correlations between HI and heading time and between HI and grain yield was -0.81 and 0.87; $P < 0.001$, respectively. RAC875 significantly showed (p = 0.001) a greater harvest index (HI = 0.36) relative to Kukri (HI = 0.30) in this environment. Four QTLs for HI were identified on chromosomes 1A, 2B, 2D and 7A and together explained 31.6% of phenotypic variation (Table 5-16). All detected QTLs overlapped with heading time QTLs. The most significant QTL for HI was located on the short arm of chromosome 2B (***QHi.aww-2BS$^{NA}$***) with a LOD of 13.7 and heritability of 15.5%. ***QHi.aww-2DS$^{NA}$*** was detected at a similar position with as the heading time QTL ***QEet.aww-2BS*** with a LOD = 8.8 and accounted for 7.8% of the phenotypic variation. A QTL for HI on chromosome 7A, ***QHi.aww-7A$^{NA}$***, was located in the *Xbarc1004–Xbarc0259* interval

and was associated with *Xbarc0259* (113.3 cM) with a LOD of 5.7 and heritability of 5.4%. For ***QHi.aww-2BS$^{NA}$*** and ***QHi.aww-7A$^{NA}$***, the 'RAC875' allele was associated with greater HI values. However, for the other two QTLs, the allele from Kukri was related to high HI values (Fig. 5-21).

#### *5.2.3.1.17 QTLs for crown rot in RAC (non-adjusted data)*

Three QTLs for crown rot score were detected on chromosomes 3B, 6A and 7A in RAC site, collectively accounted for 12.9% of the phenotypic variation (Table 5-16; Appendix K). ***QCre.aww-3BS$^{NA}$*** was located on the short arm of chromosome 3B at *Xbarc0147* (29.7 cM) in the *Xbarc0147–Xcfa2226b* interval, with a LOD of 3.4 and heritability of 4.42%. ***QCre.aww-6A$^{NA}$*** was associated with *Xstm0519actc* (87.0 cM) and peaked between *Xstm0519actc–Xbarc0118* with a LOD of 3.9 and heritability of 3.82%. This QTL overlapped TGW, screening fractions and the average screening QTLs. ***QCre.aww-7A$^{NA}$*** peaked in the *XDuPw0254–Xgwm0276* interval at 129.4 cM. This QTL overlapped with QTLs for grain yield, spikelet number, fertile and non-fertile spikelets. For ***QCre.aww-3BS$^{NA}$*** and ***QCre.aww-7A$^{NA}$***, the 'Kukri' allele was associated with more susceptibility (higher crown rot score), while for ***QCre.aww-6A$^{NA}$*** the 'RAC875' allele was associated with susceptibility to crown rot. In RAC, the reduction in spikelet fertility might be associated with crown rot disease, since the susceptibility allele came from the 'Kukri' parent in ***QCre.aww-7A$^{NA}$***.

**Table 5-16. Detected QTLs with CIM analysis for number of spikes per square meter (Spsm) in MexD, and for harvest index (HI) and crown rot (Cre) in RAC. QTL analysis was performed without taking heading time effects into account (non-adjusted data = NA). The most likely QTL position, range, interval of flanking markers, allelic additive effect, heritability and LOD for each individual QTL is presented. The italic bold loci represent putative QTLs which were detected at a 5% significance threshold. QTLs with largest trait effect are highlighted in light gray.**

| Site | QTL | Position (cM) | Range | Interval | Add | Parent | $h^2$ (%) | LOD |
|---|---|---|---|---|---|---|---|---|
| MexD | ***QSpsm.aww-1A$^{NA}$*** | 6.4 | 2.0-9.0 | *XwPt-7541–XwPt-6709* | 2.05 | Kukri | 1.6 | 3.1 |
| | ***QSpsm.aww-2B$^{NA}$*** | 37.0 | 34.0-41.1 | *XwPt-7757–Xbarc0013a* | -6.15 | RAC875 | 23.9 | 25.0 |
| | ***QSpsm.aww-2D$^{NA}$*** | 45.7 | 38.7-53.7 | *XwPt-6003–XwPt-0330* | 9.23 | Kukri | 11.6 | 15.0 |
| | ***QSpsm.aww-3D$^{NA}$*** | 116.7 | 105.1-122.8 | *Xgwm0664–Xgwm0383b* | 2.54 | Kukri | 4.1 | 5.1 |
| RAC | ***QHi.aww-1A$^{NA}$*** | 6.4 | 4.2-7.7 | *XwPt-7541–XwPt-6709* | 0.018 | Kukri | 2.96 | 3.8 |
| | ***QHi.aww-2B$^{NA}$*** | 37.0 | 33.0-39.1 | *XwPt-7757–Xbarc0013a* | -0.033 | RAC875 | 15.48 | 13.7 |
| | ***QHi.aww-2D$^{NA}$*** | 40.7 | 29.7-49.7 | *XwPt-6003–XwPt-0330* | 0.052 | Kukri | 7.79 | 8.8 |
| | ***QHi.aww-7A$^{NA}$*** | 104.2 | 90.1-113.3 | *Xbarc1004–Xbarc0259* | -0.022 | RAC875 | 5.4 | 5.7 |
| | ***QCre.aww-3B$^{NA}$*** | 29.8 | 18.8-51.9 | *Xbarc0147–Xcfa2226b* | 0.171 | Kukri | 4.42 | 3.4 |
| | ***QCre.aww-6A$^{NA}$*** | 87.0 | 70.7-98.5 | *Xstm0519actc–Xbarc0118* | -0.180 | RAC875 | 3.82 | 3.9 |
| | ***QCre.aww-7A$^{NA}$*** | 129.4 | 127.3-142.3 | *XDuPw0254–Xgwm0276* | 0.177 | Kukri | 4.69 | 3.8 |

#### *5.2.3.1.18 Leaf waxiness (non-adjusted data)*

This population segregated for leaf waxiness. The phenotypic frequency distribution of this trait was normal, and 'RAC875' was the more waxy plant compared to 'Kukri' in all tested environments. QTL analysis for this trait showed twenty six QTLs on eight chromosomes (2B, 2D, 3A, 3B, 3D, 4D, 5B and 6A) in five environments (Table 5-17; Appendix L). For all identified QTLs, the 'RAC875' allele was associated with stronger leaf waxiness compared to the 'Kukri' allele. The most significant QTL for leaf waxiness was identified on the long arm of chromosome 3A (***QW.aww-3AL$^{NA}$***), which was detected in five environments and its contribution to the phenotypic variation, depending on the environment, ranged from 4.73% to 47.82%. ***QW.aww-3AL$^{NA}$*** was associated with *Xwmc0264* (89.7 cM) in the *Xwmc0264–Xcfa2193b* interval. The second most significant QTL was detected on chromosome 2DS (***QW.aww-2D.2$^{NA}$***), in a similar position with the heading time QTL (***QEet.aww-2DS***). ***QW.aww-2D.2$^{NA}$*** was identified in four environments with LOD > 12.4 and heritability ranged from 10.13% to 21.93%. In the RAC, Minn and Bool environments, this QTL was coincident with the heading time QTL at *XwPt-0330* (80.2 cM) in the *XwPt-6003–XwPt-0330* interval. In MexI, however, ***QW.aww-2D.1$^{NA}$*** was located in the distal part of the short arm at *Xbarc0095* (0.0 cM) in the *Xbarc0095–Xwmc0111* interval, with a LOD of 16.6 and heritability of 10.13%. This QTL may be showing a pleiotropic effect of flowering time on wax deposition or it could be the *W2* gene itself, which is closely linked to *Ppd-D1* gene on chromosome 2DS (Nelson et al., 1995).

A QTL for leaf waxiness was detected on chromosome 2B (***QW.aww-2BS$^{NA}$***), with a LOD > 8.5, in two environments (Minn and MexD), in a similar position to the heading time QTL. For ***QW.aww-2BS$^{NA}$***, the 'RAC875' allele that associated with early flowering was also associated with stronger leaf waxiness, suggesting that leaf waxiness was not influenced by later flowering allele in this locus. Other leaf waxiness QTLs with smaller effects were detected on chromosomes 3B (at two sites), 3D (at three sites), 4D and 6A (at four sites). ***QW.aww-3B$^{NA}$*** was detected significantly (LOD = 4.2; 4.18% of the phenotypic variation) in Bool and it was also identified as a suggestive QTL (LOD = 2.2) in RAC. The leaf waxiness QTL on chromosome 3D (***QW.aww-3D$^{NA}$***) was identified in RAC and Minn with LOD of > 5.1, and also as suggestive QTL (LOD = 2.7) in MexI experiment. ***QW.aww-3D$^{NA}$*** did not overlap with heading time QTL and it

was located at the estimated position of 88.1 cM at *XwPt-6262* in the *Xwmc0533-XwPt-6262* interval. ***QW.aww-4D***$^{NA}$ and ***QW.aww-6A***$^{NA}$ were identified in four environments. Together they explained 7.5%, 6.85%, 12.12% and 3.8% of the observed phenotypic variation in RAC, Minn, Bool and MexI, respectively. ***QW.aww-5B***$^{NA}$ for leaf waxiness was only detected in MexI site with a LOD of 4.5 and heritability of 1.07%. This QTL did not overlap adjacent heading time QTL.

Pubescence (Pa) was scored in MexI and MexD experiments 2007. Seven QTLs for pubescence (Pa) were identified on chromosomes 1D, 2A, 2D, 3B, 6B and 7B (Table 5-17). ***QPa.aww-6B***$^{NA}$ was detected in both experiments, while other QTLs were only identified in either MexI or MexD. ***QPa.aww-1D***$^{NA}$, ***QPa.aww-2A***$^{NA}$***, QPa.aww-3B***$^{NA}$ and ***QPa.aww-7B***$^{NA}$ were detected in MexI, and ***QPa.aww-2D***$^{NA}$ was only identified in MexD.

**Table 5-17. Detected QTLs with CIM analysis for leaf waxiness in five environments and pubescence (Pa) in MexD and MexI environments. QTL analysis was performed without taking heading time effects into account (non-adjusted data = NA). The most likely QTL position, range, interval of flanking markers, allelic additive effect, heritability and LOD for each individual QTL is presented. The italic bold loci represent putative QTLs which were detected at a 5% significance threshold. Suggestive QTLs were detected at a 10% significance threshold. QTLs with largest trait effect are highlighted in light gray.**

| Trait | Site | QTL | Position (cM) | Range | Interval | Add | Parent | $h^2$ (%) | LOD |
|---|---|---|---|---|---|---|---|---|---|
| Waxiness | RAC | ***QW.aww-2D.2$^{NA}$*** | 43.7 | 36.7-49.7 | *XwPt-6003–XwPt-0330* | -1.06 | RAC875 | 19.6 | 22.7 |
| | | ***QW.aww-3A$^{NA}$*** | 91.7 | 87.9-95.7 | *Xwmc0264–Xcfa2193b* | -0.61 | RAC875 | 23.1 | 31.6 |
| | | *QW.aww-3B$^{NA}$* | 30.8 | 22.8-41.9 | *Xbarc0147–Xcfa2226b* | -0.12 | RAC875 | 0.6 | 2.2 |
| | | ***QW.aww-3D$^{NA}$*** | 86.6 | 76.6-93.1 | *Xwmc0533–XwPt-6262* | -0.21 | RAC875 | 4.2 | 5.9 |
| | | ***QW.aww-4D$^{NA}$*** | 7.0 | 3.0-8.0 | *XwPt-2379–XwPt-0431* | -0.17 | RAC875 | 2.5 | 4.2 |
| | | ***QW.aww-6A$^{NA}$*** | 102.5 | 95.5-113.5 | *Xwmc0256a–XwPt-7599* | -0.29 | RAC875 | 5.0 | 8.8 |
| | | ***QW.aww-7D$^{NA}$*** | 112.9 | 102.2-138.9 | *Xbarc0058–Xgwm0428* | -0.19 | RAC875 | 2.0 | 4.1 |
| | Minn | ***QW.aww-2B$^{NA}$*** | 37.0 | 32.3-44.1 | *XwPt-7757–Xbarc0013a* | -0.27 | RAC875 | 10.6 | 8.5 |
| | | ***QW.aww-2D.2$^{NA}$*** | 54.7 | 47.7-63.7 | *XwPt-6003–XwPt-0330* | -0.71 | RAC875 | 21.9 | 23.2 |
| | | ***QW.aww-3A$^{NA}$*** | 96.7 | 86.9-102.8 | *Xwmc0264–Xcfa2193b* | -0.19 | RAC875 | 4.7 | 5.1 |
| | | ***QW.aww-3D$^{NA}$*** | 79.6 | 69.6-91.1 | *Xwmc0533–XwPt-6262* | -0.19 | RAC875 | 4.5 | 5.1 |
| | | *QW.aww-4D$^{NA}$* | 7.0 | 3.0-8.0 | *XwPt-2379–XwPt-0431* | -0.17 | RAC875 | 2.5 | 3.0 |
| | | ***QW.aww-6A$^{NA}$*** | 104.5 | 92.5-115.5 | *Xwmc0256a–XwPt-7599* | -0.14 | RAC875 | 2.4 | 3.0 |
| | Bool | ***QW.aww-2D.2$^{NA}$*** | 50.7 | 42.7-61.7 | *XwPt-6003–XwPt-0330* | -0.70 | RAC875 | 13.3 | 12.4 |
| | | ***QW.aww-3A$^{NA}$*** | 93.7 | 87.9-102.7 | *Xwmc0264–Xcfa2193b* | -0.26 | RAC875 | 5.2 | 5.6 |
| | | ***QW.aww-3B$^{NA}$*** | 33.9 | 20.8-47.9 | *Xbarc0102–Xwmc0043* | -0.20 | RAC875 | 4.2 | 4.2 |
| | | ***QW.aww-4D$^{NA}$*** | 8.0 | 4.0-8.0 | *XwPt-2379–XwPt-0431* | -0.24 | RAC875 | 5.8 | 5.9 |
| | | ***QW.aww-6A$^{NA}$*** | 103.5 | 96.5-113.5 | *Xwmc0256a–XwPt-7599* | -0.30 | RAC875 | 6.3 | 7.0 |
| | MexI | ***QW.aww-2D.1$^{NA}$*** | 0.0 | 0.0-5.5 | *Xbarc0095–Xwmc0111* | -0.19 | RAC875 | 10.1 | 16.6 |
| | | ***QW.aww-3A$^{NA}$*** | 89.7 | 87.9-92.7 | *Xwmc0264–Xcfa2193b* | -0.46 | RAC875 | 47.8 | 77.0 |
| | | *QW.aww-3D$^{NA}$* | 88.1 | 77.6-92.1 | *XwPt-6262–XwPt-7894* | -0.06 | RAC875 | 1.0 | 2.7 |
| | | ***QW.aww-4D$^{NA}$*** | 7.0 | 3.0-8.0 | *XwPt-2379–XwPt-0431* | -0.09 | RAC875 | 2.0 | 3.5 |
| | | ***QW.aww-5B$^{NA}$*** | 55.6 | 46.7-67.4 | *Xbarc0004b–Xgwm0540a* | -0.10 | RAC875 | 2.1 | 4.5 |
| | | *QW.aww-6A$^{NA}$* | 94.5 | 86.0-103.5 | *Xwmc0256a–XwPt-7599* | -0.08 | RAC875 | 1.5 | 2.6 |
| | MexD | ***QW.aww-2B$^{NA}$*** | 41.1 | 33.0-46.1 | *Xbarc0013a–Xgwm0271a* | -0.22 | RAC875 | 6.6 | 9.5 |
| | | ***QW.aww-3A$^{NA}$*** | 90.7 | 87.9-93.7 | *Xwmc0264–Xcfa2193b* | -0.62 | RAC875 | 45.2 | 70.3 |
| Pubescence | MexI | ***QPa.aww-1D$^{NA}$*** | 120.8 | 110.8-142.4 | *Xcfd0027–XwPt-1799* | -0.081 | RAC875 | 5.0 | 4.4 |
| | | ***QPa.aww-2A$^{NA}$*** | 102.3 | 98.1-112.3 | *Xgwm0312–Xwmc0181b* | -0.061 | RAC875 | 1.5 | 3.7 |
| | | ***QPa.aww-3B$^{NA}$*** | 188.0 | 175.8-200.1 | *XwPt-4401–XwPt-9368* | -0.061 | RAC875 | 2.5 | 3.1 |
| | | ***QPa.aww-6B$^{NA}$*** | 93.1 | 90.1-95.4 | *XwPt-3581–Xgwm0626* | 0.126 | Kukri | 15.2 | 13.1 |
| | | ***QPa.aww-7B$^{NA}$*** | 23.0 | 17.0-31.4 | *Xbarc0338–Xstm0671acag* | 0.154 | Kukri | 15.7 | 18.0 |
| | MexD | ***QPa.aww-2D$^{NA}$*** | 57.7 | 46.7-91.2 | *XwPt-6003–XwPt-0330* | -0.140 | RAC875 | 9.1 | 8.8 |
| | | ***QPa.aww-6B$^{NA}$*** | 102.2 | 93.1-110.6 | *Xbarc0223–Xbarc0247* | 0.065 | Kukri | 4.8 | 4.3 |

#### *5.2.3.1.19 QTLs for chlorophyll content (non-adjusted data)*

Chlorophyll content was measured at anthesis in two environments (RAC and MexI). The population means for chlorophyll content were 55.3 and 49.6 SPAD unit in the RAC and MexI environments, respectively. Plants that grew under stress showed more chlorophyll than non-stressed plants. The population ranges for chlorophyll content were 49.2-60.7 and 44.0-54.8 in RAC and MexI, respectively. 'RAC875', generally, showed on average 11.5 SPAD units higher chlorophyll content than the 'Kukri' in both environments (Fig. 5-8). The heritability of this trait was 0.56 and 0.45 in the RAC and MexI experiments, respectively.

Fifteen QTLs for chlorophyll content (Spad) were identified on ten chromosomes in two environments. QTLs for Spad on chromosomes 1B, 3B, 4A, 5B and 7D were detected in two environments, while those on chromosomes 2B, 4D, 6B, 7A, and 7B were only detected in one environment (Table 5-18; Appendix L). The most significant QTLs were ***QSpad.aww-5B.1***$^{NA}$ and ***QSpad.aww-5B.2***$^{NA}$ which was detected on chromosome 5B with LODs of 6.6 and 7.2 in RAC and MexI, respectively. ***QSpad.aww-5B.2***$^{NA}$ was located in the distal part of the long arm of chromosome 5B at *XwPt-9013* (141.9 cM) in the *XwPt-9103–Xwmc0099* interval. This QTL explained 8.3% of the phenotypic variation for chlorophyll content in RAC. In MexI, however, ***QSpad.aww-5B.1***$^{NA}$ peaked at *XwPt-3457* (83.6 cM) in the *XwPt-3457–Xgwm0271b* interval, overlapping with heading time QTLs in this region and accounted for 6.8% of the phenotypic variation.

***QSpad.aww-1B***$^{NA}$ was detected as putative QTL (LOD = 4.9; 4.5% of the variation) in RAC, and it was also detected as a suggestive QTL (LOD = 2.6; 2.5% of the variation) in MexI. This QTL was associated with *XwPt-0944* (166.1 cM) overlapping with QTLs for grain number from sample spikes, and fertile and non-fertile spikelets. A QTL for SPAD was only detected in RAC on the long arm of chromosome 2B (***QSpad.aww-2BL***$^{NA}$) with a LOD of 4.9 and heritability of 11.8%. This QTL was located at *XwPt-3378* (129.0 cM) in the *XwPt-3378–XwPt-7360* interval in a similar position with QTL for TGW; both were clearly distinct from heading time QTL on this chromosome (Tab5-13; Figure 5-17). A QTL with small additive effect was significantly identified on chromosome 3B (***QSpad.aww-3B***$^{NA}$) with a LOD of 3.2 and heritability of 3.6%.

*QSpad.aww-3B* was also detected as a suggestive QTL in RAC and MexI (LOD = 2.7; 1.53% of the variation), which peaked at *Xbarc0102* (33.9 cM) in the *Xbarc0102–Xwmc0043*, 34.2 cM interval. ***QSpad.aww-4A***$^{NA}$ was detected (LOD > 3.6) in both environments, and was associated with *Xbarc0106* (14.2 cM). This QTL accounted for 5.1% and 3.2% of the phenotypic variation in RAC and MexI environments, respectively. Two other SPAD QTLs were identified on chromosomes 6B and 7B only in MexI. Together they accounted for 9.43% of the phenotypic variation in this environment. ***QSpad.aww-7A***$^{NA}$ (LOD = 3.2; 2.7% of the variation) was detected in a similar position with the grain yield QTL on chromosome 7A only in RAC. Another prominent QTL for SPAD was detected on chromosome 7D (***QSpad.aww-7D***$^{NA}$) with a similar additive effect in both environments. ***QSpad.aww-7D***$^{NA}$ peaked at 91.2 cM between *XwPt-4115* and *Xstm3535*, which was coincident with the QTL for flag leaf length on chromosome 7D.

Four QTLs for leaf color (Lc) were detected on chromosomes 2BS, 2DS, 3A and 3BS in RAC (Table 5-19). ***QLc.aww-2BS***$^{NA}$ and ***QLc.aww-2DS***$^{NA}$ were coincident with the heading time QTL, so that late flowering lines appeared greener than early flowering lines. ***QLc.aww-3A***$^{NA}$ and ***QLc.aww-3BS***$^{NA}$ were coincident with leaf waxiness and chlorophyll content QTLs, respectively.

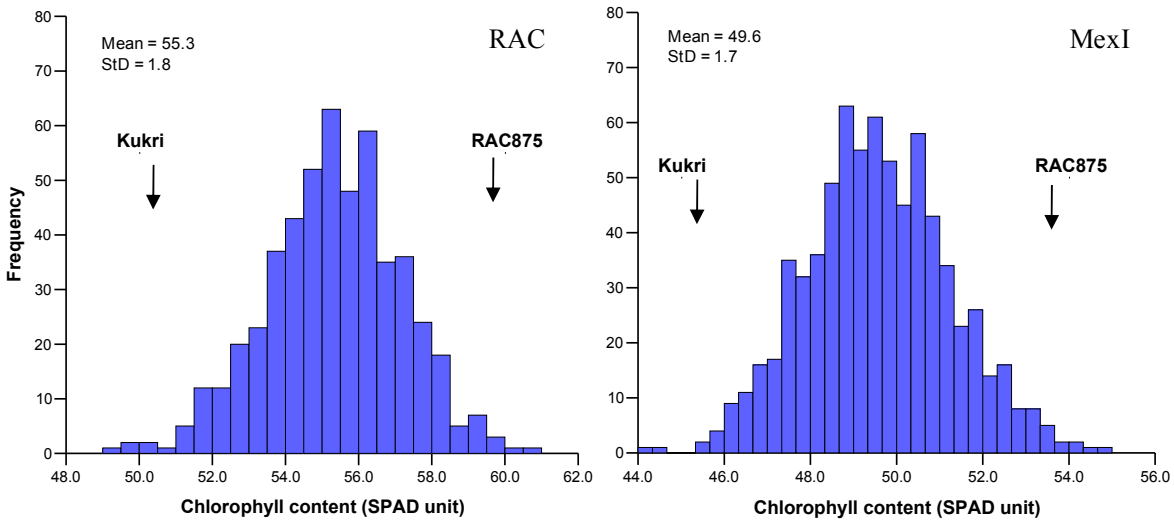


**Figure 5-8. Phenotypic frequency distribution of chlorophyll content for the RAC875/Kukri population in RAC and MexI environments. The population mean (Mean) and the standard error of deviation (StD) are shown in the figure. Arrows indicate the trait value for the two mapping parents.**

**Table 5-18. Detected QTLs with CIM analysis for chlorophyll content (Spad) in RAC and MexI and leaf color (Lc) in RAC. QTL analysis was performed without taking heading time effects into account (non-adjusted data = NA). The most likely QTL position, range, interval of flanking markers, allelic additive effect, heritability and LOD for each individual QTL is presented. The italic bold loci represent putative QTLs which were detected at a 5% significance threshold. Suggestive QTLs were detected at a 10% significance threshold. QTLs with largest trait effect are highlighted in light gray.**

| Trait | Site | QTL | Position (cM) | Range | Interval | Add | Parent | $h^2$ (%) | LOD |
|---|---|---|---|---|---|---|---|---|---|
| Chlorophyll content | RAC | ***QSpad.aww-1B$^{NA}$*** | 167.1 | 151.0-180.1 | *XwPt-9809–XwPt-4129* | -0.50 | RAC875 | 4.5 | 4.9 |
| | | ***QSpad.aww-2BL$^{NA}$*** | 133.9 | 129.0-139.3 | *XwPt-3378–XwPt-7360* | -0.46 | RAC875 | 11.8 | 4.9 |
| | | ***QSpad.aww-3BS$^{NA}$*** | 33.9 | 14.8-47.9 | *Xbarc0102–Xwmc0043* | -0.45 | RAC875 | 3.6 | 3.2 |
| | | *QSpad.aww-4A$^{NA}$* | 12.9 | 1.0-20.2 | *XwPt-7001–Xbarc0106* | -0.39 | RAC875 | 3.9 | 2.8 |
| | | ***QSpad.aww-4D$^{NA}$*** | 7.0 | 3.0-8.0 | *XwPt-2379–XwPt-0431* | -0.57 | RAC875 | 5.1 | 5.4 |
| | | ***QSpad.aww-5B.2$^{NA}$*** | 141.9 | 140.9-143.9 | *XwPt-9103–Xwmc0099* | -0.60 | RAC875 | 8.3 | 6.6 |
| | | *QSpad.aww-7A$^{NA}$* | 106.2 | 59.6-128.3 | *Xbarc1004–Xbarc0174* | -0.45 | RAC875 | 2.7 | 3.2 |
| | | ***QSpad.aww-7D$^{NA}$*** | 91.2 | 78.2-105.2 | *XwPt-4115–Xstm0535* | -0.45 | RAC875 | 4.3 | 3.6 |
| | MexI | *QSpad.aww-1BL$^{NA}$* | 145.5 | 137.6-151.0 | *Xbarc0256–XwPt-9809* | -0.28 | RAC875 | 2.5 | 2.6 |
| | | *QSpad.aww-3BS$^{NA}$* | 33.9 | 14.8-47.9 | *Xbarc0102–Xwmc0043* | -0.22 | RAC875 | 1.5 | 2.7 |
| | | ***QSpad.aww-4A$^{NA}$*** | 18.2 | 10.9-35.9 | *Xbarc0106–XDuPw0328* | -0.32 | RAC875 | 3.2 | 3.6 |
| | | ***QSpad.aww-5B.1$^{NA}$*** | 89.6 | 79.9-97.6 | *XwPt-3457–Xgwm0271b* | -0.47 | RAC875 | 6.8 | 7.2 |
| | | ***QSpad.aww-6B$^{NA}$*** | 121.6 | 109.6-146.1 | *Xbarc0247–Xbarc0134* | 0.38 | Kukri | 2.4 | 4.3 |
| | | ***QSpad.aww-7B$^{NA}$*** | 33.6 | 29.4-40.2 | *Xgwm0297–Xbarc0065* | -0.42 | RAC875 | 7.0 | 4.2 |
| | | ***QSpad.aww-7D$^{NA}$*** | 91.2 | 78.2-105.2 | *XwPt-4115–Xstm0535* | -0.63 | RAC875 | 4.3 | 3.0 |
| Leaf color | RAC | ***QLc.aww-2BS$^{NA}$*** | 34.0 | 26.8-49.0 | *XwPt-7757–Xbarc0013a* | 0.20 | Kukri | 3.3 | 3.0 |
| | | ***QLc.aww-2DS$^{NA}$*** | 47.7 | 40.7-56.7 | *XwPt-6003–XwPt-0330* | -0.86 | RAC875 | 36.7 | 13.1 |
| | | ***QLc.aww-3A$^{NA}$*** | 93.7 | 87.9-98.7 | *Xwmc0264–Xcfa2193b* | -0.43 | RAC875 | 9.4 | 12.0 |
| | | ***QLc.aww-3BS$^{NA}$*** | 6.2 | 0.0-10.6 | *XwPt-7984–Xbarc0075* | -0.24 | RAC875 | 2.8 | 4.3 |

### *5.2.3.1.20 Water soluble carbohydrates (WSC)*

In 2006, stem WSC was measured once at around anthesis in a small subset of DH lines and the parents of the population grown in the RAC experiment. The average WSC for 20 DH lines was 308.9 mg·g$^{-1}$ DW, for the Kukri parent WSC value (261.6 mg·g$^{-1}$ DW) was significantly ($p = 0.007$) lower than the RAC875 parent (312.8 mg·g$^{-1}$ DW). RAC875 accumulated about 16.4% more WSC compared to Kukri in the RAC environment. The distribution of WSC in this subpopulation was normal (Fig.5-9). This phenotypic frequency distribution suggests that this population is potentially segregating for WSC content.

In 2007, stem WSC were measured at six different time points at booting (heading in irrigation experiment), at 7, 13, 19 and 25 days post-anthesis (DPA) and at pre-harvest. At each time point, stem and spike dry weights were also recorded. The dry matter accumulation in the stem and the spike for Kukri and RAC875 plants grown under irrigated and drought stressed experiments are shown in Figure 5-10. In the irrigated experiment, the rate of dry matter accumulation in RAC875 and Kukri was similar. Under drought stress conditions, however, the pattern and the rate of dry matter accumulation in the stem and the spike were significantly different. The dry weight for the RAC875 stems were significantly ($P < 0.05$) higher than for Kukri at the stages of 7 and 13 DPA. The rate of dry matter accumulation in the spike was also higher in RAC875 ($b = 4.3$) relative to Kukri ($b = 2.9$) under drought. In this experiment, stem WSC was higher in RAC875 in irrigated and drought stressed experiments (Fig. 5-11). Under irrigation, stem WSC increased linearly to the stage of 25 DPA to 25.1% and 19.4% in RAC875 and Kukri, respectively. It then decreased dramatically to 3.3% and 1.7% in the pre-harvest sample. Under drought, however, the stem WSC value for Kukri reached the highest level at 7 DPA of 17.9%, while it was 20.8% for RAC875. The highest stem WSC value for RAC875 was 21.5% at 13 DPA; in contrast Kukri had 15.9% WSC at this stage. Stem WSC decreased to 0.75% and 5.4% at pre-harvest in the Kukri and the RAC875 stems, respectively. These data support the results of the growth room experiment for WSC (Chapter 3; Section 3.3.3), where RAC875 consistently accumulated more stem reserves compared to Kukri under well watered and drought conditions.

In the field experiment (Mexico, 2007), RAC875 had significantly larger grains, higher grain yield, a higher grain number per square meter and a greater harvest index under drought than Kukri. In the irrigated experiment, although RAC875 had significantly larger grains compare to Kukri, there were no significant differences in grain yield, number of grains per unit area and harvest index between RAC875 and Kukri (Table 5-19).

The presented stem WSC data from the two mapping parents and only 20 DH lines did not allow performing any QTL analysis. However, future work will be required to map WSC in this population.

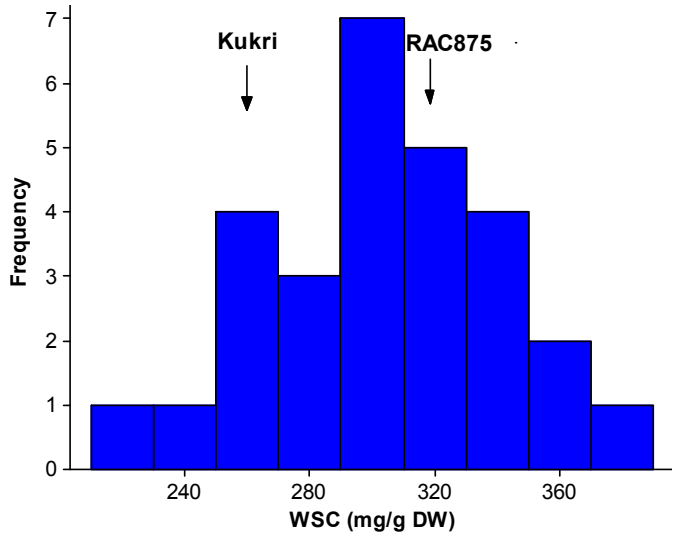


**Figure 5-9. Phenotypic frequency distribution of WSC at anthesis in a subset of 20 DH lines along with parents of the population grown in the RAC environment, 2006. Arrows indicate the trait value for the two mapping parents.**

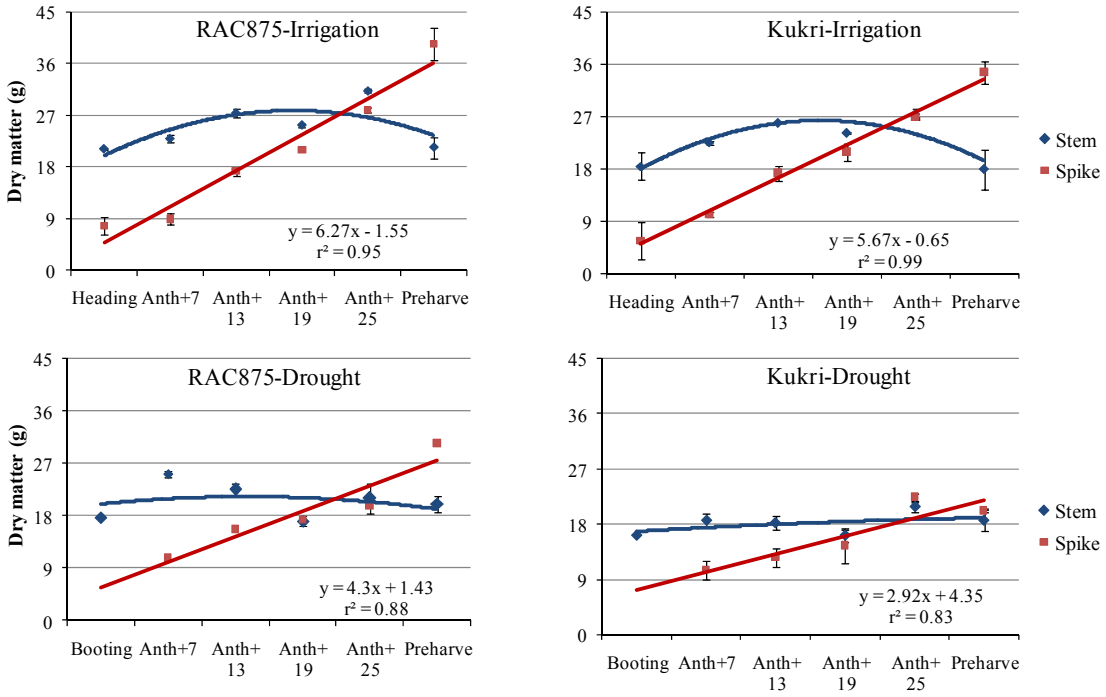


**Figure 5-10. Dry matter accumulation in stems and spikes throughout the reproductive stages from booting to pre-harvest in RAC875 and Kukri grown under irrigation and drought at CIMMYT, Mexico, 2007. $r^2$ was calculated for the spike.**

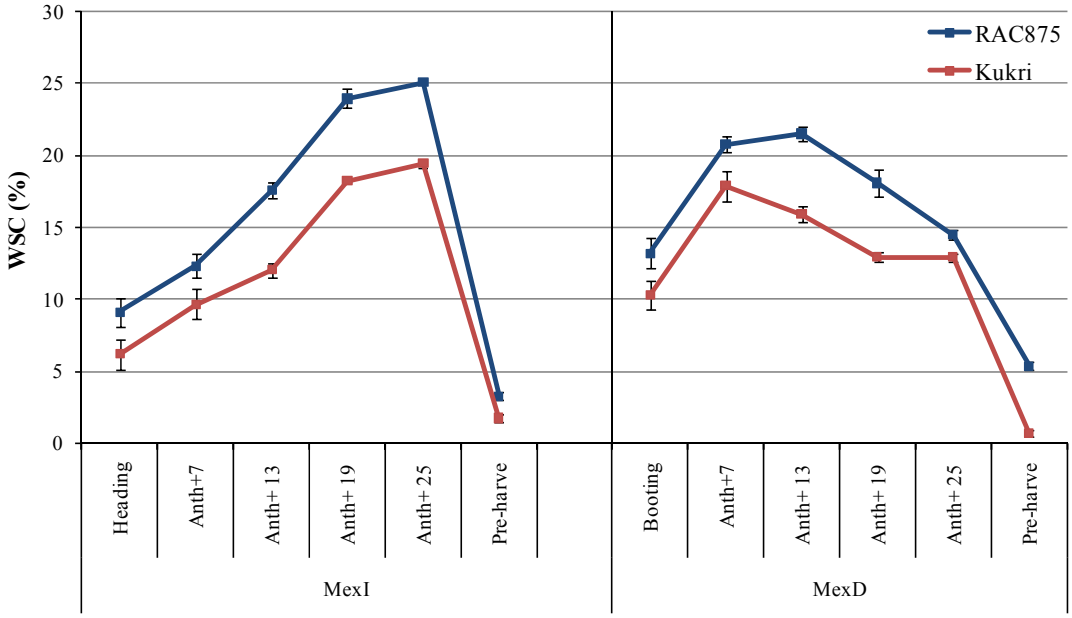


**Figure 5-11. Percentage of WSC in stem samples throughout the reproductive stages from booting to pre-harvest for Kukri and RAC875 grown under irrigation and drought at CIMMYT, Mexico, 2007. Data were kindly provided by Matthew Reynolds.**

**Table 5-19. The differences between RAC875 and Kukri for grain yield, TGW, grain number per unit area and HI under irrigation and drought experiments at CIMMYT, Mexico 2007.**

| Trial | Cultivars | YLD (g.m$^{-2}$) | TGW (g) | GM2 (No) | HI |
|---|---|---|---|---|---|
| MexI | RAC875 | 410.0 | 52.2 | 7861.0 | 0.42 |
| | Kukri | 377.0 | 43.4 | 8682.0 | 0.43 |
| | LSD (0.05) | 98.8 | 4.1 | 2835.0 | 0.04 |
| MexD | RAC875 | 199.0 | 30.9 | 6449.0 | 0.50 |
| | Kukri | 113.0 | 19.5 | 5814.0 | 0.43 |
| | LSD (0.05) | 30.9 | 1.7 | 1374.0 | 0.04 |

### 5.2.4 Identification of QTLs by taking heading time effects into account (*adjusted data*)

In the population under study, most data were confounded by genetic variation in flowering time. As mentioned in the Materials and Methods (section 5.2.3.3), to correct the relationship between heading time and other agronomical traits, especially grain yield, different approaches were implemented to deal with the confounding effect of different flowering time.

#### 5.2.4.1 QTLs for early- and late-flowering subpopulations (*split-up data*)

The phenotypic frequency distribution of heading time showed a bimodal pattern (3:1 ratio) in this population (Fig. 5-3 and 5-12). The late flowering lines were easily distinguishable based on their phenotype. Therefore, the population of 368 lines was divided into two subpopulations of 260 and 108 lines based on their heading time phenotype. The ranges of heading time, depending on the environment, were a range of 21 to 30 d for the early-flowering and a range of 15 to 28 d for the late-flowering subpopulations.

QTL analyses were conducted separately for each subpopulation (early- and late-flowering). Figure 5-12 shows the association between heading time and grain yield in the five different environments for the whole population. Although heading time had a generally large impact on grain yield in this population, there was considerable variation among DH lines for grain yield with very similar heading time in both subpopulations (Fig 5-12). The general trend can be broken up by splitting the population into two subpopulations. Therefore, QTL analysis on each individual subpopulation may reduce confounding effects of heading time on other traits.

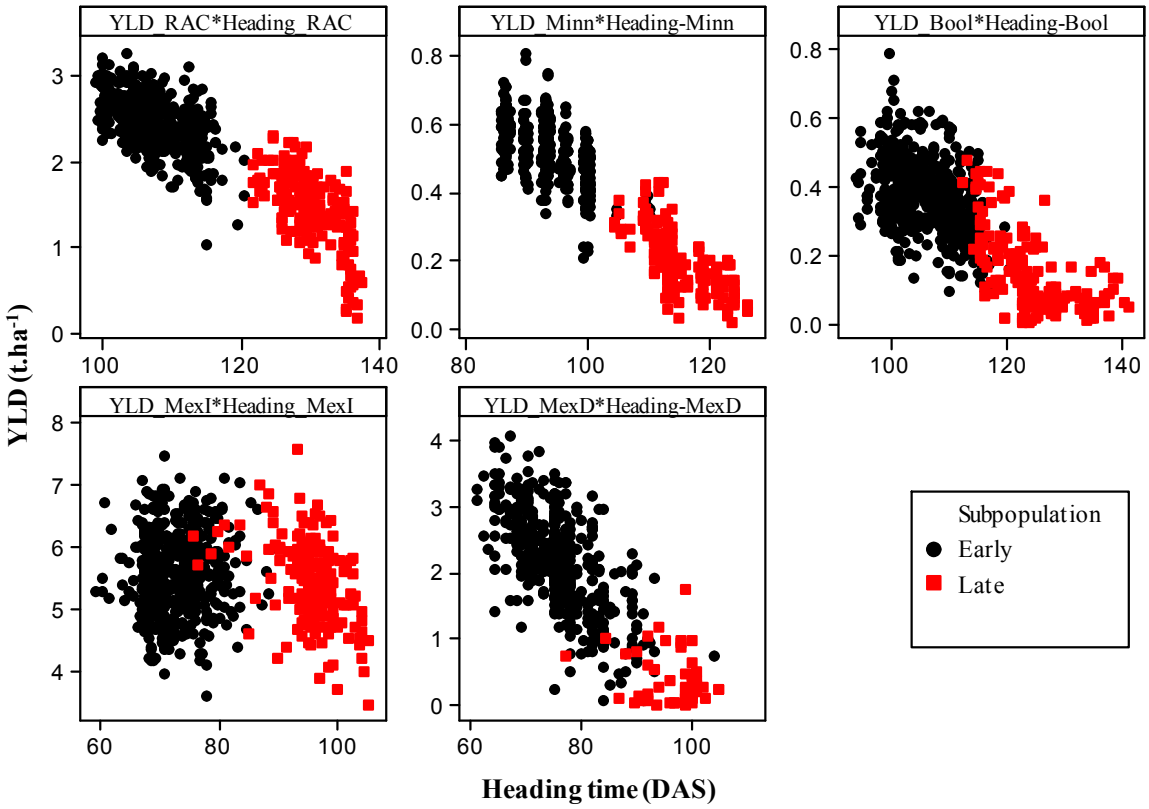


**Figure 5-12. Scatter plot between grain yield (YLD) and heading time for the RAC875/Kukri population in five environments. The population of 368 DH lines was divided into 260 early- and 100 late-flowering DH lines.**

#### *5.2.4.1.1 QTLs for heading time for the early- and late-flowering subpopulations*

By dividing the population into two subpopulations of 260 and 100 lines, the heading time QTL on chromosome 2B (***QEet.aww-2B***) disappeared (Fig. 5-21). In the early-flowering subpopulation, overall, seventeen QTLs for heading time were identified on five chromosomes (2D, 3D, 5B, 7A and 7B) in five environments (Appendix E, L and M). The most significant QTL was ***QEet.aww-2D$^{EF}$***, which was also detected for the whole population dataset.

In the late-flowering subpopulation, eleven QTLs were identified on chromosomes 4A (only one site), 5B, 7A and 7B. Heading time QTL on chromosome 5B, 7A and 7B were detected in both the early- and late-flowering subpopulations in more than three environments, almost overlapping corresponding loci that were detected for the whole population dataset (Table 5-6). Heading time QTL on chromosome 7A (***QEet.aww-***

***7A$^{EF}$*** and ***QEet.aww-7A$^{LF}$***) was detected at *Xcfa2028* (90.1 cM) in the *Xcfa2028-Xbarc1004* interval in both subpopulations (Fig. 5-21). On chromosomes 2D, 3D and 5B, the 'RAC875' alleles were associated with later flowering in the early- and late-flowering subpopulations relative to the 'Kukri' alleles. However, for two other QTLs on chromosomes 7A and 7B, the 'Kukri' alleles were associated with later flowering.

Based on the result of QTL analysis from non-adjusted data using the whole population, the RAC875 allele of ***QEet.aww-2BS*** (potentially *Ppd-B1*) was the most significant QTL for heading time in all environments. Single marker analysis showed that DArT marker locus *XwPt-7757* on chromosome 2B was significantly associated with heading time across all environments, and that the 'RAC875' allele of ***QEet.aww-2BS*** was associated with earlier flowering (Table 5-5). The second significant heading time QTL was ***QEet.aww-2DS*** (potentially *Ppd-D1*) on chromosome 2DS, at marker locus *XwPt-0330,* where the 'Kukri' allele of ***QEet.aww-2DS*** was associated with earlier flowering.

By dividing the population into two subpopulations based on the phenotypic data of heading time, the flowering effect of ***QEet.aww-2BS*** was fixed and disappeared. The phenotypic frequency distribution of heading time among the early-flowering lines (~260 DH lines) showed that alleles from both parents were rather equally distributed at *XwPt-7757-2BS*, whereas among the late-flowering lines (~100 DH lines), 90.0% of the lines possessed the later-flowering 'Kukri' allele (Fig. 5-13 and Fig. 5-14a ). Alternatively, the ***QEet.aww-2DS*** QTL was only detected in the early-flowering subpopulation at *XwPt-0330-2DS,* but it was not identified in the late-flowering subpopulation. Among the late-flowering lines, 74.7% had the later-flowering allele from 'RAC875' at *XwPt-0330-2DS* (Fig. 5-14b). The combination of two late-flowering alleles from each parent on 2BS (the 'Kukri' allele) and 2DS (the 'RAC875' allele) were associated with extreme late-flowering in this population.

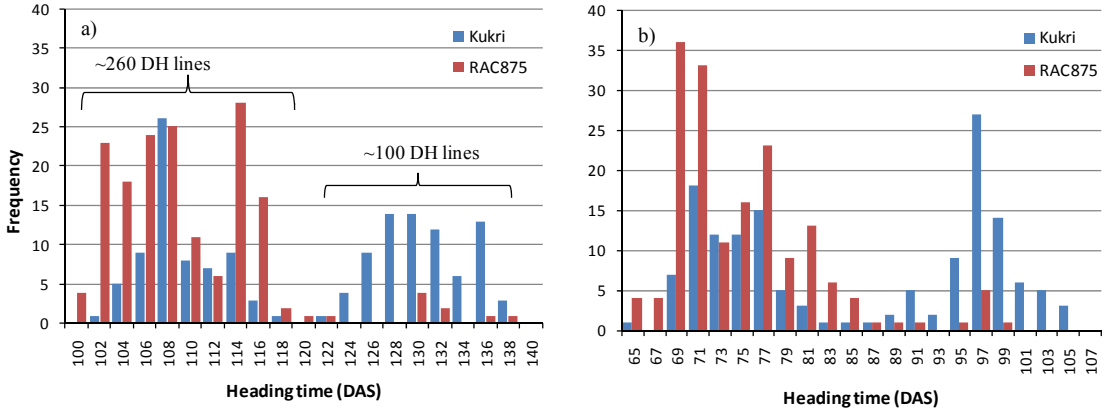


**Figure 5-13. Phenotypic frequency distribution of heading time at *XwPt-7757-2BS* controlling heading time in RAC (a) and MexI (b) environments. The majority of lines in late-flowering group possess the 'Kukri' allele conferring late flowering.**

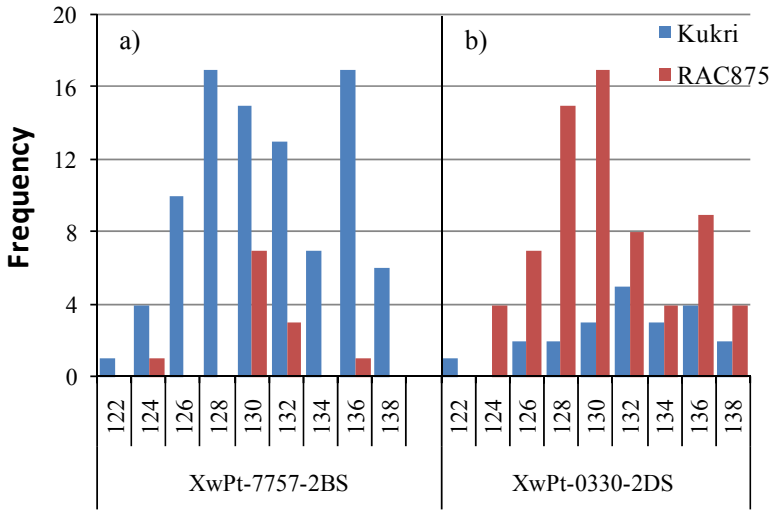


**Figure 5-14. Phenotypic frequency distribution of heading time among the late-flowering lines (~100 DH lines) at *XwPt-7757 -2BS* (a) and *XwPt-0330-2DS* (b) on chromosomes 2B and 2D, respectively for the heading time data at RAC.**

### *5.2.4.1.2 QTLs for grain yield for the early- and late-flowering subpopulations*

In the split-up populations (early- and late-flowering), 18 QTLs for grain yield were detected on four chromosomes (3B, 5B, 7A and 7B) in five environments (Table 5-20; Appendix M). The largest QTLs for grain yield were located on chromosome 7A in both subpopulations. These QTLs were only identified in the drought-affected environments including RAC, Minn, Bool and MexD (Fig. 5-13 and 5-14). For the early-flowering subpopulation ***QYld.aww-7A.1$^{EF}$*** was only detected in MexD in a similar position with heading time QTL at marker *Xcfa2028* (90.1 cM). ***QYld.aww-***

***7A.2$^{EF}$*** peaked (LOD > 4.0) in a ~30 cM interval from *Xbarc0259* (113.3 cM) to *Xgwm0276* (130.9 cM) in RAC, Minn and Bool (Fig. 5-15). In RAC and Minn, ***QYld.aww-7A.2$^{EF}$*** peaked at *Xgwm0276* with a LOD of 7.9 and 8.3 that individually explained about 12.5% of the phenotypic variation. In Bool, ***QYld.aww-7A.2$^{EF}$*** peaked at *Xbarc0259* (113.3 cM) in the *Xbarc0259* and *Xbarc0195* interval. One may assume that there are two QTLs for grain yield in this chromosomal region, but there is not enough evidence to declare that there are two separate QTLs since they are overlapping each other. Further work would be required to add more markers in the map with an even distribution throughout the chromosome 7A.

For the late-flowering subpopulation, ***QYld.aww-7A.1$^{LF}$*** was coincident with heading time QTL in RAC, while in Minn and Bool ***QYld.aww-7A.2$^{LF}$*** was located between *Xbarc0259* and *Xbarc0281*. There is a question whether the co-localization of heading time and yield performance under drought in this region are due to pleiotropy or linkage between two loci?

In the drought-affected environments, a linear relationship was observed between heading time and grain yield (Fig. 5-12). Although, splitting the population removed the strong effects of the heading time QTLs on 2B and 2D, it did not break this relationship entirely. In the early- and late-flowering subpopulations, a linear relationship still remained. In the early-flowering subpopulation in MexD, for example, where the strongest association between heading time and grain yield was observed, QTLs for yield and heading time perfectly overlapped (Fig. 5-13; d1 and d2), while in RAC with a weaker relationship these two QTLs were separated (Fig. 5-13; a1 and a2). The association between heading time and yield in this chromosomal region is possibly due to pleiotropism or linkage. However, by breaking up this close association, it might be possible to detect yield QTL independent of heading time effects. A QTL analysis taking heading time effects into account (*adjusted data*) was subsequently performed (see Section 5.3.1.3).

In the MexI dataset, two yield potential QTLs for grain yield were again detected on chromosome 3B (***QYld.aww-3B.1$^{EF}$*** and ***QYld.aww-3B.2$^{EF}$***). In MexD and RAC, ***QYld.aww-3B.1$^{EF}$*** was also detected as putative and suggestive QTL, respectively, which was not detected for non-adjusted data in these drought-affected environments.

For this QTL, the 'Kukri' allele was associated with yield increases. Other small QTLs on 5B and 7B were coincident with heading time QTLs.

**Table 5-20. Detected QTLs with CIM analysis for grain yield for the early-and late-flowering subpopulations (EF and LF) in the RAC, Minn, Bool, MexI and MexD environments. The most likely QTL position, range, interval of flanking markers, allelic additive effect, heritability and LOD for each individual QTL is presented. The italic bold loci represent putative QTLs which were detected at a 5% significance threshold. Suggestive QTLs were detected at a 10% significance threshold. QTLs with largest trait effect are highlighted in light gray.**

| Sub | Site | QTL | Position (cM) | Range | Interval | Add | Parent | $h^2$ (%) | LOD |
|---|---|---|---|---|---|---|---|---|---|
| Early-flowering (EF) | RAC | *QYld.aww-3B.1$^{EF}$* | 88.0 | 78.8-105.5 | *XwPt-8886–XwPt-9510* | 0.05 | Kukri | 2.15 | 2.4 |
| | | *QYld.aww-5B$^{EF}$* | 39.7 | 31.3-46.7 | *XwPt-3389–XwPt-5914* | 0.05 | Kukri | 2.15 | 2.7 |
| | | ***QYld.aww-7A.2$^{EF}$*** | 134.8 | 128.3-140.3 | *Xgwm0276–Xbarc0292* | -0.11 | RAC875 | 12.4 | 7.9 |
| | Minn | ***QYld.aww-7A.2$^{EF}$*** | 129.4 | 126.3-132.4 | *XDuPw0254–Xgwm0276* | -0.03 | RAC875 | 12.6 | 8.3 |
| | | ***QYld.aww-7B.2$^{EF}$*** | 127.9 | 120.9-127.9 | *XwPt-1422–Xscm0002* | -0.03 | RAC875 | 6.9 | 4.1 |
| | Bool | *QYld.aww-5A$^{EF}$* | 82.0 | 55.4-98.0 | *Xgwm0186–XwPt-1370* | 0.03 | Kukri | 6.8 | 2.3 |
| | | ***QYld.aww-7A.2$^{EF}$*** | 113.3 | 107.2-124.4 | *Xbarc0259–Xbarc0195* | -0.02 | RAC875 | 6.8 | 4.0 |
| | MexI | ***QYld.aww-3B.1$^{EF}$*** | 75.8 | 75.1-76.8 | *XwPt-6973–XwPt-8886* | 0.14 | Kukri | 6.6 | 4.4 |
| | | ***QYld.aww-3B.2$^{EF}$*** | 196.1 | 196.1-197.1 | *XwPt-8021–Xgwm0114b* | -0.20 | RAC875 | 12.9 | 8.9 |
| | MexD | ***QYld.aww-3B.1$^{EF}$*** | 81.0 | 80.8-82.0 | *XwPt-8886–XwPt-9510* | 0.18 | Kukri | 6.6 | 4.0 |
| | | ***QYld.aww-7A.1$^{EF}$*** | 90.1 | 89.6-91.1 | *Xcfa2028–Xbarc1004* | -0.20 | RAC875 | 9.5 | 6.9 |
| | | ***QYld.aww-7B.1$^{EF}$*** | 7.0 | 6.6-8.0 | *Xbarc0338–Xstm0671acag* | -0.15 | RAC875 | 4.7 | 3.1 |
| Late-flowering (LF) | RAC | ***QYld.aww-4A$^{LF}$*** | 61.3 | 41.9-77.3 | *Xgwm0637a–XwPt-7924* | 0.17 | Kukri | 10.5 | 4.3 |
| | | *QYld.aww-5B$^{LF}$* | 71.4 | 63.4-80.9 | *Xbarc0088–XwPt-4936* | 0.12 | Kukri | 7.6 | 2.6 |
| | | ***QYld.aww-7A.1$^{LF}$*** | 90.1 | 60.6-94.1 | *Xcfa2028–Xbarc1004* | -0.21 | RAC875 | 27.4 | 6.1 |
| | Minn | *QYld.aww-5B$^{LF}$* | 87.6 | 72.9-95.6 | *XwPt-3457–Xgwm0271b* | 0.02 | Kukri | 4.6 | 2.8 |
| | | ***QYld.aww-7A.2$^{LF}$*** | 117.3 | 110.0-121.4 | *Xbarc0259–Xbarc0281* | -0.05 | RAC875 | 32.2 | 10.2 |
| | Bool | ***QYld.aww-7A.2$^{LF}$*** | 104.2 | 96.1-120.0 | *Xbarc1004–Xbarc0281* | -0.05 | RAC875 | 28.1 | 9.5 |
| | | ***QYld.aww-7B$^{LF}$*** | 56.8 | 38.2-67.8 | *XwPt-4230–Xwmc0517b* | -0.05 | RAC875 | 16.1 | 5.5 |

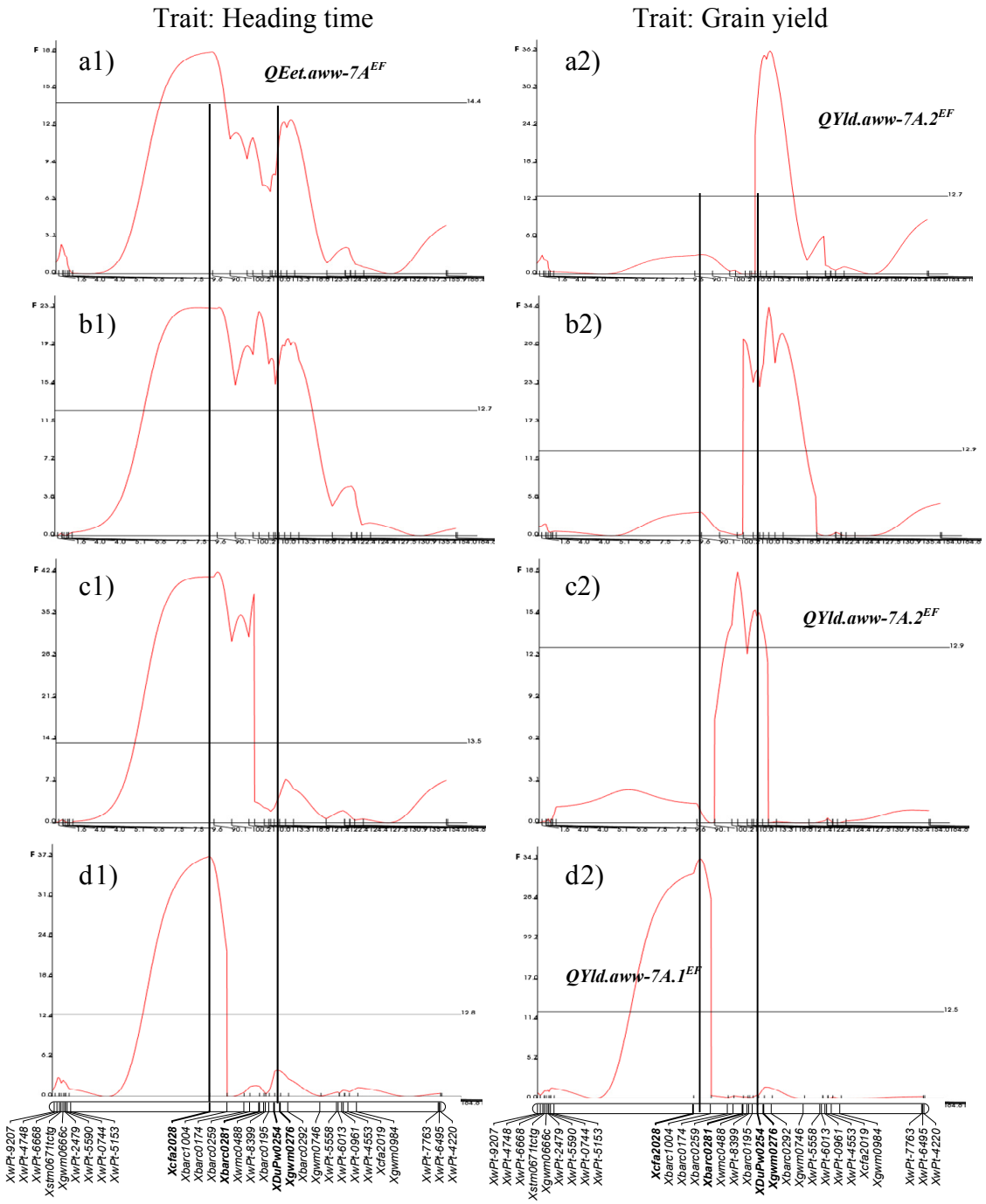


**Figure 5-15. The location of identified QTLs with CIM analysis for heading time (left) and grain yield (right) on chromosome 7A for the early-flowering subpopulation (EF) in the four drought-affected environments RAC (a1, a2), Minn (b1, b2), Bool (c1, c2) and MexD (d1, d2).**

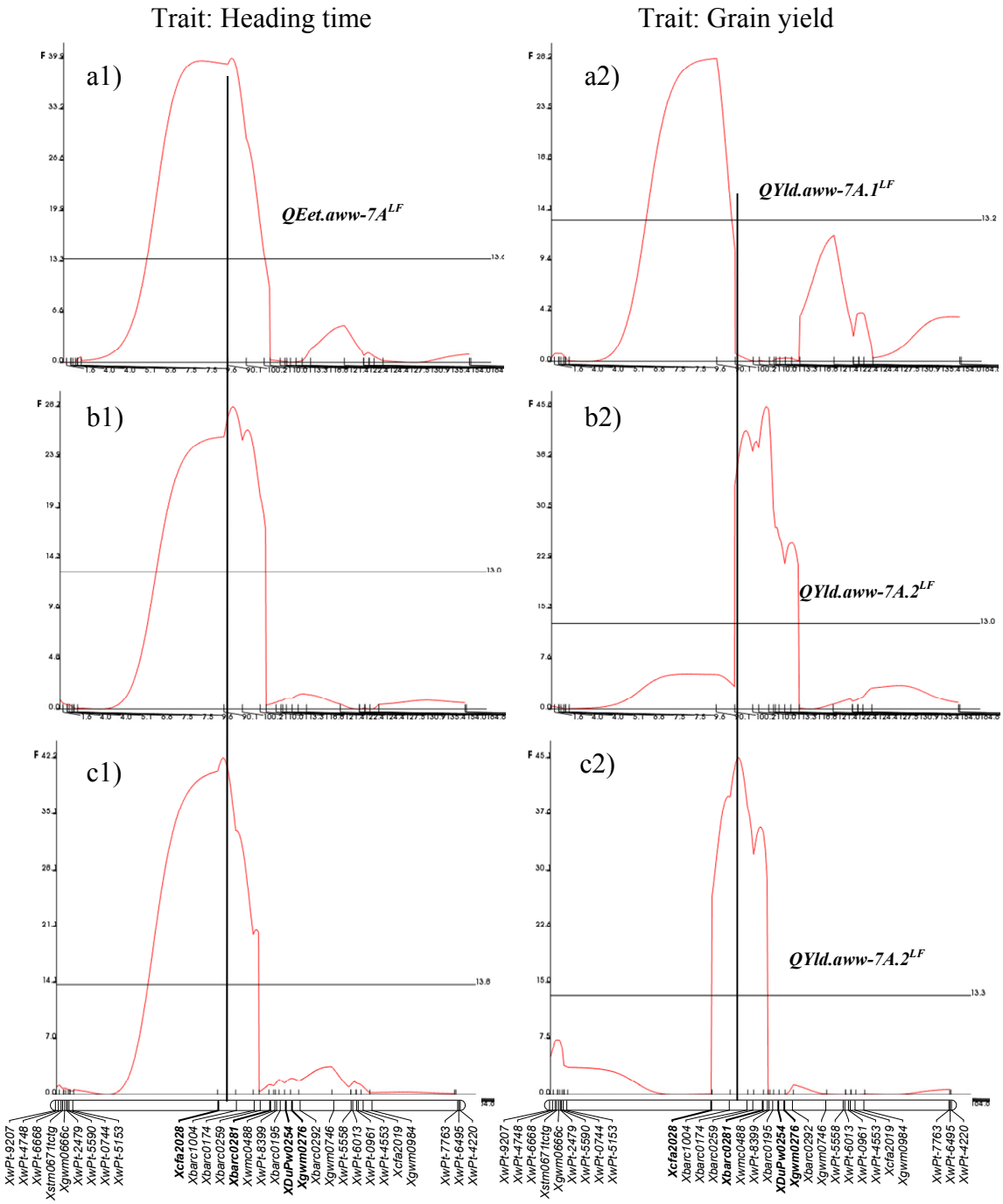


**Figure 5-16. The location of identified QTLs for heading time (left) and grain yield (right) on chromosome 7A for the late-flowering subpopulation (LF) in the three drought-affected environments RAC (a1, a2), Minn (b1, b2) and Bool (c1, c2).**

#### *5.2.4.1.3 QTLs for grains per square meter for the early- and late-flowering subpopulations*

Twenty six QTLs for G·m$^{-2}$ (Kpsm) were detected on chromosomes 1A, 2D, 3B, 4A, 4D, 5B, 6A, 7A and 7B for early- and late- flowering subpopulations (16 and 10 QTLs, respectively) at four sites (Table 5-21; Appendix M). G·m$^{-2}$ QTLs on 1A, 3B (in MexI), 5B, 7A and 7B were also identified for non-adjusted data. For split-up data no QTLs for G·m$^{-2}$ were detected on chromosome 2B and 3D. However, a QTL for G.m$^{-2}$ was only detected on chromosome 2D in Minn. A significant QTL on chromosome 3BS was identified in RAC, Minn and Bool for the early-flowering subpopulation, but they did not overlap. In RAC, ***QKpsm.aww-3B.1$^{EF}$*** peaked at *XwPt-9510* (88.4 cM) in the *XwPt-8886–XwPt-9510* interval. In Minn and Bool, ***QKpsm.aww-3BS$^{EF}$*** was located in the distal part of the short arm of chromosome 3B between *Xbarc0075* (6.6 cM) and *Xbarc0102* (33.9 cM), respectively. In MexI, two QTLs for this trait were detected on chromosome 3B (***QKpsm.aww-3B.1$^{EF}$*** and ***QKpsm.aww-3B.2$^{EF}$***) at a similar position with grain yield QTLs in this site. QTLs on chromosome 4D and 6A were only detected in RAC with LOD > 4.0. Two new QTLs for G.m$^{-2}$ on chromosome 4D (***QKpsm.aww-4D$^{EF}$***) and 6A (***QKpsm.aww-6A$^{EF}$***) were only detected in RAC, while they were not detected for non-adjusted data. ***QKpsm.aww-4D$^{EF}$*** was coincident with QTLs for leaf waxiness, chlorophyll content and larger grain size fraction (N > 2.8mm), while ***QKpsm.aww-6A$^{EF}$*** was coincident with QTLs for TGW, screening fractions and number of spikelets per spike. Another significant QTL for this trait was identified on chromosome 7A (***QKpsm.aww-7A.1$^{EF}$*** and ***QKpsm.aww-7A.2$^{EF}$***). ***QKpsm.aww-7A.1$^{EF}$*** was identified in MexI for the early-flowering subpopulation, and ***QKpsm.aww-7A.1$^{LF}$*** was also detected in Minn and Bool for the late-flowering subpopulation. ***QKpsm.aww-7A.2$^{EF}$*** was detected in Minn and Bool for the early-flowering subpopulation. For the late-flowering subpopulation, ***QKpsm.aww-7A.2$^{LF}$*** was detected in RAC. These QTLs on chromosome 7A (***QKpsm.aww-7A.1$^{EF}$*** and ***QKpsm.aww-7A.2$^{EF}$***) explained most of the phenotypic variations for grain number per square meter in both subpopulations (Table 5-21).

**Table 5-21. Detected QTLs with CIM analysis for grain number per square meter (Kpsm) for the early- and late-flowering subpopulations in the RAC, Minn, Bool, MexI and MexD environments. The most likely QTL position, range, interval of flanking markers, allelic additive effect, heritability and LOD for each individual QTL is presented. The italic bold loci represent putative QTLs which were detected at a 5% significance threshold. Suggestive QTLs were detected at a 10% significance threshold. QTLs with largest trait effect are highlighted in light gray.**

| Sub | Site | QTL | Position (cM) | Range | Interval | Add | Parent | $h^2$ (%) | LOD |
|---|---|---|---|---|---|---|---|---|---|
| Early-flowering | RAC | ***QKpsm.aww-1AL$^{EF}$*** | 182.3 | 172.0-189.1 | *XwPt-0864–XwPt-6754* | 47.0 | Kukri | 5.8 | 3.4 |
| | | ***QKpsm.aww-3B.1$^{EF}$*** | 86.0 | 78.8-110.4 | *XwPt-8886–XwPt-9510* | 133.7 | Kukri | 7.5 | 3.8 |
| | | ***QKpsm.aww-4D$^{EF}$*** | 6.3 | 1.0-8.0 | *Xbarc0288–XwPt-2379* | 135.5 | Kukri | 7.9 | 6.1 |
| | | ***QKpsm.aww-5B$^{EF}$*** | 56.4 | 53.3-64.4 | *Xbarc0088–XwPt-4936* | 131.7 | Kukri | 6.9 | 4.4 |
| | | ***QKpsm.aww-6A$^{EF}$*** | 91.1 | 87.0-98.5 | *Xbarc0118–Xwmc0256a* | 126.2 | Kukri | 5.8 | 4.0 |
| | Minn | ***QKpsm.aww-1AL$^{EF}$*** | 201.6 | 194.1-201.6 | *Xcfe0242b–Xwmc0215a* | 52.8 | Kukri | 4.8 | 3.7 |
| | | ***QKpsm.aww-2DS$^{EF}$*** | 45.7 | 32.7-61.7 | *XwPt-6003–XwPt-0330* | 137.5 | Kukri | 5.1 | 5.2 |
| | | ***QKpsm.aww-3BS$^{EF}$*** | 32.0 | 6.6-33.9 | *Xbarc0075–Xbarc0102* | 58.0 | Kukri | 3.3 | 4.0 |
| | | ***QKpsm.aww-7A.2$^{EF}$*** | 137.3 | 133.8-144.3 | *Xbarc0292–Xgwm0746* | -94.1 | RAC875 | 13.5 | 6.1 |
| | | ***QKpsm.aww-7B$^{EF}$*** | 32.6 | 28.4-36.6 | *Xgwm0297–Xbarc0065* | -69.5 | RAC875 | 7.6 | 3.9 |
| | Bool | ***QKpsm.aww-1AL$^{EF}$*** | 182.3 | 178.2-186.3 | *XwPt-0864–XwPt-6754* | 37.3 | Kukri | 5.2 | 3.7 |
| | | ***QKpsm.aww-3BS$^{EF}$*** | 32 | 20.8-41.9 | *Xcfa2226b–Xbarc0102* | 37.9 | Kukri | 4.1 | 3.7 |
| | | ***QKpsm.aww-7A.2$^{EF}$*** | 129.4 | 118.8-146.3 | *XDuPw0254–Xgwm0276* | -53.3 | RAC875 | 9.8 | 5.2 |
| | MexI | *QKpsm.aww-3B.1$^{EF}$* | 116.2 | 98.5-122.8 | *Xgwm0285–Xbarc0344* | 43.9 | Kukri | 1.9 | 2.8 |
| | | ***QKpsm.aww-3B.2$^{EF}$*** | 186.0 | 175.8-193.0 | *XwPt-4401–XwPt-9368* | -87.5 | RAC875 | 14.8 | 8.1 |
| | | ***QKpsm.aww-7A.1$^{EF}$*** | 113.3 | 104.2-118.8 | *Xbarc0259–Xbarc0281* | 46.8 | Kukri | 5.2 | 3.4 |
| Late-flowering | RAC | ***QKpsm.aww-4A$^{LF}$*** | 61.3 | 38.9-79.3 | *Xgwm0637a–XwPt-7924* | 319.5 | Kukri | 8.0 | 3.3 |
| | | ***QKpsm.aww-5B$^{LF}$*** | 65.4 | 54.3-82.9 | *Xbarc0088–XwPt-4936* | 352.5 | Kukri | 8.3 | 3.8 |
| | | ***QKpsm.aww-7A.1$^{LF}$*** | 90.1 | 63.6-95.1 | *Xcfa2028–Xbarc1004* | -410.7 | RAC875 | 26.4 | 4.5 |
| | | ***QKpsm.aww-7A.2$^{LF}$*** | 155.9 | 145.3-160.9 | *Xgwm0746–XwPt-5558* | -297.1 | RAC875 | 14.4 | 4.7 |
| | | ***QKpsm.aww-7B$^{LF}$*** | 58.8 | 44.0-72.8 | *XwPt-4230–Xwmc0517b* | -309.2 | RAC875 | 7.0 | 3.3 |
| | Minn | ***QKpsm.aww-7A.1$^{LF}$*** | 117.3 | 105.2-121.8 | *Xbarc0259–Xbarc0281* | -116.6 | RAC875 | 25.6 | 7.4 |
| | Bool | ***QKpsm.aww-7A.1$^{LF}$*** | 100.2 | 93.1-109.2 | *Xbarc1004–Xbarc0174* | -97.2 | RAC875 | 20.6 | 7.8 |
| | | ***QKpsm.aww-7B$^{LF}$*** | 42.6 | 38.2-61.8 | *Xbarc0137b–Xwmc0396* | -95.3 | RAC875 | 19.8 | 6.1 |
| | MexI | ***QKpsm.aww-3B$^{LF}$*** | 128.1 | 118.8-141.6 | *Xgwm0853–XwPt-5769* | 96.1 | Kukri | 12.6 | 3.2 |
| | | ***QKpsm.aww-4A$^{LF}$*** | 36.9 | 12.9-50.9 | *Xcfe0254–Xbarc0170* | 95.4 | Kukri | 14.3 | 3.2 |

#### *5.2.4.1.4 QTLs for plant height and peduncle length for early- and late-flowering subpopulations*

For the early-flowering subpopulation, thirteen QTLs for plant height were identified on eight chromosomes (1B, 2D, 3B, 3A, 5A, 6B, 7A and 7B) at four sites, while for the late-flowering subpopulation four QTLs were detected on chromosomes 3A, 4A and 7A (Table 5-23; Appendix M). In the early-flowering subpopulation in Bool, no QTLs were detected for plant height, and only one QTL on 7A at the same position with heading time was detected in the late-flowering subpopulation. Overall, the largest QTL for

plant height was ***QHt.aww-2DS$^{EF}$*** (LOD > 5.5) in the droughted sites RAC, Minn and MexD. This QTL was not detected in MexI, indicating a G by E interaction. Since ***QHt.aww-2DS$^{EF}$*** overlapped with the heading time QTL on 2D (***QEet.aww-2DS***), it might still indicate a residual pleiotropic effect of heading time in this region despite the separation in early- and late-flowering subpopulations. The 'Kukri' allele at this locus was associated with higher plant height relative to the 'RAC875' allele. Another significant QTL for plant height was detected on 3A (***QHt.aww-3A$^{EF}$***) in RAC, MexI and MexD sites, but not in Minn. In severely drought-affected sites like Minn and Bool, this QTL was not detected. This QTL was also detected in the late-flowering subpopulation in RAC (LOD = 5.2; 25.35% of the variation). In the early-flowering subpopulation, the phenotypic contribution of this QTL to the plant height, depending on environment, ranged from 4.17% to 11.56%. The 'RAC875' allele was associated with taller plants compared to the 'Kukri' allele for this QTL. A QTL for plant height on chromosome 5A (***QHt.aww-5A$^{EF}$***) was only detected in RAC with a LOD of 3.4 and heritability of 4.86%. ***QHt.aww-6B$^{EF}$*** was detected in MexI with a LOD of 3.9 at *Xbarc0247* (106.6 cM) in the *Xbarc0247–Xbarc0134* interval. A suggestive QTL on chromosome 3B (*QHt.aww-3B$^{EF}$*) was detected in MexD. This QTL was coincident with the yield QTL detected in MexI (***QYld.aww-3B.1$^{NA}$***), where the 'Kukri' allele was associated with increases in plant height and grain yield. A plant height QTL on chromosome 7A (***QHt.aww-7A.1$^{EF}$***) was detected at two sites (MexI and MexD) for the early-flowering subpopulation. ***QHt.aww-7A.1$^{LF}$*** was also detected in two different sites (RAC and Bool) for late-flowering subpopulation. In MexI, two QTLs for plant height were identified on chromosome 7A (***QHt.aww-7A.1$^{EF}$*** and ***QHt.aww-7A.2$^{EF}$***). ***QHt.aww-7A.1$^{EF}$*** overlapped with the heading time QTL, while ***QHt.aww-7A.2$^{EF}$*** was not associated with heading time. For ***QHt.aww-7A.1$^{EF}$***, an interaction between genotype and environment was found. At the MexI site, the 'Kukri' allele was associated with taller plants for this QTL, whereas the 'RAC875' allele was associated with taller plants at the MexD, RAC and Bool sites. A QTL on chromosome 7B (***QHt.aww-7B$^{EF}$***) was only identified in MexD at the same location with heading time QTL (***QEet.aww-7B***).

Twelve QTLs for peduncle length were detected on six chromosomes (1B, 2D, 3A, 5A, 7A and 7B) in RAC, Minn, Bool and MexD sites (Table 5-22; Appendix M). For the late-flowering subpopulation, three QTLs were detected on 5B and 7A at the three

South Australian sites (RAC, Minn and Bool). All identified QTLs for peduncle length co-localized with plant height QTLs (Table 5-22).

**Table 5-22. Detected QTLs with CIM analysis for plant height (Ht) and peduncle length (Pdl) for the early- and late-flowering subpopulations in RAC, Minn, Bool, MexI and MexD environments. The most likely QTL position, range, interval of flanking markers, allelic additive effect, heritability and LOD for each individual QTL is presented. The italic bold loci represent putative QTLs which were detected at a 5% significance threshold. Suggestive QTLs were detected at a 10% significance threshold. QTLs with largest trait effect are highlighted in light gray.**

| Sub | Site | QTL | Position (cM) | Range | Interval | Add | Parent | $h^2$ (%) | LOD |
|---|---|---|---|---|---|---|---|---|---|
| Early-flowering | RAC | ***QHt.aww-2D$^{EF}$*** | 88.2 | 79.7-97.2 | *XwPt-0330–Xbarc0328b* | 1.40 | Kukri | 7.7 | 6.4 |
| | | ***QHt.aww-3A$^{EF}$*** | 54.1 | 42.1-59.9 | *XwPt-0714–Xgwm0002* | -1.31 | RAC875 | 11.7 | 5.9 |
| | | ***QHt.aww-5A$^{EF}$*** | 171.7 | 155.7-192.5 | *Xcfa2141–XwPt-5231* | 1.08 | Kukri | 4.9 | 3.4 |
| | Minn | ***QHt.aww-2D$^{EF}$*** | 87.2 | 57.7-96.2 | *XwPt-0330–Xbarc0328b* | 0.44 | Kukri | 9.4 | 5.5 |
| | MexI | ***QHt.aww-3A$^{EF}$*** | 56.9 | 56.1-57.9 | *Xgwm0002–Xbarc0328a* | -1.58 | RAC875 | 5.6 | 3.4 |
| | | ***QHt.aww-6B$^{EF}$*** | 106.6 | 106.2-107.6 | *Xbarc0247–Xbarc0134* | 1.60 | Kukri | 6.8 | 3.9 |
| | | *QHt.aww-7A.1$^{EF}$* | 113.3 | 110.0-116.3 | *Xbarc0259–Xbarc0281* | 1.379 | Kukri | 3.0 | 2.7 |
| | | ***QHt.aww-7A.2$^{EF}$*** | 224.5 | 224.1-225.2 | *XwPt-7763–XwPt-6495* | -1.59 | RAC875 | 7.7 | 4.5 |
| | MexD | ***QHt.aww-1B$^{EF}$*** | 75.0 | 74.1-76.0 | *Xcfe0257–XwPt-6240* | -1.54 | RAC875 | 4.7 | 5.5 |
| | | ***QHt.aww-2D$^{EF}$*** | 80.2 | 79.7-81.2 | *XwPt-0330–Xbarc0328b* | 2.89 | Kukri | 13.7 | 13.0 |
| | | ***QHt.aww-3A$^{EF}$*** | 56.9 | 56.1-57.9 | *Xgwm0002–Xbarc0328a* | -1.43 | RAC875 | 4.2 | 3.7 |
| | | *QHt.aww-3B$^{EF}$* | 81.0 | 80.8-82.0 | *XwPt-8886–XwPt-9510* | 1.26 | Kukri | 3.4 | 2.9 |
| | | ***QHt.aww-7A.1$^{EF}$*** | 90.1 | 89.6-97.1 | *Xcfa2028–Xbarc1004* | -1.81 | RAC875 | 8.6 | 5.5 |
| | | ***QHt.aww-7B$^{EF}$*** | 7.0 | 6.6-8.0 | *Xbarc0338–Xstm0671acag* | -1.55 | RAC875 | 5.2 | 4.0 |
| LF | RAC | ***QHt.aww-3A$^{LF}$*** | 64.3 | 41.1-72.6 | *Xbarc0324–XwPt-4077* | -1.47 | RAC875 | 25.4 | 5.2 |
| | | ***QHt.aww-4A$^{LF}$*** | 44.9 | 29.9-79.3 | *Xbarc0170–Xgwm0637a* | 1.54 | Kukri | 9.0 | 6.3 |
| | | ***QHt.aww-7A.1$^{LF}$*** | 94.1 | 69.6-100.2 | *Xcfa2028–Xbarc1004* | -1.56 | RAC875 | 13.8 | 5.1 |
| | Bool | ***QHt.aww-7A.1$^{LF}$*** | 92.1 | 62.6-100.1 | *Xcfa2028–Xbarc1004* | -1.10 | RAC875 | 17.5 | 4.6 |
| Early-flowering | RAC | ***QPdL.aww-2D$^{EF}$*** | 90.2 | 84.2-97.2 | *XwPt-0330–Xbarc0328b* | 1.26 | Kukri | 16.7 | 10.2 |
| | | ***QPdL.aww-3A$^{EF}$*** | 39.1 | 11.0-51.1 | *XwPt-0714–Xgwm0002* | 0.97 | Kukri | 6.8 | 4.8 |
| | | ***QPdL.aww-5A$^{EF}$*** | 165.7 | 136.3-180.7 | *Xcfa2141–XwPt-5231* | 0.87 | Kukri | 5.6 | 4.4 |
| | | ***QPdL.aww-7B$^{EF}$*** | 8.0 | 2.6-21.0 | *Xbarc0338–Xstm0671acag* | -0.56 | RAC875 | 4.1 | 2.8 |
| | Minn | ***QPdL.aww-2D$^{EF}$*** | 86.2 | 50.7-93.2 | *XwPt-0330–Xbarc0328b* | 0.74 | Kukri | 12.2 | 7.3 |
| | | ***QPdL.aww-5A$^{EF}$*** | 164.7 | 124.3-182.7 | *Xcfa2141–XwPt-5231* | 0.52 | Kukri | 5.2 | 3.3 |
| | Bool | ***QPdL.aww-2D$^{EF}$*** | 49.7 | 36.7-74.7 | *XwPt-6003–XwPt-0330* | 0.91 | Kukri | 8.4 | 4.9 |
| | | ***QPdL.aww-5A$^{EF}$*** | 101.0 | 86.0-143.3 | *Xgwm0186–XwPt-1370* | 0.52 | Kukri | 5.2 | 3.2 |
| | MexD | ***QPdL.aww-1B$^{EF}$*** | 75.0 | 73.1-81.8 | *Xcfe0257–XwPt-6240* | -0.84 | RAC875 | 5.1 | 4.6 |
| | | ***QPdL.aww-2D$^{EF}$*** | 105.1 | 83.2-114.1 | *Xbarc0328b–XwPt-6574* | 1.03 | Kukri | 6.4 | 5.7 |
| | | ***QPdL.aww-7A$^{EF}$*** | 94.1 | 69.6-107.2 | *Xcfa2028–Xbarc1004* | -0.95 | RAC875 | 9.4 | 4.5 |
| | | ***QPdL.aww-7B$^{EF}$*** | 15.0 | 1.0-24.0 | *Xbarc0338–Xstm0671acag* | -1.22 | RAC875 | 9.9 | 5.6 |
| LF | RAC | ***QPdL.aww-5B$^{LF}$*** | 87.6 | 71.4-97.6 | *XwPt-3457–Xgwm0271b* | 0.89 | Kukri | 14.6 | 3.7 |
| | Minn | ***QPdL.aww-7A$^{LF}$*** | 72.6 | 53.6-97.1 | *XwPt-5153–Xcfa2028* | -0.61 | RAC875 | 16.8 | 4.3 |
| | Bool | ***QPdL.aww-7A$^{LF}$*** | 78.6 | 56.6-99.1 | *XwPt-5153–Xcfa2028* | -0.58 | RAC875 | 20.2 | 5.5 |

#### *5.2.4.1.5 QTLs for flag leaf length and spike length for early- and late-flowering subpopulations*

Overall, seventeen QTLs for flag leaf length (Fl) were identified at the four sites. Eleven and six QTLs in the early- and late-flowering subpopulations, respectively. These QTLs were detected on chromosomes 2B, 2D, 4A, 5B, 6A, 7A and 7D in one or more sites (Appendix G and M). Flag leaf QTLs on chromosome 2B, 2D, 5B and 7A were coincident with heading time QTLs. For most detected QTLs, the 'Kukri' allele was associated with a longer leaf except for QTLs on chromosome 2B (***QFl.aww-2BS$^{EF}$***) and 4A (***QFl.aww-4A$^{EF}$***), where the 'RAC875' allele was associated with a longer flag leaf. Those alleles that associated with early flowering were also associated with longer flag leaf, except the QTL locus on chromosome 7A (***QFl.aww-7A$^{EFand\ LF}$***), where the early flowering allele came from the 'RAC875' parent, while allele from 'Kukri' was associated with longer flag leaf. The similar result was also obtained for non-adjusted data.

For spike length, eight QTLs were detected for two subpopulations in RAC, Minn, Bool and MexD, of those, seven QTLs for the early- and only one QTL for the late-flowering subpopulations were identified on chromosomes 2A, 3A, 3D, 4A and 7A (Appendix G). A QTL for spike length on chromosome 3D (***QEl.aww-3D$^{EF}$***) was detected at three sites (RAC, Bool and MexD). This QTL was coincident with heading time QTL. Spike length QTLs on chromosome 2A (***QEl.aww-2A$^{EF}$***) and 4A (***QEl.aww-4A$^{EF}$***) were only detected in the MexD site with LOD of 4.8 and 3.5, respectively. Another significant QTL for spike length was ***QEl.aww-7A.1***. This QTL was detected was located about 46.6 cM from *Xbarc0259* (113.3 cM) in the *Xbarc0259–Xbarc0281* interval with a LOD of 14.6 and the phenotypic variation explained by this QTL was 17.5% in MexD. However, in Minn only ***QEl.aww-7A.2*** was detected at *Xgwm0746* (154.0 cM) in the *Xgwm0746–XwPt*-5558 interval (Fig. 5-17; Appendix G).

### 5.2.4.2 QTLs for grain yield after adjusting data for heading time (Eet)

To make heading time constant for all 368 DH lines of the mapping population, a linear regression was performed (see the Material and Methods; Section 5.2.3.3) and subsequent QTL analysis was carried out on the adjusted grain yield data.

After adjustment for heading time, fewer QTLs were detected for grain yield. In total seven QTLs (putative and suggestive) were identified on chromosomes 1B, 2D, 3B, 5A and 7A in the four droughted environments (Table 5-23; Appendix N). For the adjusted grain yield data, a suggestive QTL (LOD = 2.9; 4.18% of variation) was detected on chromosome 1B (*QYld.aww-1B*$^{Eet}$) in RAC. A significant QTL on the short arm of chromosome 3B (*QYld.aww-3BS*$^{Eet}$) was also identified in RAC. This QTL was located in the *Xbarc0147–Xcfa2226b* interval (22.8 cM) and explained 3.71% of the observed phenotypic variation for the adjusted data. The most significant QTL was ***QYld.aww-7A***$^{Eet}$ with a LOD of 10.1, 4.6, 2.6 and 3.4 in RAC, Minn, Bool and MexD environments, respectively (Fig. 5-17). The inability to detect ***QYld.aww-7A***$^{Eet}$ in Bool significantly could be due to the low phenotypic variability of grain yield after adjustment. ***QYld.aww-7A***$^{Eet}$ peaked between *Xbarc0259* and *Xbarc0281* (113.3 cM). The saw-toothing in the LOD profiles might be as a result of missing genotypic data for some markers or the uncertainty in marker ordering. Two other QTLs suggestively detected on chromosomes 2D (*QYld.aww-2D*$^{Eet}$) and 5A (*QYld.aww-5A*$^{Eet}$) in Bool with a LOD of 4.5 and 2.7 overlapped heading time QTLs.

**Table 5-23. Detected QTLs with CIM analysis for grain yield when heading time effects were taken into account (superscripe Eet) in four drought environments; RAC, Minn, Bool and MexD. The most likely QTL position, range, interval of flanking markers, allelic additive effect, heritability and LOD for each individual QTL is presented. The italic bold loci represent putative QTLs which were detected at a 5% significance threshold. Suggestive QTLs were detected at a 10% significance threshold. QTLs with largest trait effect are highlighted in light gray.**

| Site | QTL | Position (cM) | Range | Interval | Add | Parent | $h^2$ (%)[a] | LOD |
|---|---|---|---|---|---|---|---|---|
| RAC | *QYld.aww-1B*$^{Eet}$ | 146.5 | 131.6-158.0 | *Xbarc0256–XwPt-9809* | -0.048 | RAC875 | 4.2 | 2.9 |
| | *QYld.aww-3BS*$^{Eet}$ | 22.8 | 0.0-35.9 | *Xbarc0147–Xcfa2226b* | -0.049 | RAC875 | 3.7 | 3.0 |
| | ***QYld.aww-7A***$^{Eet}$ | 113.3 | 111.0-117.3 | *Xbarc0259–Xbarc0281* | -0.082 | RAC875 | 9.7 | 10.1 |
| Minn | ***QYld.aww-7A***$^{Eet}$ | 114.3 | 111.0-120.8 | *Xbarc0259–Xbarc0281* | -0.017 | RAC875 | 5.8 | 4.6 |
| Bool | *QYld.aww-2D*$^{Eet}$ | 85.2 | 53.7-95.2 | *XwPt-0330–Xbarc0328b* | -0.021 | RAC875 | 3.4 | 2.7 |
| | *QYld.aww-5A*$^{Eet}$ | 55.4 | 45.6-83.0 | *Xgwm0304b–Xbarc0360* | 0.016 | Kukri | 3.2 | 2.7 |
| | *QYld.aww-7A*$^{Eet}$ | *113.3* | 110.0-117.3 | *Xbarc0259–Xbarc0281* | -0.022 | RAC875 | 1.5 | 2.6 |
| MexD | ***QYld.aww-7A***$^{Eet}$ | 113.3 | 110.0-124.4 | *Xbarc0174–Xbarc0195* | -0.081 | RAC875 | 3.9 | 3.4 |

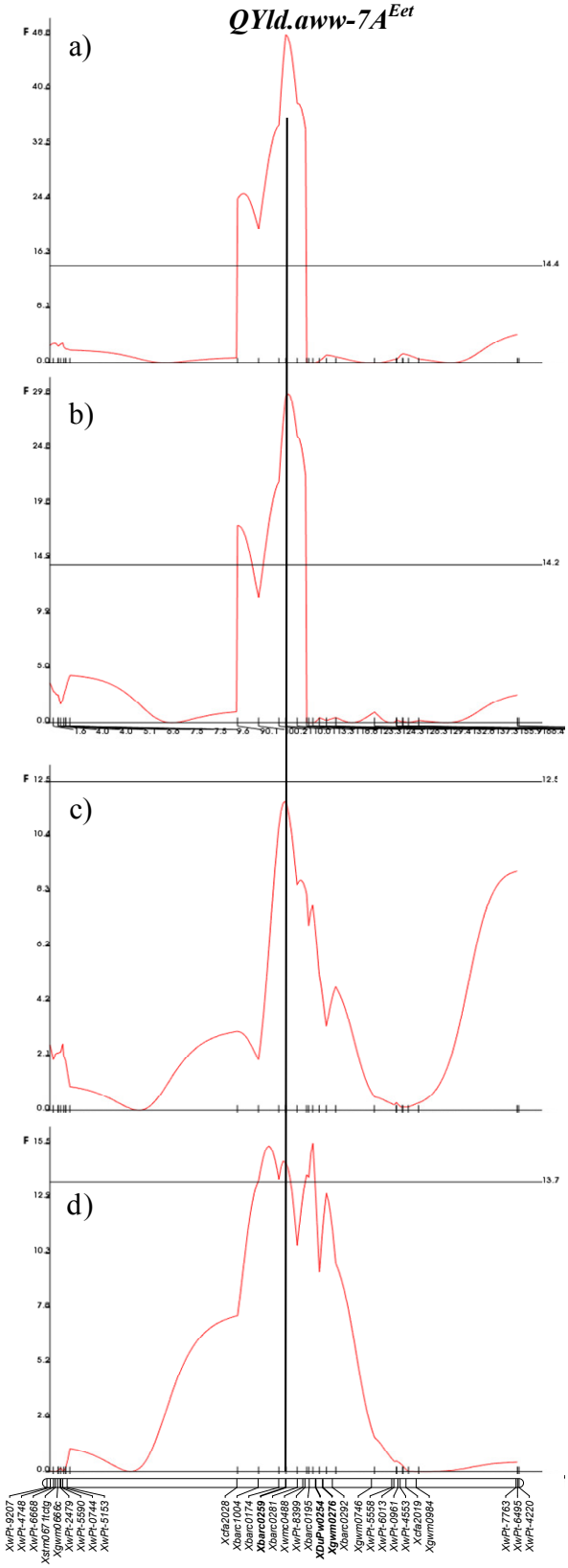


**Figure 5-17. The detected QTL for grain yield after adjusting for heading time effects on chromosome 7A (*QYld.aww-7A*$^{Eet}$) in the four drought-affected environments RAC (a), Minn (b), Bool (c) and MexD (d).**

### 5.2.4.3 QTL analysis using drought indices

Quantitative trait loci detected for drought resistance indices are listed in Table 5-25. Relationships between drought response index (DRI), stress tolerance index (STI), drought susceptible index (DSI), heading time (Eet), grain yield under stress and non-stress conditions based on the principal component analysis (PCA) are given in Figure 5-18. The PCA was performed to classify these variables based on their relationships. The first component was considered as yield under drought-stressed conditions (yield response), and the second component was considered as yield under non-stressed conditions (yield potential). Grain yield in all four drought-stressed environments was positively correlated with grain yield in the non-stress environment (MexI), which came together in the same direction in the biplots (Fig. 5-18a,b,c,d). DRI was not correlated with either yield potential or flowering time, while other drought indices (STI and DSI) showed correlations with flowering time and grain yield. DRI was located in a separate direction of heading time and yield potential in the biplot (Fig. 5-18a, b, c, d). These data indicated that DRI successfully eliminated the effects of heading time and yield potential from the yield data under drought stress. STI (tolerance index), yield under stress and yield potential were correlated and all came together in the same direction for the four droughted environments (Fig. 5-18a, b, c, d). This supported the idea that STI selects genotypes with both high yield under stress and non-stress environments (Fernandez, 1992). DSI (susceptibility index) was negatively correlated with STI and was located in the opposite direction with STI (Fig 5-18).

#### *5.2.4.3.1 Drought response index (DRI)*

In this study, grain yields at the four drought-affected sites were simultaneously regressed on yield potential, heading time and DRI to evaluate the individual contribution of these three factors explaining the phenotypic variation in grain yield under drought-stressed conditions (Table 5-24). Heading time was the major factor in all environments, explaining 75.4, 80.2, 50.3 and 71.8% of the variation in grain yield in RAC, Minn, Bool and MexD, respectively. DRI was the second factor after the heading time that explained 19.4, 15.6, 40.4 and 28.2% of the variation in grain yield in the stressed environments, respectively. Yield potential, generally, made a negligible contribution (Table 5-24). In the drought-affected environments the severity of terminal

drought stress as well as extreme delay in flowering time greatly disadvantaged late-flowering lines, whereas early-flowering lines escaped from terminal drought stress.

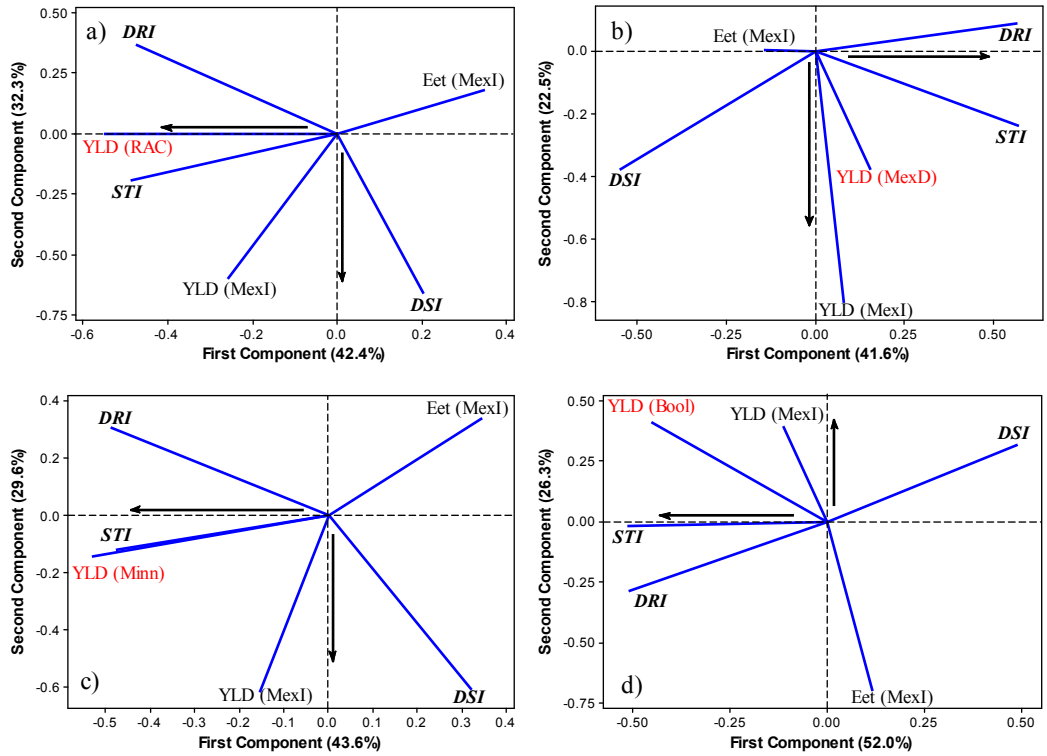


**Figure 5-18. The biplot display of principal component analysis for drought indices, actual yield under stress environment (in red colour), yield potential and heading time (Eet) under non-stressed environment (MexI). The first component was considered as yield response under stress, and the second component was considered as yield potential. Components were calculated from the correlation matrix to study the interrelationship between the drought indices, heading time, yield potential and yield under drought conditions in RAC (a), MexD (b), Minn (c) and Bool (d). Drought indices are presented in italic format.**

**Table 5-24. The $R^2$ values (%) of three factors including time to heading, drought response index (DRI) and yield potential (in MexI) explaining the variation in grain yield under drought stress in RAC, Minn, Bool and MexD. $R^2$ was estimated from stepwise regression analysis in which grain yield under stress was considered as response; heading time, DRI and yield potential were fitted as predictors.**

| Site | Heading time | DRI | YLD potential (MexI) |
|---|---|---|---|
| RAC | 75.4 | 19.4 | 0.86 |
| Minn | 80.2 | 15.6 | 0.05 |
| Bool | 50.3 | 40.4 | 1.64 |
| MexD | 71.8 | 28.2 | 0.06 |

From composite interval mapping (CIM), only one significant QTL remained when the DRI was used for QTL mapping. ***QDri.aww-7A$^{M}$*** or ***QDri.aww-7A$^{R}$*** was detected on chromosome 7A with a LOD > 2.3 in the four droughted environments. The superscript M and R stand for MexI and RAC as reference site for DRI estimation (see Section 5.2.3.3). The results from CIM results were presented in Table 5-25 and Figure 5-19. Results from from CIM (Fig. 5-19) showed one QTL for DRI (***QDri.aww-7A***), which peaked at *Xbar0259* (113.3 cM). ***QDri.aww-7A*** coincided with yield QTLs for the non-adjusted, split-up and adjusted data. For this QTL, the 'RAC875' allele was associated with higher DRI relative to the 'Kukri' allele. These results indicated that the QTL for yield under drought on this region may be different from heading time QTL and it could be a yield response region under drought.

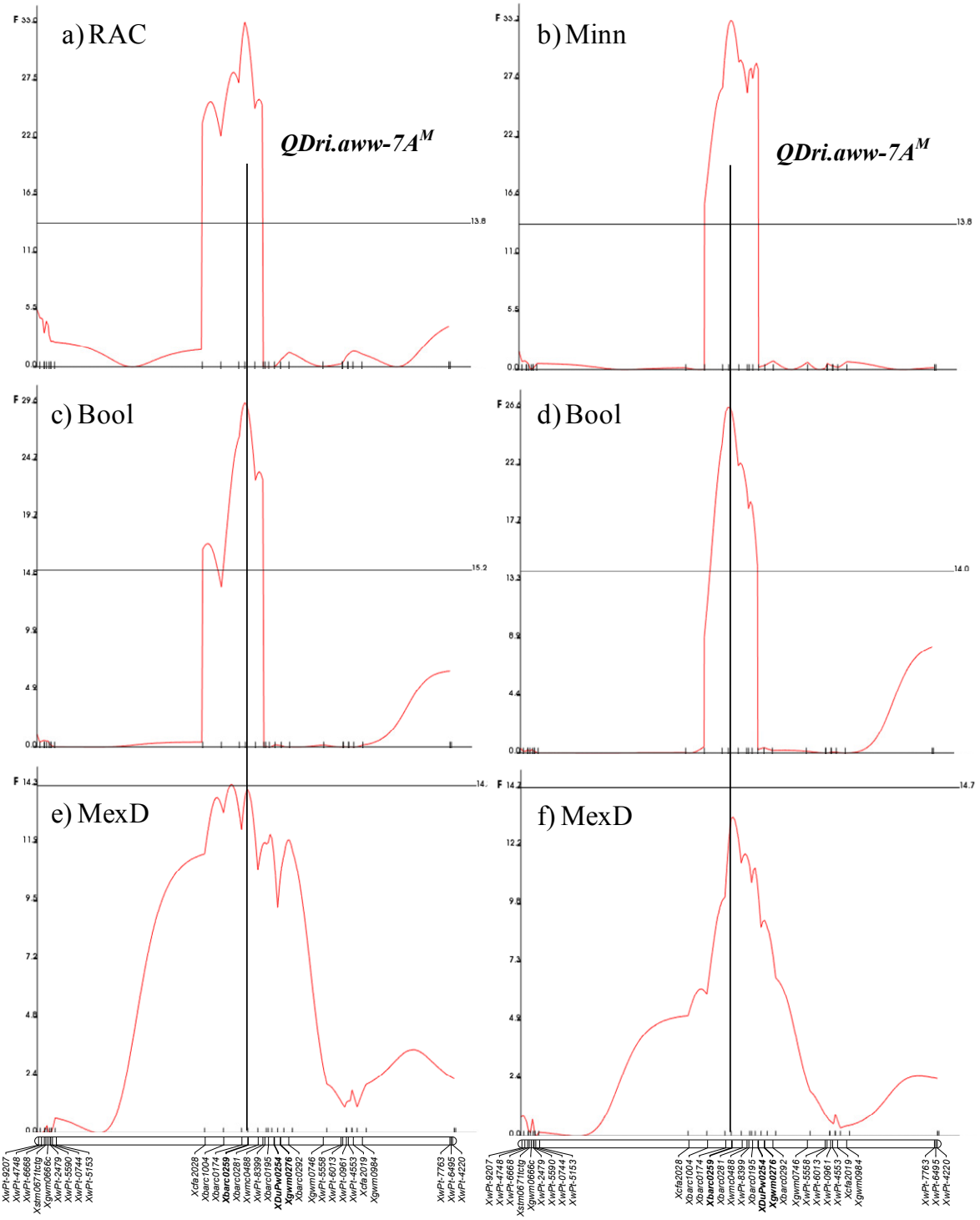


**Figure 5-19. Composite interval mapping QTL for drought response index (DRI) on chromosome 7A in RAC, Bool, Minn and MexD environments. DRI for yield under drought was estimated from yield performance and time to heading in MexI (superscript M). For the South Australian experiment, DRI was also calculated from yield and time to heading in RAC (superscript R). QTL for DRI in (a) RAC (*QDri.aww-7A*$^M$), (b) Minn (*QDri.aww-7A*$^M$), (c) and (d) in Bool (*QDri.aww-7A*$^M$ and *QDri.aww-7A*$^R$), (e) and (f) in MexD (*QDri.aww-7A*$^M$ and *QDri.aww-7A*$^R$).**

#### *5.2.4.3.2 Stress tolerance index (STI)*

A total of 17 QTLs for STI were identified, and the contribution of each QTL to the observed phenotypic variation ranged from 2.2% to 12.7%. These QTLs were detected on chromosomes 1B, 2B, 2D, 3B, and 7A in one or more environments (Table 5-25; Appendix M). A QTL for STI on 1B (LOD = 4.4) was only detected in RAC. In RAC, more QTLs were identified and collectively explained 23.2% of the phenotypic variation.

A QTL on 2D (LOD = 3.6; 4.4% of variation) was detected only in Bool in a similar position with the heading time QTL in this region. However, the identified QTLs for STI on chromosome 2B, 3B and 7A were detected either significantly or suggestively in all four drought environments. The QTLs on 2B and 3B (***QSti.aww-3B.1*** and ***QSti.aww-3B.2***) were coincident with yield QTL in MexI dataset, while 7A overlapped with yield QTLs in drought stressed environments (Table 5-25). For most of the identified loci, except ***QSti.aww-3B.1*** locus**,** alleles form the 'RAC875' parent were associated with larger STI values (tolerance alleles) relative to the 'Kukri' alleles (susceptible alleles). Those lines that had higher STI values may possess those alleles for yield potential as well as yield response under drought stress. This result indicated that using the STI index for QTL mapping is able to detect yield potential and stress response alleles.

#### *5.2.4.3.3 Drought susceptibility index (DSI)*

In total, nine QTLs for the drought susceptibility index (DSI) were identified on chromosomes 2D, 3B, 5A and 7A in one or four environments (Table 5-26; Appendix M). QTLs for DSI on chromosomes 3B and 7A again were detected in three out of four environments. In Bool, only two QTLs for DSI were detected on chromosome 2D and 5A that both were coincident with heading time QTLs. The alleles from both parents (Kukri and RAC875) were associated with larger DSI values on 3BS (***QDsi.aww-3B.1***) and 3BL (***QDsi.aww-3B.2***) QTLs, respectively. However, for the DSI QTL on chromosome 7A (***QDsi.aww-7A***), the susceptibility allele from Kukri was associated with bigger DSI value.

Overall, the results from using drought indices in QTL mapping indicated that DRI can eliminate the interfering effects of heading time and yield potential variations from the

actual response under drought. While eliminating heading time from the data, STI and DSI detect alleles that are involved in high yield potential under non-stress conditions as well as high yield under stress conditions.

**Table 5-25. Detected QTLs with CIM analysis for estimated drought indices including drought response index (DRI), stress tolerance index (STI) and drought susceptibility index (DSI). The most likely QTL position, range, interval of flanking markers, allelic additive effect, heritability and LOD for each individual QTL is presented. Drought indices were estimated from yield performance and time to heading in MexI (superscript M) and also from yield and time to heading in RAC (superscript R). The italic bold loci represent putative QTLs which were detected at a 5% significance threshold. Suggestive QTLs were detected at a 10% significance threshold. QTLs with largest trait effect are highlighted in light gray.**

| Index | Site | QTL | Position (cM) | Range | Interval | Add | Parent | $h^2$ (%) | LOD |
|---|---|---|---|---|---|---|---|---|---|
| DRI | RAC | ***QDri.aww-7A$^M$*** | 113.3 | 110.0-118.3 | *Xbarc0259–Xbarc0281* | -0.29 | RAC875 | 8.6 | 7.2 |
| | Minn | ***QDri.aww-7A$^M$*** | 114.3 | 110.0-121.8 | *Xbarc0259-Xbarc0281* | -0.31 | RAC875 | 9.2 | 7.2 |
| | Bool | ***QDri.aww-7A$^M$*** | 113.0 | 107.2-118.3 | *Xbarc0174-Xbarc0259* | -0.23 | RAC875 | 5.2 | 6.2 |
| | | ***QDri.aww-7A$^R$*** | 113.0 | 107.2-121.8 | *Xbarc0174-Xbarc0259* | -0.2 | RAC875 | 5.2 | 5.8 |
| | MexD | ***QDri.aww-7A$^M$*** | 113.0 | 90.1-122.0 | *Xcfa2028– Xbarc0259* | -0.27 | RAC875 | 2.8 | 3.1 |
| | | ***QDri.aww-7A$^R$*** | 114.3 | 105.2-121.8 | *Xbarc0259–Xbarc0281* | -0.52 | RAC875 | 3.7 | 2.9 |
| STI | RAC | ***QSti.aww-1B$^M$*** | 149.5 | 140.5-159.0 | *Xbarc0256–XwPt-9809* | -0.013 | RAC875 | 5.9 | 4.4 |
| | | *QSti.aww-2B$^M$* | 59.2 | 49.6-73.6 | *XwPt-0335–XwPt-0950* | -0.012 | RAC875 | 3.8 | 2.8 |
| | | ***QSti.aww-3B.1$^M$*** | 86.0 | 71.1-98.5 | *XwPt-8886–XwPt-9510* | 0.015 | Kukri | 4.7 | 4.5 |
| | | ***QSti.aww-3B.2$^M$*** | 185.0 | 175.8-219.6 | *XwPt-4401–XwPt-9368* | -0.012 | RAC875 | 3.6 | 3.1 |
| | | ***QSti.aww-7A$^M$*** | 117.3 | 111.0-122.8 | *Xbarc0259–Xbarc0281* | -0.015 | RAC875 | 5.2 | 5.3 |
| | Bool | *QSti.aww-2B$^M$* | 54.2 | 49.6-61.2 | *XwPt-0335–XwPt-0950* | -0.003 | RAC875 | 2.7 | 2.6 |
| | | ***QSti.aww-2D$^M$*** | 82.2 | 52.7-94.2 | *XwPt-0330–Xbarc0328b* | -0.004 | RAC875 | 4.4 | 3.6 |
| | | *QSti.aww-7A$^M$* | 117.3 | 113.3-122.8 | *Xbarc0259–Xbarc0281* | -0.003 | RAC875 | 2.2 | 2.1 |
| | | ***QSti.aww-2D$^R$*** | 89.2 | 73.7-99.1 | *XwPt-0330–Xbarc0328b* | -0.011 | RAC875 | 7.5 | 5.7 |
| | | ***QSti.aww-7A$^R$*** | 112.0 | 107.2-118.3 | *Xbarc0174–Xbarc0259* | -0.01 | RAC875 | 6.2 | 5.1 |
| | Minn | ***QSti.aww-2B$^M$*** | 54.2 | 50.6-62.2 | *XwPt-0335–XwPt-0950* | -0.003 | RAC875 | 5.1 | 3.5 |
| | | ***QSti.aww-3B.1$^M$*** | 74.1 | 46.9-80.8 | *Xwmc0043–XwPt-6973* | 0.003 | Kukri | 4.4 | 3.9 |
| | | *QSti.aww-3B.2$^M$* | 172.6 | 164.2-179.8 | *XwPt-5704–Xbarc0077* | -0.003 | RAC875 | 2.7 | 1.5 |
| | | *QSti.aww-6B$^M$* | 156.3 | 150.9-163.3 | *XwPt-0171–XwPt-9423* | 0.003 | Kukri | 2.5 | 2.7 |
| | | ***QSti.aww-7A$^M$*** | 117.3 | 111.0-124.3 | *Xbarc0259–Xbarc0281* | -0.003 | RAC875 | 4.5 | 4 |
| | | *QSti.aww-6B$^R$* | 161.3 | 156.3-164.4 | *XwPt-0171–XwPt-9423* | 0.008 | Kukri | 3.0 | 2.5 |
| | | ***QSti.aww-7A$^R$*** | 114.3 | 111.0-118.3 | *Xbarc0259–Xbarc0281* | -0.016 | RAC875 | 12.7 | 10.8 |
| | MexD | ***QSti.aww-3B.1$^M$*** | 76.8 | 72.1-85.0 | *XwPt-6973–XwPt-8886* | 0.026 | Kukri | 5.3 | 2.8 |
| | | ***QSti.aww-3B.2$^M$*** | 195.1 | 185.0-202.1 | *XwPt-9368–XwPt-8021* | -0.034 | RAC875 | 5.0 | 3.6 |
| DSI | RAC | *QDsi.aww-1D$^M$* | 116.8 | 99.5-148.4 | *Xcfd0027–XwPt-1799* | -0.02 | RAC875 | 3.6 | 3 |
| | | *QDsi.aww-2A$^M$* | 79.2 | 73.3-88.1 | *Xwmc0296–XwPt-7306* | -0.017 | RAC875 | 4.2 | 3 |
| | | ***QDsi.aww-3B.1$^M$*** | 76.8 | 69.1-81.0 | *XwPt-6973–XwPt-8886* | 0.027 | Kukri | 4.5 | 3.9 |
| | | ***QDsi.aww-3B.2$^M$*** | 187.0 | 174.8-195.0 | *XwPt-4401–XwPt-9368* | -0.024 | RAC875 | 4.9 | 5.1 |
| | | ***QDsi.aww-7A$^M$*** | 113.3 | 111.0-116.3 | *Xbarc0259–Xbarc0281* | 0.023 | Kukri | 5.3 | 5.8 |
| | Bool | ***QDsi.aww-2D$^M$*** | 87.2 | 49.7-99.1 | *XwPt-0330–Xbarc0328b* | 0.004 | Kukri | 4.7 | 3.8 |
| | | *QDsi.aww-5A$^R$* | 56.4 | 45.6-84.0 | *Xgwm0304b–Xbarc0360* | -0.01 | RAC875 | 3.8 | 3 |
| | Minn | ***QDsi.aww-3B.2$^M$*** | 198.1 | 179.8-207.1 | *XwPt-8021–Xgwm0114b* | -0.003 | RAC875 | 4.1 | 3.2 |
| | | ***QDsi.aww-7A$^M$*** | 114.3 | 111.0-126.2 | *Xbarc0259–Xbarc0281* | 0.003 | Kukri | 3.9 | 2.7 |
| | MexD | ***QDsi.aww-3B.2$^M$*** | 195.1 | 185.0-202.1 | *XwPt-9368–XwPt-8021* | -0.034 | RAC875 | 4.9 | 3.4 |
| | | *QDsi.aww-7A$^M$* | 104.2 | 93.1-117.3 | *Xbarc1004–Xbarc0174* | 0.03 | Kukri | 3.0 | 2.3 |

**Figure 5-20. The estimated location of all detected QTLs for the non-adjusted (NA), split-up (EF and LF) and adjusted data (Eet) on chromosomes 2B, 2D and 7A. QTLs for heading time (Eet) is shown in red colour. QTLs for plant height (Ht), peduncle length (Pdl), spike length (El) and flag leaf length (Fl) are shown in blue colour. QTLs for grian yield (Yld) and yield components such as number of grains per $m^2$ (Gnm), number of spikelets per spike (Spn), the fertile spikelets (Fspn), the non-fertile spikelets (Nspn), grain weight per spike (Gwe), grain number per sampeled spikes (Gnu), harves index (Hi), thousand grain weight (Tgw) and screening (scr) are shown in black colour. The dark green colour loci showing physiological traits such as leaf waxiness (W), chlorophyll content (Spad) and pubescence (pa). The underlined loci are drought indices QTLs for adjusted data. The putative QTLs (at $P < 0.05$) are shown in bold font and solid vertical bars, while the suggestive QTLs (at $P < 0.1$) are represented in non-bold and dashed lines adjacent to chromosomes.**

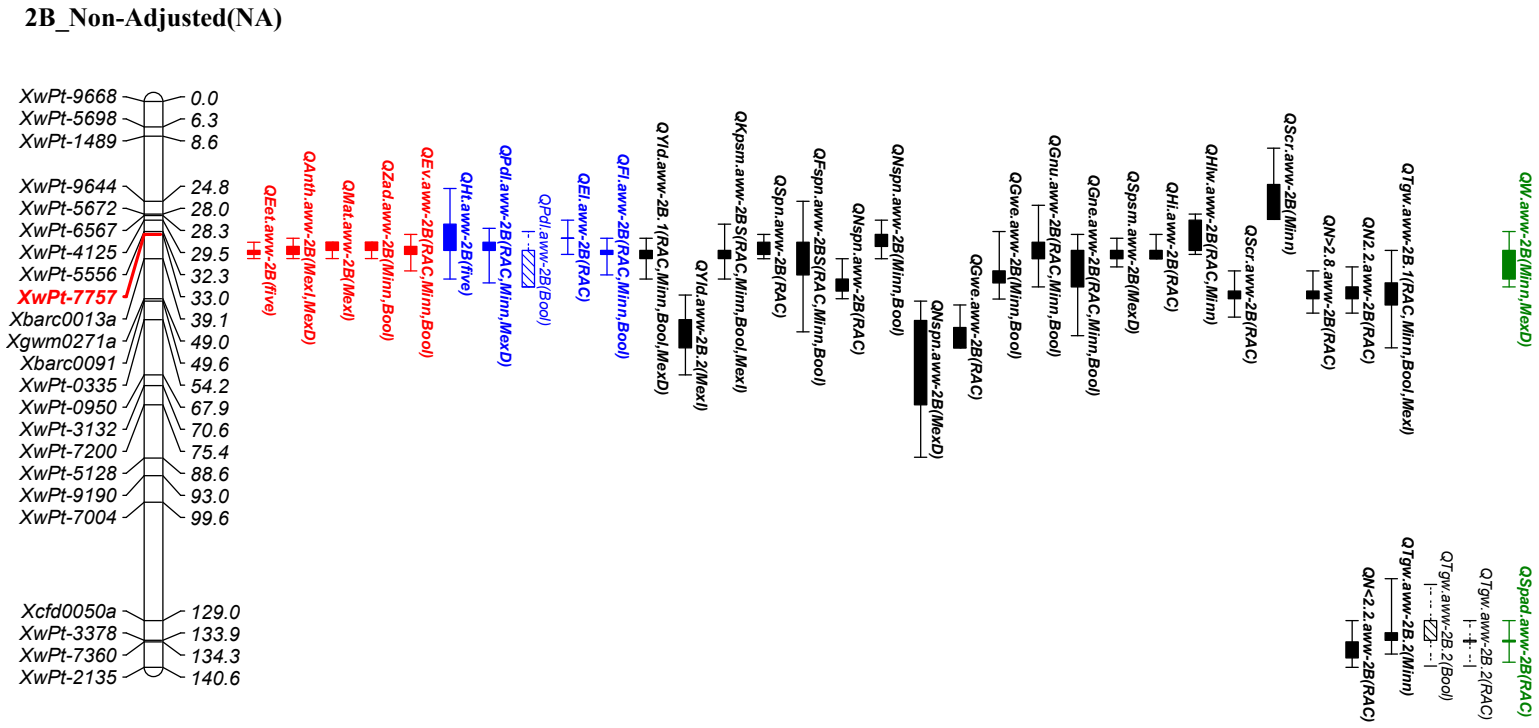

**Figure 5-20. Continued**

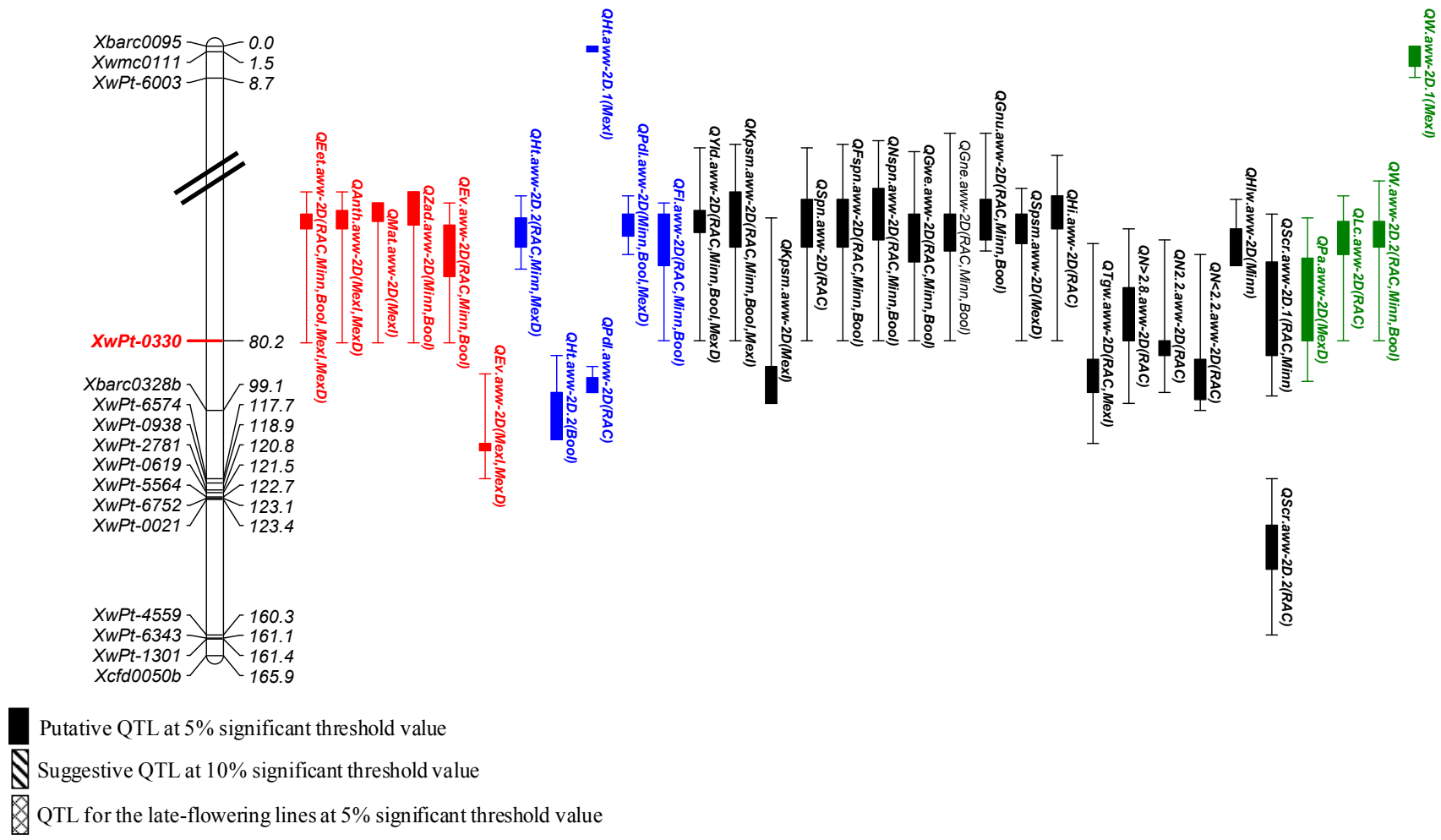


Putative QTL at 5% significant threshold value

Suggestive QTL at 10% significant threshold value

QTL for the late-flowering lines at 5% significant threshold value

**Figure 5-20. Continued**

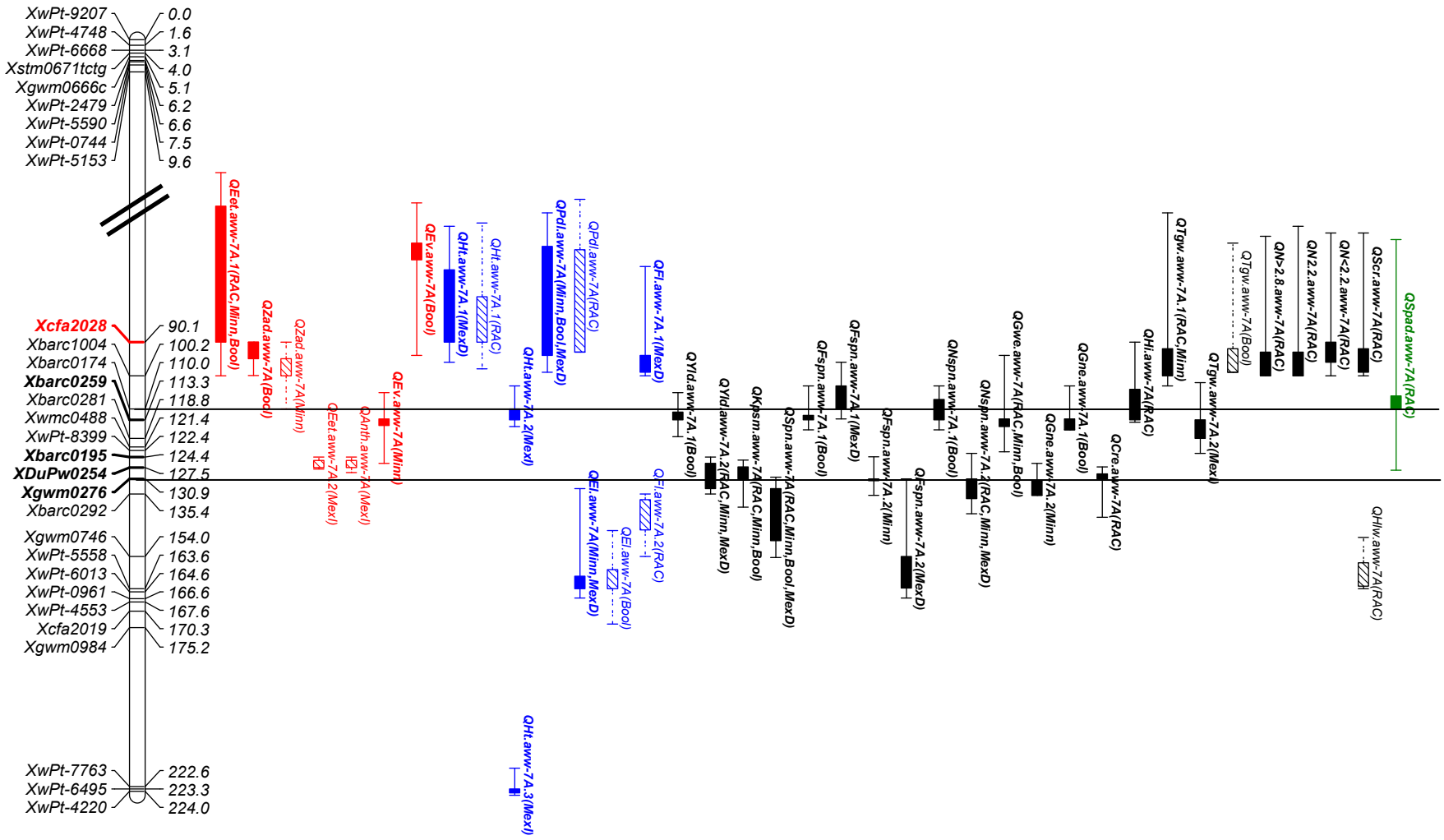

**Figure 5-20. Continued**

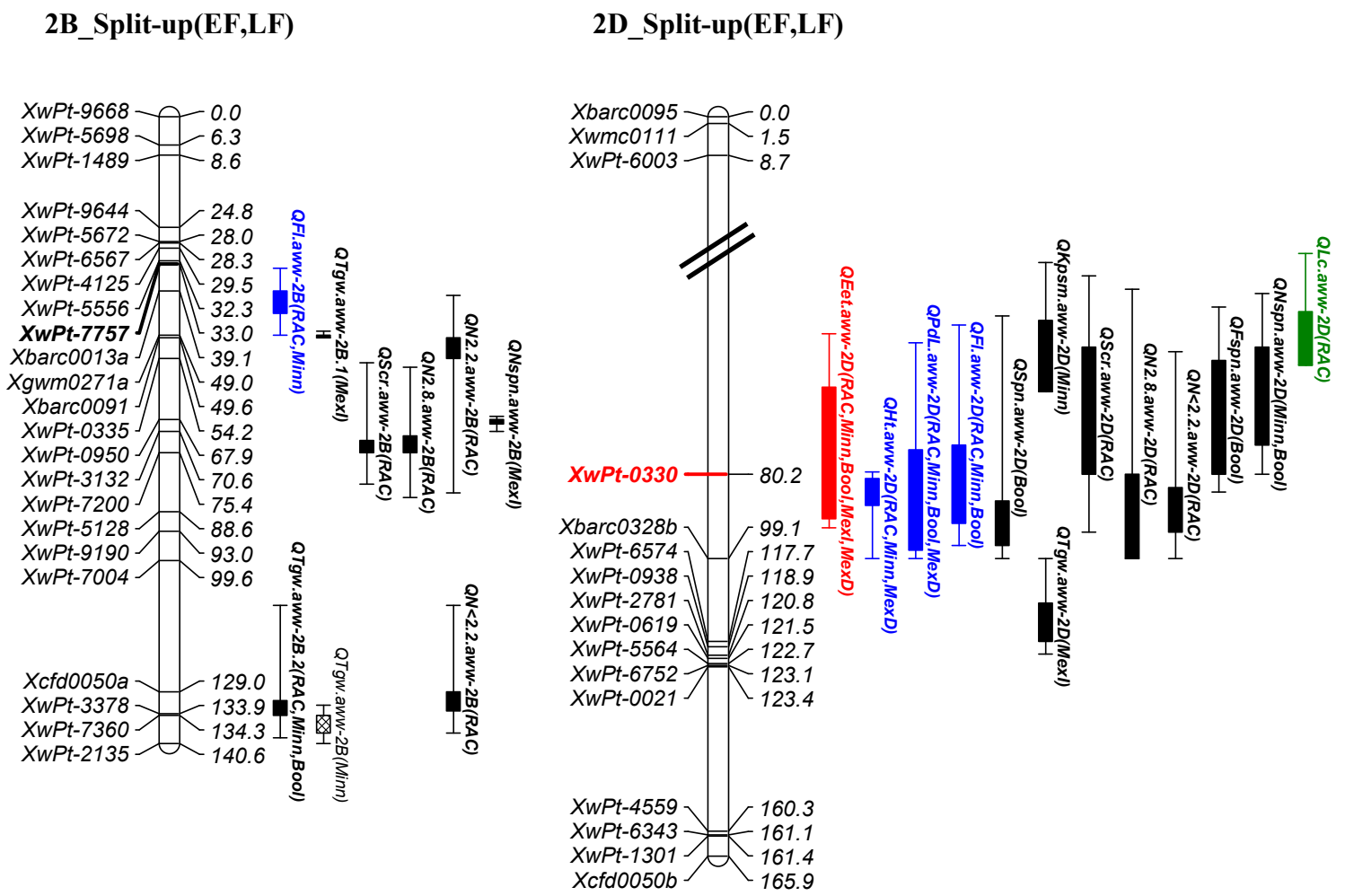

**Figure 5-20. Continued**

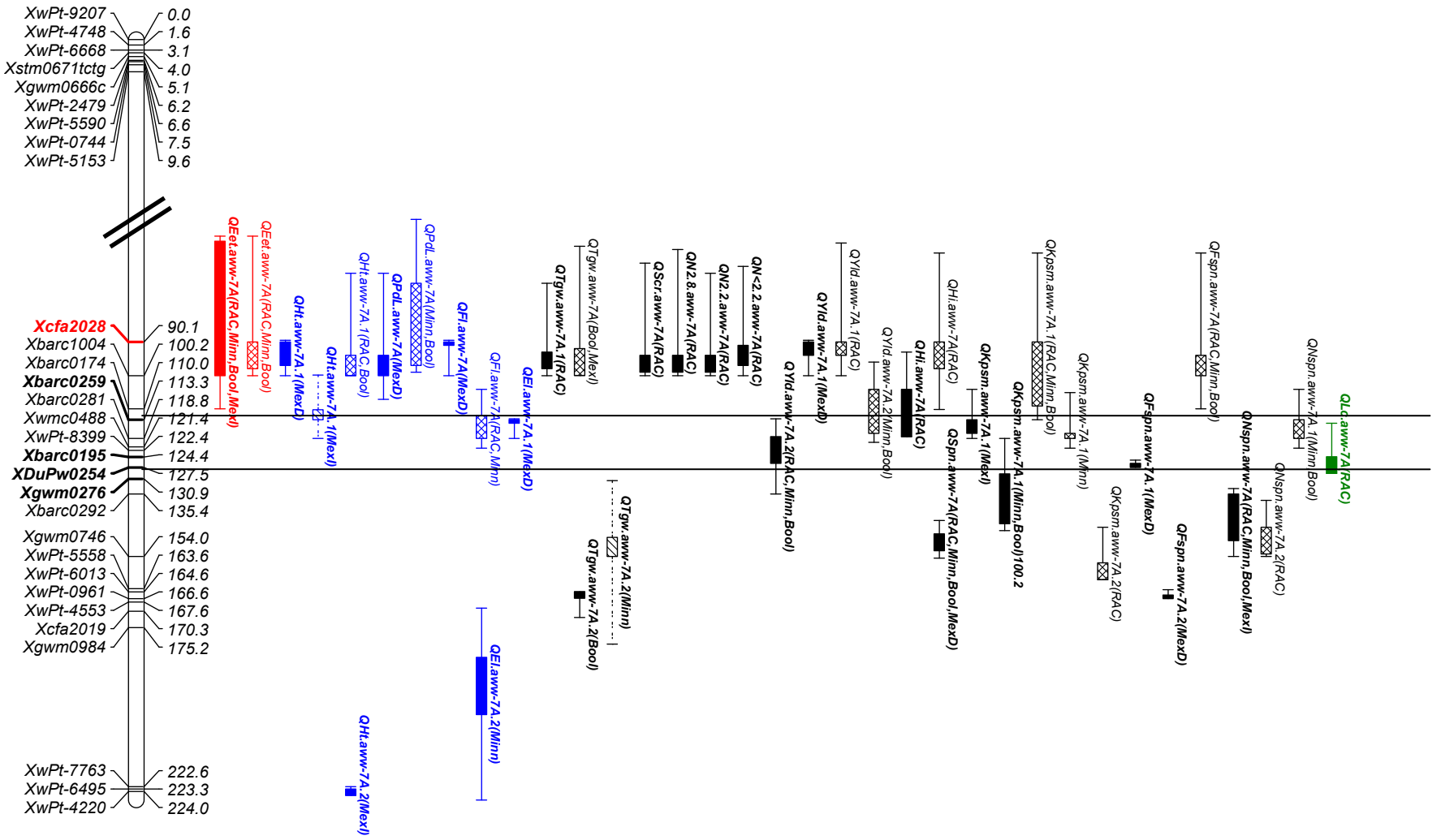

**Figure 5-20. Continued**

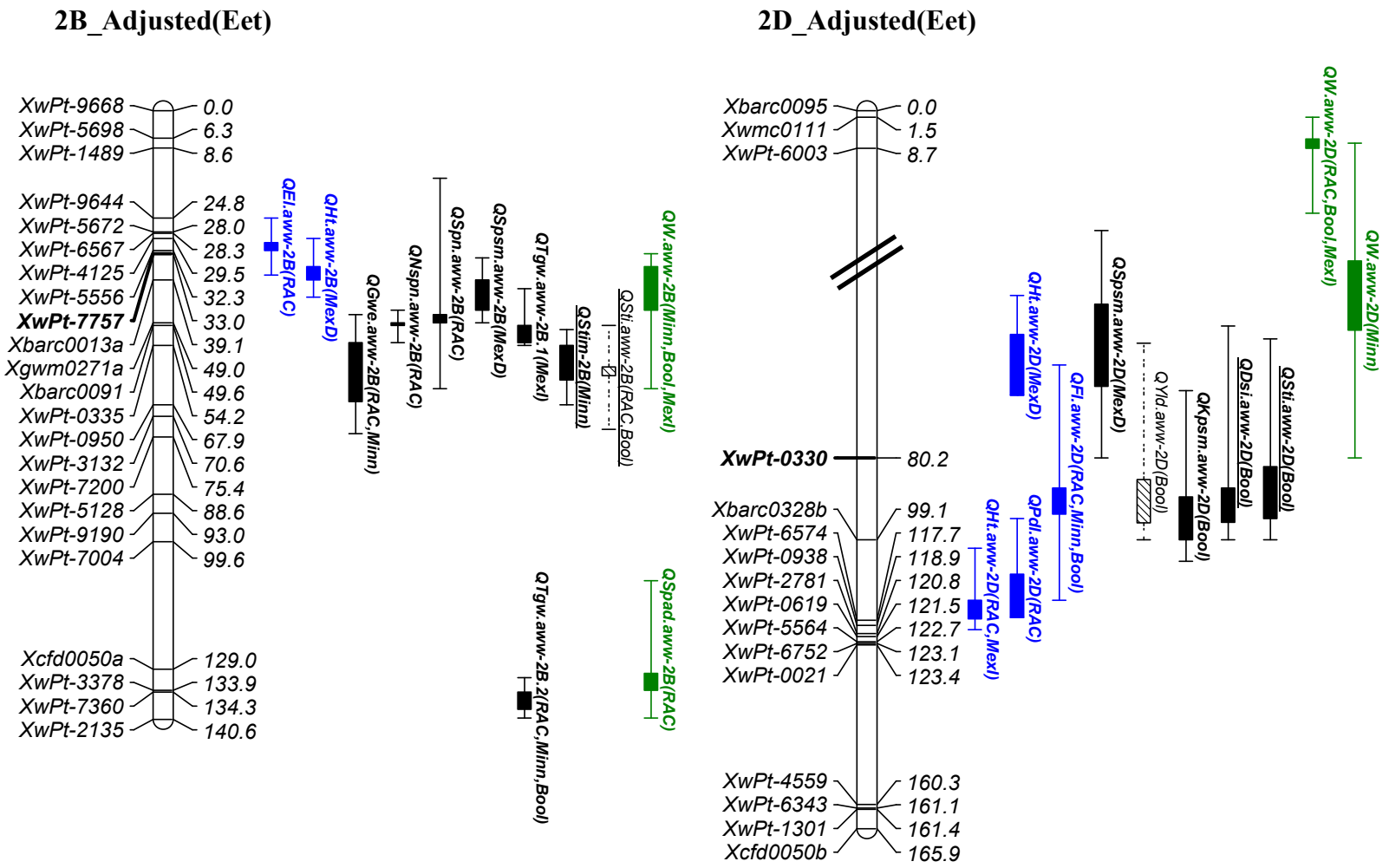

**Figure 5-20. Continued**

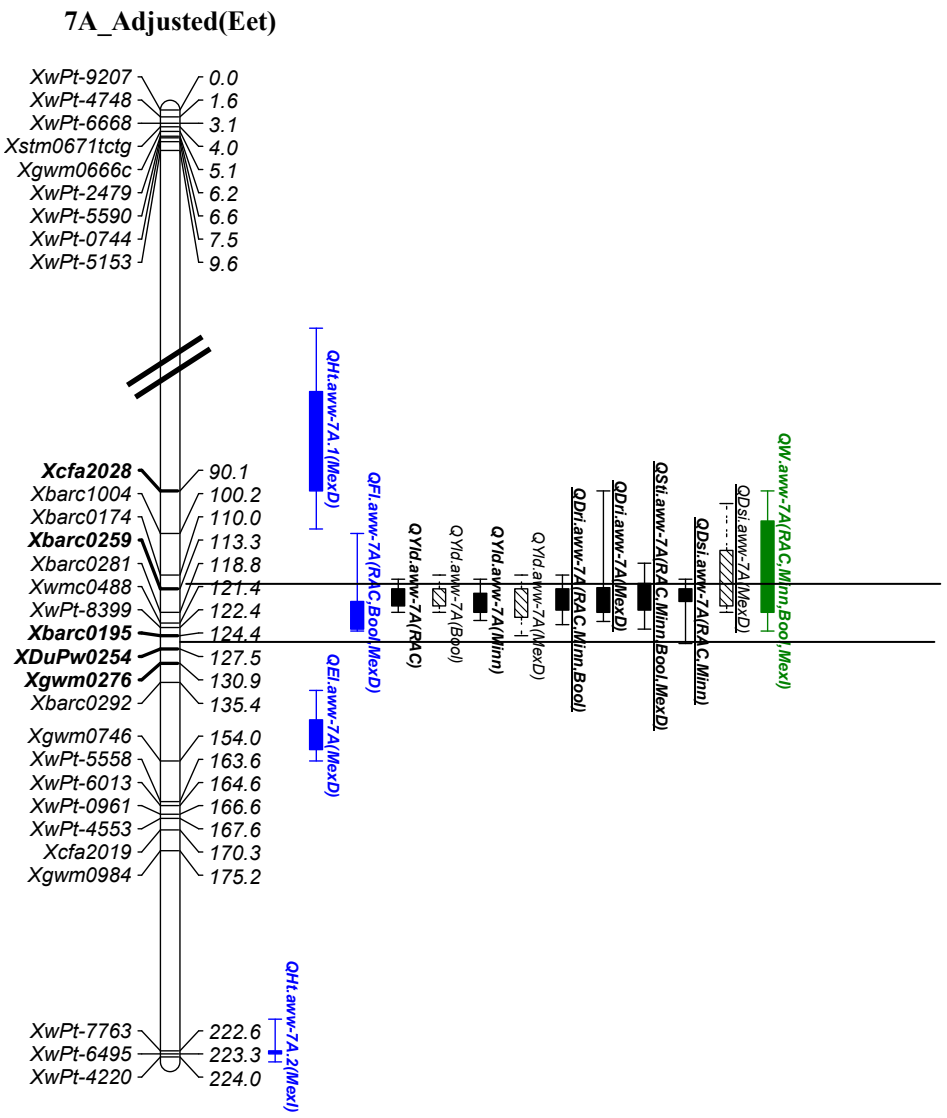

## 5.3 Discussion

### 5.3.1 Drought escape associated with different phenological development

Maturity and plant height are two agronomic traits of great importance in producing grain yield in wheat. In the population under study, heading time was clearly the most important factor affecting grain yield under all four drought stress conditions. In this study, the early flowering lines outyielded the late flowering lines. In an environment with unpredictable rainfall and low moisture availability late in the growing cycle, early flowering confers drought tolerance via escape (Fischer and Maurer, 1978). In the southern Australian environments, in particular, the late-season is characterised by intermittent high temperatures and a rapid progression towards water shortage (Turner, 2004). Therefore, the ability of lines to flower earlier is advantageous because plants can complete development and grain-filling before the onset of high temperatures as well as the late-season water deficit. Consequently the alleles associated with the early flowering in this population lead to an increase in grain yield.

The extent of variation observed for heading time in this population was relatively large, indicating the action of several genes resulting in the observed transgressive segregation. Seven QTLs for heading time were found on chromosomes 1A, 2B, 2D, 3D, 5B, 7A and 7B. Heading time in the field is influenced by interactions between environment and the three genetic factors responsible for photoperiod sensitivity (*Ppd*), vernalization requirement (*Vrn*) and/or earliness *per se* (*Eps*) (Shindo et al., 2003; Dubcovsky et al., 2006). In this study, the largest QTLs were located on the short arm of chromosomes 2B and 2D. These two QTLs are coincident with previously known *Ppd-B1* and *Ppd-D1a* genes, respectively (Worland and Sayers, 1996; Beales et al., 2007). Two QTLs for earliness *per se* on 2B, distal to *Ppd-B1*, were also reported (Shindo et al., 2003; Kuchel et al., 2006). The photoperiod response gene *Ppd-D1a* plays a major role in regulating flowering time in wheat (Worland et al., 1996; 1998a). The dominant *Ppd* genes reduce sensitivity to photoperiod and accelerate flowering under short- and long-day conditions (Cockram et al., 2007). In this population, it is very likely that the presence of both photoperiod sensitivity alleles at '*ppd-B1*' and '*ppd-D1*' from 'Kukri' and 'RAC875', respectively, were associated with the extreme

delay in heading time. A similar result was found by Quarrie et al. (2005) in the CS/SQ1 population, in which different alleles of both *Ppd-B1* and *Ppd-D1* from both parents (CS and SQ1) were associated with photoperiod-insensitivity.

Several QTLs were reported to be involved for photoperiod insensitivity in hexaploid wheat, apart from *Ppd-B1* and *Ppd-D1*on 2B and 2D. Shindo et al. (2003) suggested that genes involved in photoperiod sensitivity can be categorized into at least two group of genes; genes responding to photoperiod independent of vernalization requirement, and genes, including *Ppd-B1*, dependent on the vernalization requirement; they cannot fulfill their effect until the vernalization requirement is met. Shindo et al. (2003) reported QTLs for heading time on chromosome 5B and 7A that were involved in both photoperiod sensitivity and heading time under non-vernalized short-day conditions. Kuchel et al. (2006) identified QTLs associated with time to heading on chromosomes 1A, 2A, 2B, 6D, 7A and 7B in the Trident/Molineux DH population grown in South Australian environments.

The heading time QTL on the short arm of chromosome 1A (***QEet.aww-1AS***) is possibly related to the genes for photoperiod sensitivity, which were previously identified on the homoeologous chromosome 1H (*Ppd-H2)* in barley (Laurie et al., 1995; Law et al., 1998). Law et al. (1998) showed that genes for time to heading were present on the short arm of homoeologous group 1 chromosomes in wheat. Kuchel et al. (2006), in contrast, reported a photoperiod-responsive locus on the long arm of chromosome 1A in wheat, which did not respond to vernalisation. In our study, this QTL (***QEet.aww-1AS***) was detected at the South Australian sites, while in the Mexican sites there was a weak association of this locus with time to heading, indicating G × E interaction. In this population, no further QTLs associated with time to heading were found on chromosomes 1B and 1D.

The heading time locus on chromosome arm 3D (***QEet.aww-3D***) may correspond to an earliness *per se* (*Eps*) gene. Börner et al. (2002) identified a flowering time QTL on 3AL in the International Triticeae Mapping Initiative (ITMI) 'Opata 85' × 'W7984' population. They suggested that by changes of the RFLP maps (Pestsova et al., 2000), the QTL for *Eps* may be located on chromosome arm 3DL instead of 3AL. Paillard et al. (2004) reported a QTL associated with heading time on 3DL in the Arina /Forno population. Narasimhamoorthy et al. (2006) reported a QTL for day to heading on 3DS

in an advanced backcross of a hard winter wheat × synthetic wheat population. In barley, QTLs determining flowering time were also detected in the distal region of chromosome arm 3HL (Laurie et al., 1995).

A significant QTL for heading time was detected on the long arm of chromosome 5B (***QEet.aww-5BL***), and one weak heading time QTL was also identified in a poorly covered region on chromosome 5A (***QEet.aww-5A***) in the *Xgwm0186-XwPt-1370* interval. It has been reported that the genes *Vrn-A1*, *Vrn-B1* and *Vrn-D1* are homoeo-allelic and are localized on chromosomes 5A, 5B and 5D, respectively (McIntosh et al., 2003). The gene *Vrn-B1* was mapped on the long arm of chromosome 5B, closely linked to the marker *Xgwm408* (Leonova et al., 2003). Kato et al.(1999) reported a locus for earliness *per se* on chromosome 5AL of hexaploid wheat. Hanocq et al. (2004) found four QTLs for earliness *per se* on chromosomes 2B, 2D, 5B and 7A which together described between 27.2% and 28.6% of the observed phenotypic variation under the vernalized treatment. In this study the QTLs detected for heading time on 5A and 5B could be *Vrn* and/or *Eps* genes. Further investigation would be required to find out the mode of action for the genes underlying these QTLs and their impact on the ear-emergence.

In this study, QTLs for heading time were also identified on homologues group 7 chromosomes. ***QEet.aww-7A*** and ***QEet.aww-7B*** were detected in all environments on chromosomes 7A and 7B, respectively, while ***QEet.aww-7D*** was detected in a poorly covered region on chromosome 7D, only in one environment (Bool). It seems that the chromosome 7A and 7B loci presented here are homoeoloci, given the similarity of their chromosome locations. These QTLs are possibly associated with *Vrn3* (previously called *Vrn5* or *Vrn-B4*) on the short arm of the group 7 chromosomes (Yan et al., 2006; Bonnin et al., 2008). *Vrn3* is completely linked to *TaFT* and 1 cM distal to *Xabc158-7B* on 7BS (Yan et al., 2006). In both wheat and barley *Vrn3* is associated with a flowering promoter gene homologous to the Arabidopsis *FT* gene (Yan et al., 2006). Bonnin et al. (2008) confirm the presence of FT in the group 7 chromosomes using both an association study and QTL mapping. The *TaFTA* and *TaFT* (*Vrn3*) and *TaFTD* were physically assigned in the short arm of chromosomes 7A, 7B and 7D, respectively, where major QTLs for flowering time traits were also detected in wheat. *FT* genome A was assigned to the 7AS8-0.45-0.59 bin, at an estimated position near the marker *barc154,* 0.4 cM from *Xcfa2028.* The marker *Xcfa2028* was assigned to the C-7AS8-

0.45 bin close to the centromere. The marker *Xcfa2028* in our map showed a significant association with heading time across all environments. Quarrie et al. (2006) also found a QTL for flowering time on the short arm of chromosome 7A, possibly in the same bin as *FTA*. Hanocq et al. (2007) reported a QTL for heading date and earliness *per se* and Kuchel et al. (2006) reported a QTL for ear-emergence time on the short arm of chromosome 7A, these loci are also located in a 30 cM region around *Xbarc154*. For chromosome 7B, one meta-QTL for heading date and earliness *per se* (Hanocq et al. 2007) and one QTL for heading date (Kuchel et al., 2006) were located in the same bin as *FT* (Bonnin et al., 2008). In the present study, when the population was divided into two early- and late-flowering groups, the most significant QTLs in the early-flowering group were ***QEet.aww-2DS$^{EF}$*** and ***QEet.aww-7AS$^{EF}$***. However, for the late-flowering group ***QEet.aww-5B$^{LF}$***, ***QEet.aww-7AS$^{LF}$*** and ***QEet.aww-7B$^{LF}$*** were detected. The presence of heading time QTL on chromosome 7A for all datasets indicates that ***QEet.aww-7AS*** is associated with early flowering in both subpopulations. Further investigation would be required to find out whether these loci are associated with the vernalization, photoperiod or earliness *per se* response. The presence of *FTA* should be tested in the parents and possibly mapped in this population.

### 5.3.2 A major QTL for grain yield on chromosome 7A independent of heading time

In this study most detected QTLs for the non-adjusted yield data at the four drought-affected environments co-located with the heading time QTLs on chromosome 1AS, 2BS, 2DS, 3D, 5B, 7A and 7B. However, in the non-stressed environment (MexI), two QTLs for yield were detected on chromosome 3B. These were not identified in the four droughted environments, indicating a strong G × E interaction for grain yield at these loci. As mentioned previously, grain yield was influenced noticeably by heading time. Those loci having a large impact on phenology, particularly ear emergence loci on chromosomes 2B (*Ppd-B1*) and 2D (*Ppd-D1*), were strongly associated with QTL for grain yield. Although the heading time QTL on chromosome 7A (***QEet.aww-7AS***) was detected in all tested environments (putatively or suggestively), most QTLs for grain yield, $G \cdot m^{-2}$, number of grains per sampled spike and grain weight per spike were mapped in clusters in the 25 cM interval from the marker *Xbarc0259* (113.3 cM) to the marker *Xbarc0292* (135.4 cM). Although this QTL was strongly associated with grain

yield, their effects on time to ear-emergence were minor, and certainly less than observed for the *Ppd-B1* and *Ppd-D*1. Interestingly, for the split-up data most grain yield QTLs disappeared, only 7A (***QYld.aww-7A$^{EF}$*** and ***QYld.aww-7A$^{LF}$***) locus was consistently detected with a stronger additive effect at the four droughted sites (Fig. 5-21). By taking heading time effects into account (adjusted data), the grain yield QTL on chromosome 7A (***QYld.aww-7A$^{Eet}$***) was also detected, while the effects of other QTLs were eliminated. Further by mapping the drought response index (DRI), only one QTL was detected on chromosome 7A for DRI (***QDri.aww-7A$^{M}$*** and ***QDri.aww-7A$^{R}$***). This QTL was associated with markers *Xbarc0259* (113.3 cM). From the results of this study it is, therefore, likely that the yield QTL on chromosome 7A (***QYld.aww-7A***) is a yield response to drought stress.

The identified grain yield QTL on 7A (***QYld.aww-7A***) in this work may correspond to the QTL for grain yield reported by Quarrie et al. (2006) on chromosome 7AL. However, Quarrie et al.(2005, 2006) mapped a yield QTL on the proximal long arm of chromosome 7A in deletion bin 7AL16-0.86-0.90 for the CS/SQ1 DH population across several different environments.

In addition to a major QTL for grain yield on chromosome 7A, several QTLs for yield components including number of grains per $m^2$, number of spikelets per spike, number of fertile and non-fertile spikelets, grain weight per spike, grain number per sampled spike, harvest index and TGW were also identified on chromosome 7A (Fig. 5-21). Traits that are correlated, as in the case of yield and yield components, are likely to have QTL mapping to similar locations (Kato et al., 2000; Gardner and Latta, 2007). The coincidence of QTL in a cluster on chromosome 7A mean that several closely-linked genes for performance under stress are located together or it may correspond to a single major gene involved in regulating the drought response pathway (pleiotropic effects). Further study will be necessary to unravel the molecular basis of the detected grain yield and yield component QTLs.

Among yield components, it has been shown that grain yield is more closely associated with grain number than with grain weight (Zamski and Grunberger, 1995). However, grain weight is not only a major grain yield component, but also has an impact on end-use quality (Gupta et al., 2006) and is often used as a grain receival and marketing standard (Kuchel et al., 2007a). Therefore, genetic dissection of grain size may also help

to elucidate the genes regulating grain yield. Each yield QTL could be the consequence of variation in one or more of the yield components such as number of spikes per square meter, grain per spike and TGW (Quarrie et al., 2005). Quarrie et al. (2005) reported that grain yield QTLs were primarily associated with grain number per ear (Gne) and to a lesser extent with number of spike per plant. In our study, number of grains per $m^2$, number of grains per spike, and spike fertility were associated with the major grain yield QTL on chromosome 7A. Börner et al. (2002) identified a QTL for grain number per ear at the distal part of chromosome 7DL in the ITMI wheat mapping population. Quarrie et al. (2005) suggested that this locus is in a homoeologous position to 7AL and 7BL QTLs which clustered around the *Xwmc273* locus in the CS/SQ1 population. A QTL for the number of spikelets per spike was also identified by Börner et al. (2002) on 7AL in the ITMI mapping population.

Although flowering time may influence grain size and grain number through its effect on the dry mass accumulation in spike, stem elongation, duration of the late reproductive phase, and number of florets at anthesis (Gupta et al., 2006), several physiological factors also influence these traits by their effects on seed set and grain size throughout the grain-filling period (reviewed by Yang and Zhang, 2006). These factors include rate of photosynthesis, mobilization of reserves and sink capacity (e.g. number and size of cells in developing grain). In this study reduction in number of grains and grain weight was observed under drought stress. This could be due to pollen sterility and/or abortion of grains as a result of failure of grain development (Saini and Westgate, 2000). The lack of source activity (current photosynthetic assimilates) and strength (stem water soluble carbohydrates) is probably associated with a reduction in the number of endoplast cells and amyloplasts in the grain (Saini and Westgate 2000). On the base of results from the WSC measurements in the parents and in a small subset of DH lines, it seems that higher percentage of WSC in the stem and the rate of dry matter accumulation in the spike in the higher yielding parent 'RAC875' may help maintain a certain number of grains per spike with a reasonable grain size under drought stress conditions. Our result is in agreement with Kuchel et al. (2007a) who suggested that the semi-dwarf wheat genotypes adapted to the South Australian environments achieves relatively high grain yield through increases in seed set and little compensatory loss in grain weight. Interestingly, the 'RAC875' allele showed a strong association with high $G \cdot m^{-2}$, higher number of grains per spike and high TGW on chromosome 7A.

One can speculate that QTLs for number of grain per spike (or spikelet fertility) and TGW are independent. Regardless of the effects of the heading time, the effects of this locus on grain yield components were consistent, showing little G × E interaction.

In this study we identified three major QTLs for TGW on chromosomes 2B, 6A and 7A which were co-located with screening fractions in the four tested environments. A QTL for TGW was also detected on chromosome 3A in a similar position with the leaf waxiness QTL only in the MexI environments. A previous study reported QTL for TGW on chromosome 7D (Börner et al., 2002; Kuchel et al., 2007a). Röder et al. (2008) recently fine mapped the previously identified grain weight QTL in the most telomeric bin 7DS4-0.61-1.00 in the physical map of wheat chromosome 7DS in the *Xgwm295–Xgwm1002* interval. It was reported that 84.7% of the observed phenotypic variation was explained by the microsatellite marker *Xgwm1002-7D*. We also identified a QTL for the largest screening grain size fraction (***QN2.8.aww-7D$^{NA}$***) on the short arm of chromosome 7D, which was associated with microsatellite marker *Xgwm295*. QTLs for grain size related traits such as TGW and screening fractions, were also identified on the short arm of chromosome 7A for the non-adjusted as well as split-up data. The coincidence of grain size with heading time may be a pleiotropic effect of heading time, or the locus might be in a homoelogous position to the 7DS locus controlling grain size on the short arm of chromosome 7A. The poor marker coverage in this region may have hidden this QTL. The 'RAC875' allele, which conferred higher relative grain yield, was also associated with larger grain.

Our results showed that the yield QTL on chromosome 7A (***QYld.aww-7A***) was also associated with QTL for HI. Quarrie et al. (2006) also found coincidence of the grain yield, HI QTLs and biomass production at anthesis QTLs on the distal region chromosome 7AL. Quarrie et al. (2006) pointed out that genetic variation in grain yield has to be due to either variation in biomass production or HI, or a combination of the two. They suggested that a higher biomass at anthesis would lead to more fertile florets per spike, creating a larger sink demand for assimilates, thus increasing HI. Further research would be required to investigate the sink-source relationship, and the role of WSC accumulation and remobilization in this population. Yang et al. (2007) identified a QTL for remobilization of water soluble carbohydrates on the long arm of chromosome 7A at marker *Xwmc488* that was coincident with TGW in the Hanxuan103/Lumai14 DH population.

Additional genomic regions were also associated with yield components, but not grain yield, on the long arm of chromosome 1AL and 6A. Although influencing the number of $G \cdot m^{-2}$, fertile and non-fertile spikelets, TGW and screening fractions, no association between this region and grain yield was detected.

### 5.3.3 Plant height and peduncle length

In wheat, plant height is an important component of grain yield. Although this population did not segregate for major *Rht* genes (*Rht-B1b* and *Rht-D1b*), it seems that some genes were segregating that modulated plant height. In this study, several QTLs for non-adjusted plant height data were identified on chromosomes 1AS, 2BS, 2DS, 3A, 3D, 5A, 5B, 7A and 7B (Appendix K). The plant height QTLs on 1AS, 2BS, 2DS, 3D, 5B and 7B were coincident with heading time QTLs, while the other loci seem distinct from the heading time effect. Two major QTL for plant height were located on chromosomes 2DS (***QHt.aww-2DS***$^{NA}$) and 3A (***QHt.aww-3A***$^{NA}$), with a relatively large contribution to the observed phenotypic variation. These two QTLs were detected for both the split-up and adjusted data. Two major QTL for peduncle length were also coincident with plant height QTLs on chromosome 2DS (***QPdl.aww-2DS***$^{NA}$) and 3A (***QPdl.aww-3A***$^{NA}$). ***QHt.aww-2DS***$^{NA}$ was associated with a heading time QTL ***QEet.aww-2DS***, whereas ***QHt.aww-3A***$^{NA}$ was not coincident with any heading time QTLs. For ***QHt.aww-2DS***$^{NA}$, it appears that the variation at the *Ppd-D1* locus may be causing the variation in the plant height, since there is a well established relationship between maturity and plant height (Worland et al., 1998b). Worland et al. (1998b) located *Ppd-D1* on chromosome 2DS, 20.9 cM proximal to *Rht8* at the SSR marker *Xgwm261*(Korzun et al., 1998). Based on analysis of the pleiotropic effects, Worland et al. (1998b) concluded that *Ppd-D1,* in addition to accelerating ear emergence time, reduced plant height, tillering, spikelet numbers.

Whether the presence of plant height and peduncle length QTL on chromosome 2DS is due to the pleiotropic effect of *Ppd-D1* or the presence of *Rht8* gene in this population is not clear, possibly due to a lack of markers in the region harboring the QTL. The poor resolution of the map in the short arm made it difficult to assess whether the height QTL is different from the heading time QTL in this region. The addition of more markers to fill gaps in the map may lead to the clearer identification QTLs for heading time and plant height.

Cadalen et al.(1998) identified QTLs associated with reduced plant height on chromosomes 4BS, 7AL, and 7BL in the Courtot/CS population. Börner et al. (2002) identified QTLs on chromosomes 3B, 4A, 5D, and 6A that affected plant height in the ITMI population. Ellis et al. (2005) mapped the *Rht5* gene approximately 10cM from *Xbarc102* on chromosome 3B. Only one QTL associated with plant height has been reported on chromosome 3A (http://www.shigen.nig.ac.jp/wheat/komugi/genes/macgene/2007/GeneSymbol.html). Eriksen et al. (2003) detected a QTL associated with plant height on the centromeric region between markers *Xwmc505* and *Xwmc264* on chromosome 3A. In this study a QTL associated with plant height was also detected on chromosome 3A at the three out of five sites.

Other significant plant height QTL was detected on chromosome 7A with the G × E interaction effects observed at RAC, MexD and MexI for this locus. In RAC and MexD (the drought-affected sites), ***QHt.aww-7A.1***$^{NA}$ was coincident with the heading time QTL at marker *Xcfa2028-7AS*, where the 'Kukri' allele was associated with reduced plant height. In MexI (the non-stressed experiment), two QTLs were found on chromosome 7A. ***QHt.aww-7A.2***$^{NA}$ was located between SSR marker *Xbarc0174* and *Xbarc0259*, and the 'RAC875' allele was associated with reduced height in this environment. ***QHt.aww-7A.3***$^{NA}$ was detected in the proximal region of the long arm of chromosome 7A between DArT marker *XwPt-7763* and *XwPt-6495***,** where the 'Kukri' allele was associate with reduce height.

Peduncle elongation is required for exertion the ear from the flag leaf sheath in cereals especially in rice (Ji et al., 2005). In semi-dwarf wheat, the peduncle has been reported to contribute approximately 30% of the total plant height (Powell and Schlehuber, 1967). Ehdaie et al. (2006a) reported 37 to 47% of the stem length in modern dwarf and semi-dwarf wheat was associated with variation in peduncle length. In this study, the peduncle comprised 32 to 39% of plant height. Drought stress slows or halts peduncle elongation. Most current improved semi-dwarf varieties have good ear exertion. However, under severe drought stress peduncle might be stunted. Briggs and Aytenfisu (1980) found an association between short peduncles and high grain yield in spring wheat. Carbohydrates are remobilised from the peduncle and flag leaf to the grain during the grain-filling period (Zamski and Grunberger, 1995). Villegas et al. (2007) although found a positive correlation between the peduncle length and grain yield ($r^2$ =

0.97, $P < 0.05$), watering regimes were reported as the main factor in explaining variations in grain yield and peduncle length. They suggested that peduncle length was not a good indicator of grain yield for breeding purposes (Villegas et al., 2007). In this study, late-flowering lines that encountered severe drought stress in Bool and Minn, showed dramatic reduction in peduncle length.

Several QTLs were identified for peduncle length. For the non-adjusted data, most detected QTLs (on chromosomes 1A, 2B, 2D, 3A, 3D, 5A, 5B, 7A and 7B) were coincidence with heading time except ***QPdl.aww-3A***$^{NA}$ and ***QPdl.aww-5A***$^{NA}$. For the early-flowering subpopulation, QTLs for peduncle length were detected on chromosome 2D, 3A, 5A, 7A and 7B, while for the adjusted data, 2D, 3A, 5A, 6D and 7A loci were detected. Börner et al. (2002) identified a QTL for peduncle length on chromosome 6A coincident with plant height QTL. By eliminating the heading time effect from peduncle length it might be possible to find loci that control peduncle length under drought stress conditions.

### 5.3.4 Drought indices to reduce phenological effects on grain yield

In this study, drought responses were confounded by genetic variation in flowering time. While the early-flowering lines escaped from progressive water stress, the late-flowering lines were disadvantaged by high temperatures and dry conditions in the terminal season. Therefore, the plant response can be confounded by the environmental covariates as a result of differing phenology. In order to determine the genetic basis of drought tolerance mechanisms, which are likely to be complex, the confounding effect of phenology must be addressed (Reynolds and Tuberosa, 2008).

Here we found that heading time strongly influenced different traits especially grain yield under drought stress conditions. These traits are often correlated both genetically and non-genetically (Jiang and Zeng, 1995). To reduce correlated trait effects on QTL detection and to obtain an improved genetic description of the trait of interest, we decided to remove the relationship between correlated traits by adjusting for the major confounder (heading time). Adjustment for potentially important confounders is important to protect against the occurrence of false associations. Adjusting trait values by using covariates that are causally related to a QTL will reduce the heritability estimates and decrease the power to detect the QTL (Zeegers et al., 2004).

If we assume that drought tolerance is an independent genetic character, yield of a genotype in an drought-affected environment can be expressed as a function of yield potential (yield in the non-stressed environment), phenology (heading time) and drought response (Fig 5-21). The actual contribution of drought tolerance to grain yield under stress may not be large, relative to that of yield potential and phenology (Ouk et al., 2006). Edmeades et al. (1989) pointed out that drought escape should not be equated with drought tolerance, since there is little evidence that early-flowering genotypes are more drought tolerant than late-flowering genotypes with a similar genetic background. Drought escape depends upon the time of flowering relative to the timing of the stress, and an early-flowering genotype, which has an advantage in a terminal stress may be more seriously affected in a midseason stress than a late genotype would be (Bidinger et al., 1987). Edmeades et al. (1989) and Bidinger et al. (1987) suggested that "considerable care must be taken in selecting for drought tolerance among cultivars which vary in flowering date and in maturity". Therefore , a selection index that holds maturity constant is desired (Edmeades et al., 1989). One strategy that has been used to reduce the genetic variance of heading time on the other phenotypic data, particularly grain yield, was the estimation of drought tolerance indices, including drought response index (Bidinger et al., 1987), stress tolerance index STI (Fernandez, 1992) and drought susceptibility index (Fischer and Maurer, 1978). The DRI corrects grain yield under drought for variation in time to heading and yield potential under non-stressed conditions. DRI has been used in different crops such as pearl millet (Bidinger et al., 1987), bean (Abebe et al., 1998) and rice (Garrity and O'Toole, 1994; Pantuwan et al., 2002; Ouk et al., 2006) to select genotypes which have drought tolerance traits. Yue et al. (2005) used DRI for the first time in rice mapping population to remove confounding effect of flowering time.

Our results are in agreement with the results from Bidinger et al. (1987) and Yue et al. (2005) showing that DRI can eliminate the effect of variation of yield potential and flowering time. DRI appears useful for identifying drought tolerance QTLs in populations segregating for major heading time genes, since DRI was not confounded by yield potential and heading time.

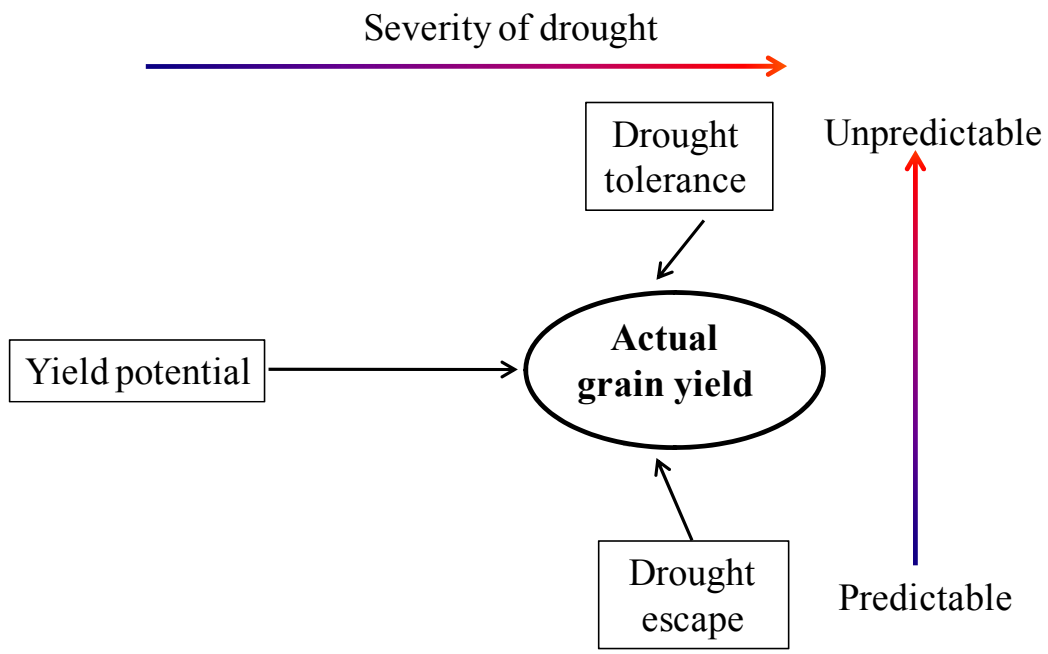


**Figure 5-21. The association between yield potential, phenology and drought tolerance in determining grain yield under various drought conditions (after Ouk et al., 2006).**

Drought indices, such as STI and DSI, can simulate the responses of plants carrying diverse combinations of alleles expressing under stress and non-stress environments. Limitations of using the DSI have already been described in wheat (Clarke et al., 1992). DSI does not differentiate between potentially drought-tolerant genotypes and those that possessed low overall yield potential (Clarke et al., 1992; Golabadi et al., 2006). Large values for DSI represents lines relatively more sensitivity to stress. Selection based on this index favors genotypes with low yield potential under non-stress conditions and high yield under stress conditions. Conversely, high values of STI identify genotypes with higher stress tolerance as well as yield potential (Fernandez, 1992; Ehdaie et al., 2003). In this study these two indices detected those yield potential QTLs on chromosome 3B and also a drought-specific yield QTL on chromosome 7A. DSI, a susceptibility index, can identify those alleles that are associated with lower grain yield under stress, while STI, a tolerance index, combined those alleles that were associated in higher grain yield under non-stressed and drought stressed environments.

## 5.4 Conclusions

The primary objective of this study was to determine the number and location of QTLs for important agronomic traits in the RAC875/Kukri population in drought stressed environments. A doubled-haploid population of 368 lines was used to map QTLs for the maturity-related traits, some morpho-physiological traits such as plant height, peduncle length, flag leaf length, leaf waxiness and chlorophyll content, grain yield and yield components traits across five different stressed and non-stressed environments. The results of this QTL study are a first step towards fine mapping of drought tolerance QTLs using recombinant inbred lines (RILs) and also the design of a marker-assisted selection program for wheat improvement under South Australian environments. The QTL mapping information provides a starting point to clone genes underlying specific QTL.

This study shows that the genetic control of flowering time in this population is complex. Multiple genes for time to heading, including vernalization and photoperiod sensitivity as well as earliness *per se*, presumably exerted their effects on the adaptability of wheat cultivars in the South Australian environments. We identified seven loci controlling heading time in this population, of those two putative QTLs, ***QEet.aww-2BS*** and ***QEet.aww-2DS***, showed the strongest effect. For the ***QEet.aww-7A*** locus further investigation is required to understand the impact that this locus has on grain yield and the G × E interaction for grain yield.

The present study identified QTLs controlling grain yield and its components on chromosome 7A in the drought-stressed environments, and confirmed that these grain-yield QTLs were correlated with QTLs for yield components. Two major grain yield QTLs on chromosome 3B were also found under non-stressed conditions. These are possible yield potential QTLs. In summary, chromosome 7A appears to carry important genes for grain yield under drought stress. Further work is needed to verify the effect of this region in various genetic backgrounds and environments.

Results of this study showed that drought stress indices worked well in mapping studies. DRI successfully eliminated the heading time and yield potential effect. Our results showed that yield potential QTLs are independent of stress tolerance loci for grain yield suggesting that breeding for high yield potential alone under optimal conditions will not

necessarily lead to stable or higher yields under drought stress. However, it is possible to improve yield stability by combining yield QTLs expressed under contrasting environments (stress and non-stress environments). In particular, combining the 'RAC875' alleles on chromosomes 3BS (***QYld.aww-3B.1***) and 7A (***QYld.aww-7A***) as well as the 'Kukri' allele on chromosome 3BL (***QYld.aww-3B.2***) into wheat genetic backgrounds having both drought response alleles may increase yield potential as well as improve yield stability.

# CHAPTER 6

# THE VALIDATION OF LEAF WAXINESS QTL USING RIL POPULATION

# 6 Chapter 6: The validation of leaf waxiness QTL using RIL population

## 6.1 Introduction

Waxiness or glaucousness refers to the visible waxy bloom or bluish-green appearance on the plant cuticles. The waxy or less waxy appearance of the plant organs is correlated with the presence and amounts of β-diketones in the surface waxes (Bianchi et al., 1982). In wheat, the presence of a large amount of β-dicarbonyl compounds is responsible for waxiness. However, non-waxy appearance of the plant does not mean absence of β-diketones (Bianchi et al., 1982; Bianchi and Figini, 1986). Bianchi and Figini, (1986) evaluated wheat varieties and mutants for epicuticular wax composition. They concluded that the wax structures in waxy wheats were characterized by the presence of long, thin tubes (also called rods and spicules). Whereas, non-waxy (green, smooth "waxless") wheat lines were associated with plate-type wax structures. Waxiness first appears on the leaf sheath at the time of stem elongation. It rapidly reaches maximum expression, particularly on the flag leaf sheath and the abaxial surface of the flag leaf lamina, as well as on the emerging head (Richards et al., 1986). Richardson et al. (2005) suggested that cuticular waxes are deposited along the growing grass leaf independent of cell age or developmental stage.

An important function of epicuticular waxes has been suggested to increase the efficiency of stomatal control by reducing water loss after stomatal closure (Rawson and Clarke, 1988), to protect plants against ultraviolet (UV) radiation (Steinmüller and Tevini, 1985) and to reduce water retention on the plant surface, thus minimizing deposition of dust, pollen and air pollutants. Moreover, it reduces sprouting by increasing water repellency of the mature ear (King and von Wettstein-Knowles, 2000). Leaf waxiness is believed to enhance yield in wheat by increasing water use efficiency (WUE) or transpiration efficiency (Richards et al., 1986). It has been suggested as a useful trait that may improve WUE in dryland conditions (Qariani et al., 2000). In wheat, waxy genotypes were reported to reduce leaf temperature, and consequently to reduce both stomata and cuticular transpiration (Yang et al., 1991).

There have been several studies on the inheritance and localisation of genes controlling waxiness in wheat. The inheritance studies of waxiness demonstrated that the expression of the waxiness gene (*W1*) is dominant over non-waxy, but waxiness is inhibited by the epistatic influence of the dominant inhibitor of the waxiness gene (*Iw1*). These genes were located on the short arm of chromosome 2BS (Driscoll, 1966; Tsunewaki and Ebana, 1999). Additional waxines and inhibitor genes (*W2* and *Iw2*) are located in a homoeologous on chromosome 2DS (Tsunewaki and Ebana, 1999; Watanabe et al., 2005; Liu et al., 2007). In this study (Chapter 5), we found a novel QTL for leaf waxiness on chromosome 3A with relatively high phenotypic main effects in five different environments. Primary objective of this work was to test out the idea of moving from the DH population for preliminary mapping to the large RILs population developed from the cross between RAC875 and Kukri. Since leaf waxiness is highly heritable and is easy to score, which can visually be done on a single plant basis, the leaf waxiness QTL was targeted for fine mapping using a small subset of 380 RILs.

## *6.2 Materials and methods*

### 6.2.1 Plant materials, phenotyping and genotyping

Five hundred recombinant inbred lines (RILs; F2-derived, F4:5 lines) were randomly sampled from 2,976 RILs that were generated by single-seed-descent (SSD) from a cross between Kukri and RAC875. To evaluate leaf waxiness, 500 RILs were planted in five 104-well trays in two replicates in the glasshouse (two plants per RIL family), the two parents as check were also replicated ten times in the experiment. Eventually, 380 RILs were used for genotyping as well as phenotyping for leaf waxiness. DNA was extracted from freeze-dried wheat leaf using high-throughput DNA extraction method (see the Materials and Methods; section 4-2). For marker screening on chromosome 3A, four DNA samples from two parents (Kukri and RAC875) and two bulks of DNA from DH lines contrasting in leaf waxiness were used. Based on the knowledge from the DH population assay in the field, twelve DH lines contrasting in leaf waxiness as well as showing genotypic differences at marker locus *Xwmc264* were selected to bulk DNAs (Table 6-1). The concentration of DNA was determined using NanoDrop spectrophotometer (ND-1000, Wilmington, Delaware USA). DNA concentrations for parents and bulks were made up of 96, 84, 148, and 165 ng/µl for Kukri, RAC875, Bulk-A and Bulk-B, respectively.

**Table 6-1. Bulks of DNA from DH lines that possess Kukri and RAC875 alleles (A and B, respectively) at marker *Xwmc0264*.**

| No | Bulk A (Kukri allele) | Bulk B (RAC875 allele) |
|---|---|---|
| 1 | DH_R035 | DH_R009 |
| 2 | DH_R196 | DH_R101 |
| 3 | DH_R275 | DH_R147 |
| 4 | DH_R086 | DH_R255 |
| 5 | DH_R213 | DH_R297 |
| 6 | DH_R119 | DH_R066 |

Seventy-one SSR markers were selected from the Multiplex-Ready Marker database and the Multiplex-Ready CMAP Interface. All these markers were all expected to be located on chromosome 3A in wheat. The BINNER software was used to create the marker panels comprising SSRs with non-overlapping allele sizes for the selected markers (http://www.genica.net.au). To screen this set of markers, the Automated Designer macros (version 2.0), developed by Dr. M. Hayden, the University of Adelaide, was used to design experiments and for the analysis of marker data. Marker dilution and allocation was performed as suggested by the Automated Designer macros. PCR profile and post-PCR protocols are given in Chapter 4 (Section 4-2). Polymorphic markers were used to genotype the 380 RILs. For linkage analysis, the Haldane mapping function (Haldane, 1919) was used to estimate distances between markers using Map Manager version QTXb20 (Manly et al., 2001).

At the stage of stem elongation, excess tillers were removed maintaining the main stem for each line. Leaf waxiness was scored on the flag leaf sheath and blade twice throughout the experiment at heading and anthesis for each line. Clear differences in surface wax between waxy and non-waxy plants were observed (Fig. 6-1). Scoring for leaf waxiness was described in Chapter 5 (Materials and Methods; Section 5-2). Score 1 was assigned to no visible wax deposition on the abaxial surface of the leaf and score 8 was assigned to extreme wax deposition on the abaxial as well as adaxial surface of the leaf. Single marker analysis and interval mapping were performed to identify strongly associated markers as well as the best possible interval in QTL analysis using Windows QTL cartographer ver. 2.5 (Wang et al., 2006).

**Figure 6-1. Differences between waxy and non-waxy lines grown in the glasshouse, the left leaf is from a non-waxy line with the score of 1 and the right leaf is from a waxy line with waxiness score of 7.**

## 6.3 Results

The largest QTL for leaf waxiness was identified on the long arm of chromosome 3A (***QW.aww-3A***) in the DH population grown in the field. ***QW.aww-3A*** was strongly associated with *Xwmc0264* in the *Xwmc0264–Xcfa2193b* interval (Fig. 6-2).

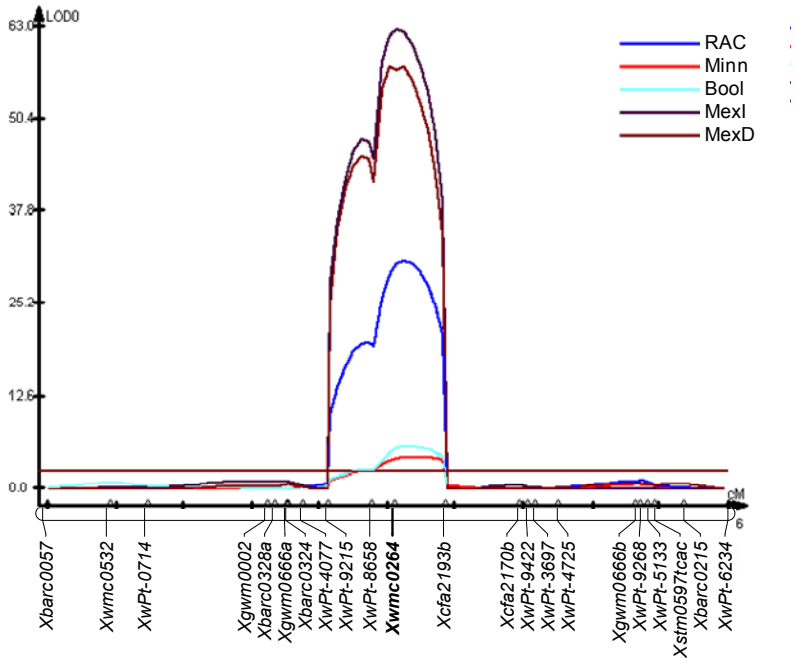


**Figure 6-2. Detected QTL with CIM for leaf waxiness on chromosome 3A (QW.aww-3A) in DH population grown at five sites; Roseworthy (RAC), Minnipa (Minn), Booleroo (Bool), Mexico irrigated (MexI) and Mexico droughted (MexD).**

In the glasshouse, segregation for visible waxiness was also observed in the parents and RILs (Fig. 6-3). The scoring of this trait was easy, despite the plants were grown in the

controlled conditions. Frequency distribution of leaf waxiness suggested that this trait was quantitatively inherited.

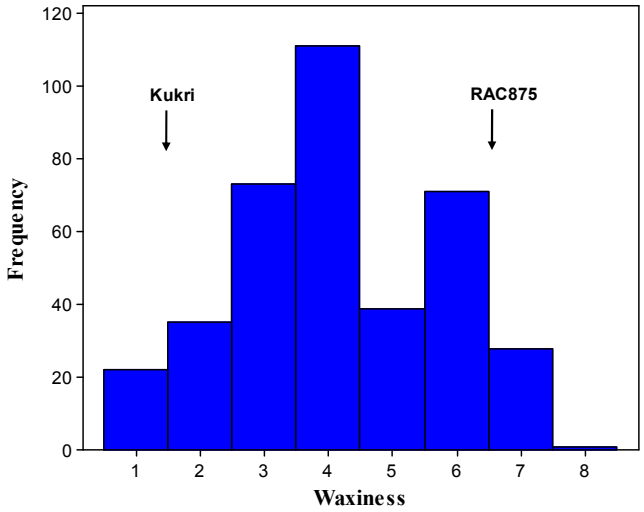


**Figure 6-3. Phenotypic frequency distribution of leaf waxiness in 380 RILs from the RAC875/Kukri population grown in glasshouse Arrows indicate the trait value for the two mapping parents.**

In the marker screen, thirty four SSR markers (~48%) were found polymorphic. These 34 markers along with eight markers that had previously been mapped in the DH lines were used for genotyping. Therefore, 42 markers were genotyped in the 380 RILs. In total, fourteen marker loci were mapped in two linkage groups on chromosome 3A (Fig. 6-4). One linkage group consisted of 10 loci which were significantly linked with LODs of more than 6.5. One redundant marker was excluded for QTL analysis. No additional marker mapped in the *QW.aww-3A* region of the RILs between *Xbarc0324* and *Xcfa2123b* spanning around 35.9 cM; *Xwmc0264* showed the closest association with *QW.aww-3A* similar to the mapping in the DH lines. The chromatogram of *Xwmc0264* segregating in the RILs is shown in Figure 6-5. In this population, the allele with 170 bp came from the Kukri parent, while the 175 bp allele came from RAC875.

The estimated distances between *Xbarc0324* and *Xwmc0264* and between *Xwmc0264* and *Xcfa2123b* were 16.8 and 19.1 cM, respectively. Based on the DH linkage map data the average distances between these markers were 27.7 and 13.1 cM, resulting in a 40.8 cM interval for this region. In the F1-derived DH lines the interval is 40.8 cM, whereas in the RILs it is only 35.9 cM. In RILs effective recombination can occur at every meiosis until the plants become relatively homozygous. Therefore the recombination frequencies between two markers are increased during line development from the F1 to the F5 generation (Messmer et al., 1999). The RILs have undergone four more meiotic

events to F5 but genetic recombination is somewhat similar to the F1-derived DH lines for chromosome 3A. The presence of heterozygosity and excess double-crossovers events in RILs might be contributed to the long interval (Knox and Ellis, 2002). Although map length is important, the correct marker order is of more benefit for genome analysis and marker-assisted breeding. However, the availability of sufficient lines (2,976 RILs) makes it possible for further fine mapping of this region.

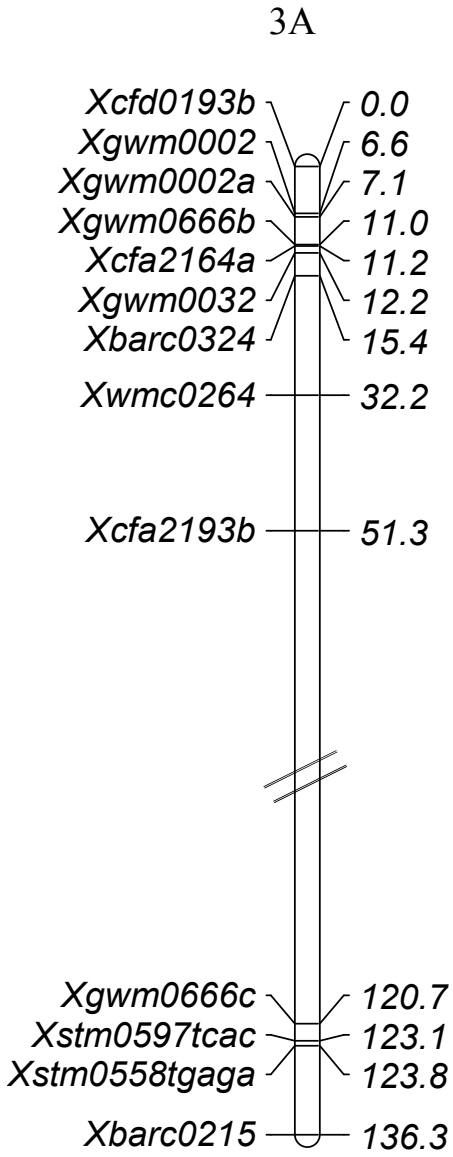


**Figure 6-4. The estimated position of SSR markers on chromosome 3A in 380 RILs from cross between Kukri and RAC875.**


**Figure 6-5. The GeneMapper chromatogram showing *Xwmc0264* (Ta0137) in the Kukri/RAC875 RIL population. The chromatogram for this marker peaked at 170 bp (Kukri allele size) and at 175 bp (RAC875 allele size) and showed a strong association with leaf waxiness in the Kukri/RAC875 DH and RIL populations.**

Single marker analysis showed significant ($P < 0.00001$) association between markers *Xbarc0324*, *Xwmc0264* and *Xcfa2193b* and leaf waxiness. Marker *Xwmc0264* merely explained only 27.0% of the phenotypic variation. Composite interval mapping in the RILs showed a significant QTL, *QW.aww-3A*, with a LOD value of 24.0 at *Xwmc0264* in the *Xbarc0324-Xcfa2123b* interval, which explained 34.7% of the phenotypic variation. This data confirmed the results from the field studies, where the largest QTL for leaf waxiness was identified on chromosome 3A in the same position with marker *Xwmc0264*.

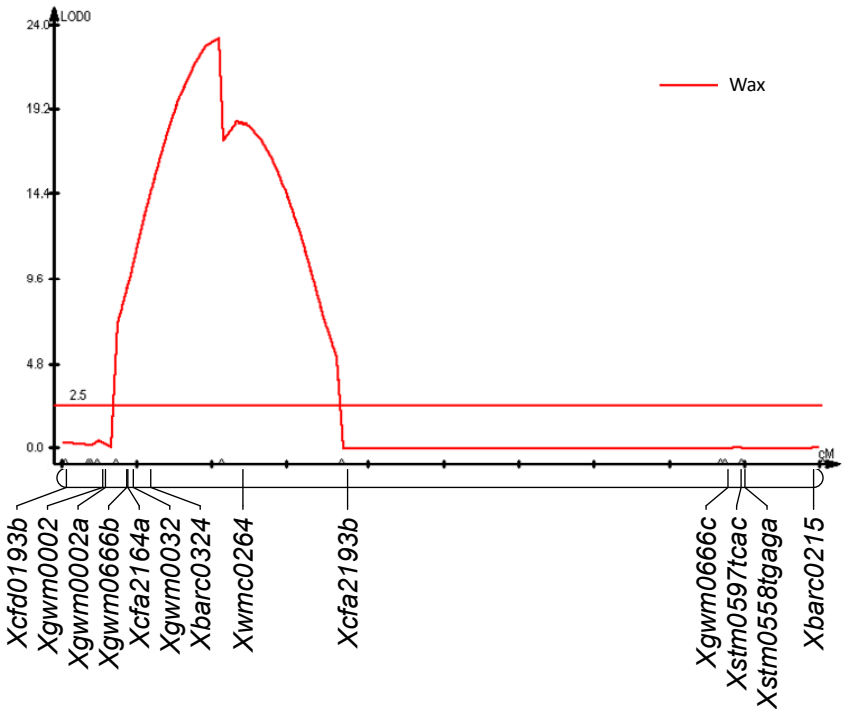


**Figure 6-6. Detected QTL with CIM for leaf waxiness on chromosome 3A (*QW.aww-3A*) in the RIL population from the cross between RAC875 and Kukri. Composite interval mapping was performed using QTL Cartographer vr 2.5.**

## 6.4 Discussion

This study validated the presence of a major novel leaf waxiness QTL (*QW.aww-3A*) in the RAC875/Kukri RIL population on chromosome 3A near the marker locus *Xwmc0264*. Several genetic studies indicated that two dominant waxy loci (*W1* and *W2*) controlling leaf glaucousness are located on chromosomes 2BS and 2DS, respectively (Driscoll, 1966; Tsunewaki, 1966). Two dominant wax inhibitor loci (*Iw1* and *Iw2*) were also located on 2BS and 2DS and were shown to inhibit the waxy phenotypes epistatically via *W1* and *W2*. *Iw2* originated from *T. tauschii* and it was reported as being non-allelic to *W2* on chromosome 2D (Tsunewaki and Ebana, 1999; Watanabe et al., 2005; Liu et al., 2007). Nelson et al. (1995) mapped the waxiness trait on 2DS. Kulwal et al. (2003) found markers on chromosomes 2B, 2D and 6A highly associated with leaf waxiness. Simmonds et al. (2008) mapped the *Vir* (viridescent appearance) gene to the distal end of the short arm of chromosome 2B. A survey in the literature showed that a QTL for leaf waxiness has not been reported on chromosome 3A. It appears that leaf waxiness in these South Australian cultivars used in the present study is genetically different from the materials used in these previous studies.

Although the waxy locus on chromosome 3A did not show a positive effect on grain yield under drought, it might provide other effects such as disease resistance, insect resistance and heat tolerance, which have not been investigated in this population. Future work is required to dissect the effect of leaf waxiness on other traits.

The relationship of leaf waxiness to yield benefits in this population is not clear. Despite the higher grain yield increases observed in RAC875 (waxy plant) under drought conditions), in the population no association was evidenced between grain yield and leaf waxiness QTL on chromosome 3A (*QW.aww-3A*). However, the structure of the wax deposition and the layer order are very important toward improved drought/heat tolerance. The type of ultra-structure of wax deposition and order were not evaluated for this QTL. There might be other waxiness loci (on other chromosomes) conferring drought/heat tolerance due to differences in the structure and order. For thorough understanding of these effects further investigation is required.

Previously, leaf waxiness has been found advantagous for yield in durum and bread wheat cultivars, especially under drought stress. Glaucousness/waxiness was associated with higher yield in dry-land barley cultivars (Febrero et al., 1998), durum wheat (Merah et al., 2000) and bread wheat (Richards et al., 1986), whereas in the present study, no association between leaf waxiness and yield was found on chromosome 3A. Simmonds et al. (2008) in contrast, found a converse relationship between leaf waxiness and yield. They found a QTL for *Vir* which exhibited a significant delay in leaf senescence and a prolonged grain-filling period in UK wheats. However, the delay in leaf senescence could be independent of leaf waxiness. The yield maintenance in the Vir genotypes might be associated with the delay in leaf senescence but not for the presence of absence of waxiness.

## 6.5 Conclusion

This work was an example to fine map the leaf waxiness QTL (*QW.aww-3A*) using the secondary mapping population of RILs. In this study, the presence of *QW.aww-3A* has been confirmed on a subset of 380 RILs population. There are enough resources (2,976 RILs) available to further fine map this QTL. Applying this strategy would allow targeting other interesting QTLs, such as QTL clusters on chromosome 7A for grain yield under drought.

# CHAPTER 7

# GENERAL DISCUSSION

# 7 Chapter 7: General discussion

## 7.1 Introduction

This study comprised three major objectives: completion of a comparative physiological study to evaluate three South Australian wheat cultivars for their agronomic and physiological responses to cyclic water stress under controlled conditions (Chapter 3); construction of a framework genetic map of a doubled-haploid (DH) population developed from a cross between Kukri and RAC875, lines with contrasting grain yield under drought conditions (Chapter 4); and identification of QTLs associated with agronomic or physiological traits that may contribute to the maintenance of yield in drought-affected environments (Chapter 5).

In this concluding chapter, the major findings presented in Chapter 3 to 6 will be discussed in the light of past and current research, and on the base of this knowledge, the possibilities for future work will be described.

## 7.2 Physiological characterization under controlled conditions

The overall strategy of characterising the three wheat cultivars to the cyclic water stress under controlled conditions was to study a range of morpho-physiological traits, and to test the relationship between these parameters and grain yield under drought conditions in the field in the South Australian target environment. Our data from the growth room experiments (Chapter 3) showed that, with target environment considerations, drought experiments under controlled conditions can relate to field performance.

Grain yield data of the three wheat cultivars at the ten different sites across the South Australian wheatbelt showed that Excalibur and RAC875 outyielded Kukri by 10 to 40% (Chapter 1). Interestingly, the differences between lines in grain yield were more noticeable under the drier conditions (Chapter1; Figure 1-4). Under moderate to high rainfall conditions, Kukri (the drought susceptible cultivar) showed a similar yield to Excalibur and RAC875, while under more severe water stress, Kukri produced far less grain yield. A similar result for grain yield production was also observed in the growth room experiments for these three tested cultivars (Chapter 3).

Although the cyclic drought experiment in the growth room worked for a small number of cultivars, there are limitations that make it difficult to assess a large number of genotypes or mapping populations. In particular, controlling watering regimes is very labour intensive. Therefore, we aimed to move from growth room characterisation of the response to field evaluation. However, in the future, a high-throughput, automated phenotyping technology (produced by LemnaTec; http://www.lemnatec.com) will become available in a new facility (http://appf.acpfg.com.au/), which will decrease laborious scoring tasks in the glasshouse. The LemnaTec platform, called a Scanalyser, may help to phenotype, non-destructively, a large number of genotypes from drought mapping populations.

### 7.2.1 Major components of the drought tolerance response

Overall, the results presented in Chapter 3 showed that, among yield components, the number of grains per spike (spike fertility) was the primary yield component that associated with yield maintenance under water stress conditions in the growth room. The results from the field study (Chapter 5) also showed that grain number per square meter, number of grains per spike and spike fertility were major components associated with grain yield in the drought-affected environments. Based on field evaluation (Chapter 5), several QTLs for grain yield and yield components were identified across the genome. The most important QTL cluster for grain yield and associated traits mapped to chromosome 7A.

### 7.2.2 Genetic basis for the source-sink relationship

Genetic variation in grain yield under drought is largely dependent on the sink-source relationship. Therefore, increases in both source- and sink-related traits are important to increase genetic gain in yield (Reynolds et al., 2001; Snape et al., 2007). The main traits associated with the source are the rate of photosynthesis during grain-filling (green leaf area and chlorophyll content), the maintenance of green leaf area during grain-filling (stay-green) and the amount of assimilates available for remobilization (stem water soluble carbohydrates). The number of grain per unit area, rate of grain-filling, and grain size are major traits associated with the sink.

In this study, reductions in the number of grains and grain weight were observed under drought stress, which could be due to pollen sterility and/or abortion of grains as a result

of failure in embryo development (Saini and Westgate, 2000). The lack of source activity (current photosynthetic assimilates) and strength (stem water soluble carbohydrates) probably associate with the reduction in the number of endosperm cells and amyloplasts in the grain (Saini and Westgate, 2000). From WSC measurements in the parents as well as a small subset of DH lines, RAC875 showed a relatively greater rate and/or extent of dry matter accumulation in stem and subsequently in the spike, possibly as a result of re-mobilization of more WSC from stem. It seems that a higher percentage of WSC in the stem and the rate of dry matter accumulation in the spike in the higher yielding parent (RAC875) may lead to the maintenance of more grains per spike with a reasonable grain size under drought stress conditions. This result is in agreement with Kuchel et al. (2007a), who suggested that the semi-dwarf wheat genotypes adapted to the South Australian environments achieve relatively higher grain yield through increases in seed set and little compensatory loss in grain weight.

From the results of this study (Chapters 3 and 5), it is likely that osmotic adjustment (OA) capacity and accumulation of stem WSC, two major physiological attributes in both drought-adapted cultivars, may associate with drought tolerance and higher relative productivity under drought stress conditions. Variation in OA and WSC were observed between three different parental lines. Excalibur and RAC875 showed the highest and moderate levels of osmotic adjustment (OA), respectively, compared to Kukri (Chapter 3; Section 3.3.3). Excalibur (data from field was not shown) and RAC875 had a greater capacity for WSC storage under both stress and non-stress treatments (Chapter 3 and 5). Segregation for WSC was also observed in a small subset of DH lines in the RAC875/Kukri population (Chapter 5). The capacity to adjust osmotically may enhance spikelet fertility due to pollen and spike development (Morgan, 1984), and the capacity for high WSC accumulation and remobilization may allow grain development during the grain-filling period (Nicolas and Turner, 1993; Blum, 1998; Shearman et al., 2005; Ehdaie et al., 2006b; Ruuska et al., 2006; Rebetzke et al., 2007; Ehdaie et al., 2008; Xue et al., 2008). Moreover, the two drought tolerant cultivars showed a stay-green characteristic under water stress conditions. High chlorophyll content and stay-green likely contributed to high yielding capacity (Borrell et al., 2000). A QTL for chlorophyll content (*QSpad.aww-7A*$^{NA}$) co-located with a QTL for grain yield on chromosome 7A (*QYld.aww-7A*$^{NA}$).

Further research would be required to investigate the genetic basis underlying the relationship between the source and the sink capacity in this population. Additional morpho-physiological traits relevant for wheat productivity under drought stressed conditions will also need further investigations. These traits could be osmotic adjustment (Morgan and Tan, 1996; Teulat et al., 1998; Zhang et al., 1999), water soluble carbohydrate accumulation and remobilization (Teulat et al., 2001a; Rebetzke et al., 2007), photosynthetic capacity (Sanchez et al., 2002; Jiang et al., 2004; Verma et al., 2004), carbon isotope discrimination (Rebetzke et al., 2002; Teulat et al., 2002; Laza et al., 2006) and root and leaf morphology and angle, which will provide important clues on the functional basis of the effects that exerted by the chromosome 7AL QTL cluster. Further work to verify the effect of this region in various genetic backgrounds and environments is needed.

The role of leaf morphology also needs to be considered. Differences in leaf morphology may play an important role under dry and hot conditions. Reduction in leaf size in RAC875, which results in a smaller transpiring leaf area, is an adaptive response to water deficit (Tardieu, 2005). Leaf rolling, which was high in Excalibur, can also reduce effective leaf area, reducing radiation intercepted and consequently transpiration under water stress (Loss and Siddique, 1994). An upright leaf canopy can also use radiation more efficiently while intercepting less radiation (Reynolds et al., 2000).

## *7.3 Genetic studies*

To study the genetic basis of drought tolerance (productivity), a framework map was constructed using the DArT and locus specific SSR markers (Chapter 3). The map generated in this study was produced with the aim to identify major genetic components of the drought response in terms of yield production in the field. Overall, the framework map made in this study had a reasonably good coverage in comparison with previously published maps in wheat (Röder et al., 1998; Messmer et al., 1999; Chalmers et al., 2001; Paillard et al., 2003; Sourdille et al., 2004; Liu et al., 2005c; Quarrie et al., 2005; Akbari et al., 2006; Semagn et al., 2006). However, there are some gaps in the map on chromosome 2DS, 3DS, 4A, 4B, 4D, 5A, 5D, 6D, 7AS and 7D, with a lack of markers and poor coverage. Further work is required to add new markers to the existing map, particularly in the genomic regions of interest. Although the existing map was constructed based on 368 DH lines, the population segregated for photoperiod-

insensitivity genes (*Ppd-B1* and *Ppd-D1a*), which made phenotyping less accurate. Thus, the population was divided into two subpopulations of the early- and late-flowering lines based on their differences in time to heading. The late-flowering lines were not of interest because the long delay in flowering time meant that their maturity class did not fit the target environment. Therefore, they were culled from the population, and the early-flowering lines were selected for further QTL studies. Although splitting the population eliminated the effect of heading time (Chapter 5), the allelic frequency may be biased as a result of uneven crossovers in the selected subpopulation (Brown et al., 2000; Vision et al., 2000; Xu et al., 2005). In this case, selective mapping as a strategy for increasing genome-wide QTL map resolution is proposed (Vision et al., 2000).

From the 260 early-flowering DH lines, it would be possible to select a subset of lines on the basis of observable crossover events – e.g. 200 individuals that collectively represent a good coverage of the crossover sites in the whole population (Vision et al., 2000; Ronin et al., 2003; Xu et al., 2005). All new markers to be mapped are genotyped only on the selected individuals and their positions inferred relative to the previously mapped framework markers as described by Vision et al. (2000).

### 7.3.1 Major loci for yield response under drought

In this study (Chapter 5), the molecular basis for drought tolerance was investigated by identifying major QTLs for grain yield under drought. Different strategies were implemented to eliminate the possible confounding effects of heading time on grain yield and yield components. A major QTL cluster for grain yield was identified on chromosome 7A only in the drought-affected environments (Chapter 5). This QTL cluster could be used as a good target for positional cloning and gene isolation. However further work would be needed to confirm and validate the identified QTLs in this preliminary QTL analysis.

### 7.3.2 Confirmation and validation of identified QTLs

QTL analysis employed in Chapter 5 is restricted to the detection of the main additive effects in a single environment basis without considering the QTL-by-environment interactions as well as epistatic interactions between QTLs. Although it improved our understanding of the genetic basis of complex traits such as grain yield, conclusions are

limited by the scope of the environments selected for examination. Future studies are needed to confirm and validate the identified QTLs in this study. Data from several environments and years would be required to confirm the position of major QTLs as well as minor QTLs with G x E interactions. Multi-environment QTL analysis may facilitate the prediction of QTL effects along with QTL-by-environment (Boer et al., 2007; Kuchel et al., 2007b; Malosetti et al., 2008). A detailed understanding of QTL-by-environment interactions may assist breeders in the design and implementation of breeding strategies targeted at improving the grain yield and adaptation of wheat to both specific and mega environments (Kuchel et al., 2007b).

In addition, the identified QTLs presented in this study related to alleles that segregate in a bi-parental cross between RAC875 and Kukri. To be useful in marker-assisted selection in breeding programs, alleles with important effects that segregate within other populations with some similarities in genetic background, such as Excalibur/Kukri and Gladius/Drysdale, would also be required.

Having identified additive QTLs, it is important to test for interactions either among QTLs or with other factors such as sexual, parental and environmental factors (Mackay, 2001; Yang et al., 2007). The identification of epistatic interactions between QTLs is a valuable starting point for a more thorough understanding of genetic networks (Carlborg and Haley, 2004). Thus, further work would be required to test for epistatic interactions between identified QTLs.

### 7.3.3 Pleiotropy versus linkage

The test for pleiotropy versus linked QTL is another area that needs further investigation. Pleiotropy is an important feature of the genetic architecture of any quantitative trait. Most loci involved in development contribute to several developmental pathways (Mackay, 2001). In this study some genomic regions, for instance chromosome 7A, were associated with various traits in the drought and/or non-drought environments. It is not clear whether this association is due to linkage or pleiotropy. For gene discovery and positional cloning of gene(s), it is important to know if one or two genes are responsible for the genetic correlation (Monforte and Tanksley, 2000). Thus, by applying an appropriate statistical approach (Jiang and Zeng, 1995; Lebreton et al., 1998) and/or by substitution-mapping (Tuinstra et al., 1998; Monforte

and Tanksley, 2000) it may become possible to distinguish between linkage and pleiotropy.

This work highlighted the issues of dealing with maturity and plant height in assessing drought responses. To design and generate mapping populations for QTL analysis of drought tolerance traits, future work should include a detailed characterization of the potential parents for major phenology genes (*Ppd*, *Vrn* and possibly for *Eps*) and also for major plant height genes (*Rht-B1b* and *Rht-D1b*) to avoid segregation for maturity and plant height in the segregating population.

### 7.3.4 High-resolution mapping

Since QTL analysis is based on a statistical calculation, it is difficult to determine the precise location of an individual QTL, despite using a large population and many genetic markers. Thus, it is difficult to perform precision linkage mapping of QTLs. Therefore, high-resolution mapping is required to narrow down the candidate genomic region of a target QTL (Tuberosa and Salvi, 2006).

The accuracy of QTL mapping can be improved by increasing population sizes. The DH mapping population is not appropriate for fine mapping of QTLs since it segregates whole parental chromosomal segments (Wan et al., 2006), despite its large pouplation. Therefore, a secondary mapping population is required to facilitate the more comprehensive analysis of target QTLs. A population of 2,976 RILs (single-seed-descent, F2-derived, F4:5 lines) has been developed from a cross between RAC875 and Kukri. Given that, this population segregates for two major heading time genes, possibly *Ppd-B1* and *Ppd-D1*, for further fine mapping, this problem should be taken into account. To fix for these major heading time loci genotypically, it is possible to select individuals with the early alleles on chromosome 2BS and 2DS simultaneously. Based on the information from DH population, around one-quarter of the RILs population (~750 RILs) should have this allele combination. High-resolution mapping can then be done on the selected lines which would be relatively similar in heading time.

The semi-automated Multiplex-ready PCR technique (Hayden et al., 2007) for genotyping will provide high density SSR and SNP genetic maps. Meanwhile, using DArT markers (Akbari et al., 2006) to fill in the map would be useful. Cleaved

amplified polymorphic sequence (CAPS) markers can be used for targeting specific regions in the map. Eventually, thousands of markers can be used to refine the position of the identified QTL.

Fine mapping of the identified QTLs from the primary DH mapping population will enable breeding programs to employ marker-assisted selection and will also allow positional candidate gene analyses to proceed with high levels of accuracy and precision.

In this study, the strategy of using RILs was tested to fine map the leaf waxiness QTL (QW.aww-3A) using a subset of 380 RILs (Chapter 6). Fine mapping of a specific region can also be applied for the interesting chromosome 7A, which harbors several QTLs for grain yield and associated traits. As mentioned previously, for fine mapping of grain yield QTLs, which are more complex, the population should be fixed for the major heading time loci (*Ppd-B1* and *Ppd-D1a*), e.g, using a quarter of the population possessing both the early flowering alleles for *Ppd-B1* and *Ppd-D1a*. For this reason, a partial linkage map for chromosome 7A is constructed.

Finding highly associated loci for grain yield expressed under drought would allow pyramiding of QTLs using marker assisted selection in the breeding programs for the target environment. They can be used as diagnostic markers for breeders, and provide opportunities to screen for novel variation (new alleles) at the target locus. They allow understanding new tolerance strategies based around the mechanisms involved in drought tolerance.

## *7.4 Conclusions*

In conclusion, three wheat cultivars which are the parents of DH populations have been evaluated under controlled conditions to try to identify underlying physiological differences which confer drought tolerance or susceptibility.

This study also showed that there are different adaptive mechanisms in two drought tolerance cultivars (RAC875 and Excalibur), which are involved in conferring drought tolerance or adaptation. RAC875 was found to be more ‘conservative’ in its responses, with moderate OA, high leaf waxiness, high chlorophyll content and high stem WSC. RAC875 showed lowest tiller number *per se*, thick green leaves, stay-green phenotype.

Excalibur was most 'responsive' to cyclic water availability. It showed a strong interaction with the environmental conditions. Excalibur produced more tillers (high pre-anthesis biomass) in the first place and aborted tillers under stress, concentrating resources on the main stems (higher number of spikelet per spike). It produced greater total biomass and had a higher root-shoot ratio under water stress than Kukri and RAC875. It showed leaf rolling and moderate leaf waxiness under stress. Excalibur showed the highest OA capability, highest stomatal conductance, lowest ABA content under stress and rapid recovery after re-watering.

Within the two drought-adapted cultivars in this study, the capacity for osmotic adjustment and stem water soluble carbohydrates might be the main physiological attributes associated with high tolerance and productivity under water stress conditions.

A genetic map was developed for a DH population from the two South Australian wheat cultivars, Kukri and RAC875. This study shows that the genetic control of flowering time in this population is complex. Multiple genes for time to heading, including vernalisation and photoperiod sensitivity as well as earliness *per se*, presumably exerted their effects on the adaptability of wheat cultivars in the South Australian environments.

The present study identified QTLs controlling grain yield and its components on chromosome 7A in the drought-stressed environments, and confirmed that these grain yield QTLs were correlated with QTLs for yield components, e.g. grain number per $m^2$, number of grain per spike and spike fertility. In summary, chromosome 7A appears to carry important genes for grain yield under drought stress. Dissection of these yield traits with physiological studies and fine mapping of this region to determine the molecular basis of these yield traits and their underlying physiological basis is now possible and is likely to reveal interesting insights into mechanisms of drought tolerance in southern Australian wheats.